AN INVESTIGATION OF TUNNEL DIODE-COMMON-BASE TRANSISTOR COMBINATIONS FOR LARGE GAIN-BANDWIDTHS

A THESIS

Presented to

The Faculty of the Graduate Division

by

James Stephen Gray

In Partial Fulfillment

of the Requirements for the Degree

Doctor of Philosophy

in the School of Electrical Engineering

Georgia Institute of Technology

August, 1967

In presenting the dissertation as a partial fulfillment of the requirements for an advanced degree from the Georgia Institute of Technology, I agree that the Library of the Institute shall make it available for inspection and circulation in accordance with its regulations governing materials of this type. I agree that permission to copy from, or to publish from, this dissertation may be granted by the professor under whose direction it was written, or, in his absence, by the Dean of the Graduate Division when such copying or publication is solely for scholarly purposes and does not involve potential financial gain. It is understood that any copying from, or publication of, this dissertation which involves potential financial gain will not be allowed without written permission.

3/17/65
b

AN INVESTIGATION OF TUNNEL DIODE-COMMON-BASE

TRANSISTOR COMBINATIONS FOR LARGE GAIN-BANDWIDTHS

APPROVED:

Chairman

Date Approved by Chairman: August 31, 1967

Dedication

To my father and in memory of my recently
deceased father-in-law.

ACKNOWLEDGMENTS

The author wishes to thank his thesis advisor, Dr. D. T. Paris, for his assistance and encouragement throughout this research. He would also like to thank Dr. B. J. Dasher and the School of Electrical Engineering for providing support during the author's academic career in the form of an NSF Traineeship Fellowship, Teaching Assistantships, and Research Assistantships. Special thanks are due as well to Dr. J. B. Peatman and Dr. K. L. Su for their services as members of the reading committee and to J. H. Dwight for his assistance in proofreading the rough draft. The many suggestions obtained from stimulating discussions with Dr. R. D. Hayes are gratefully acknowledged.

TABLE OF CONTENTS

TABLE OF CONTENTS (Continued)

LIST OF ILLUSTRATIONS

LIST OF ILLUSTRATIONS (Continued)

LIST OF ILLUSTRATIONS (Continued)

LIST OF ILLUSTRATIONS (Continued)

LIST OF TABLES

SUMMARY

The maximum achievable gain-bandwidth for transistor low-pass product amplifiers is currently about ω_T, the frequency at which the short circuit current gain in the common-emitter configuration is equal to one. As a means of achieving gain-bandwidths greater than ω_T, it was initially proposed to use the tunnel diode as an interstage element between common-base transistor stages. To this end, a class of tunnel diode-common-base transistor combinations was evolved and methods of investigating combination behavior were developed and validated. The investigation can be divided into seven related parts. These are:

1. Evolution of the class of tunnel diode-common-base transistor combinations.
2. Modeling for the active devices.
3. Development of theoretical methods to investigate combination behavior using the digital computer.
4. Computer studies.
5. Development of biasing techniques for the combinations.
6. Experimental verification.
7. A design example to illustrate combination use.

For several combinations with either six or seven normalized network variables, it was found that gain-bandwidths as large as ten times ω_T are obtainable. The introduction of the tunnel diode as an interstage element generates biasing and small signal stability considerations that are not present for ordinary interstages. In studying combination behavior,

only values of the network variables were allowed that corresponded to actual devices and also satisfied stability and biasing requirements.

The main disadvantage of the class of combinations was found to be the biasing requirements. One of the bias sources must have very low internal impedance, be capable of fine voltage adjustments, and exhibit good stability with regard to environmental changes and time. The investigation of other members of the infinite possibilities in the class could easily lead to further gain-bandwidth improvements.

CHAPTER I

INTRODUCTION

In a classical multiple-stage amplifier, the design for an overall frequency response can be made in terms of the pole-zero configurations of the individual stages since the input and output circuits of each stage are essentially isolated. The concept of gain-bandwidth is very useful and relatively simple to apply to the pentode amplifier. The equivalent small signal model for a single stage pentode amplifier with resistive load is given in Figure 1. The gain-bandwidth product

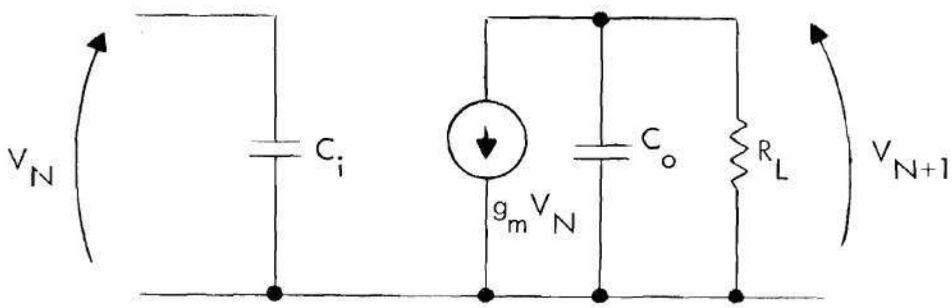

Figure 1. Single Stage Pentode Amplifier Equivalent Circuit.

(GBW) equals g_m/C_o, a constant, and thus gain may be easily traded for bandwidth and vice versa. The bandwidth limitation in cascaded pentode amplifiers is due to the presence of the tube and stray capacitances. For an N-stage amplifier, one may define a factor F, the GBW factor.

$$F = \frac{\text{MGBW}}{(\text{GBW of single RC interstage})} \tag{1.1}$$

where

$$\text{MGBW} = (\text{overall gain})^{1/N}(\text{overall bandwidth}) \qquad (1.2)$$

is the mean gain-bandwidth product. Now the gain-bandwidth of a single RC interstage is given by

$$\text{GBW}\Big|_{RC} = \frac{g_m}{C} \qquad (1.3)$$

where $C = C_o + C'$, and C' is the capacitance in the output due to the input of the next stage plus stray capacitance. The constancy and the form of the denominator of F normalizes the expression with respect to the tube parameters. This normalization allows one to easily compare various broadbanding techniques.

In a multiple-stage pentode amplifier, the stages are isolated and the only limitations on the frequency response are due to the input and output capacitances of each stage. This greatly simplifies the problem of finding the maximum value of F which can be obtained using one-port or two-port interstage networks. Bode[1] has shown that, for the optimum low-pass one-port network, $F_{max} = 2$ and that, for the optimum two-port low-pass network, $F_{max} = 4.94$. Hanson[2] has shown that, for the optimum two-port bandpass interstage network, $F_{max} = 5.06$.

In a transistor amplifier the input and output circuits of any stage are not isolated and thus analysis and design of the overall response must include the effects of interaction between stages. Although analysis is more complicated, the procedure is simple and direct. The main difficulty is in the development of design procedures. A design for an overall response may require a cut and try procedure involving complicated expressions with tedious computation.

For a single-stage common-emitter transistor circuit with a resistive load the small signal equivalent model is that shown in Figure 2. Here

$$C_i = \frac{1 + R_L C_{ob} \omega_T}{r_e' \omega_T} \tag{1.4}$$

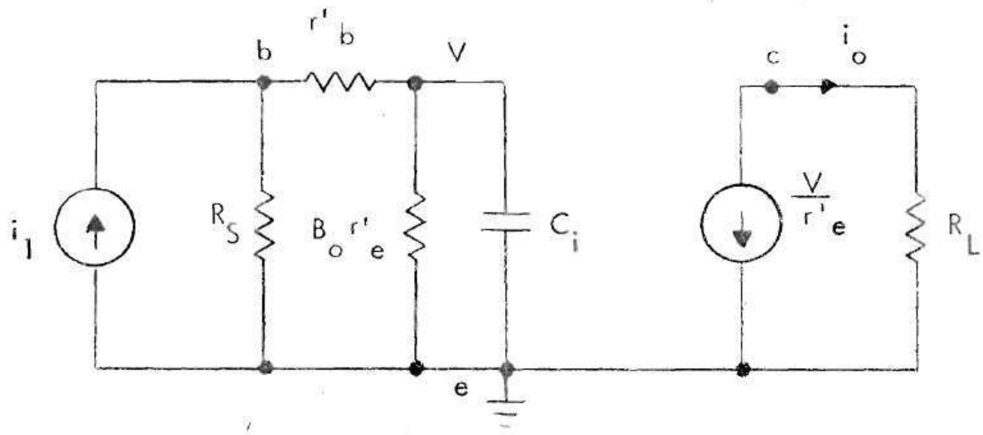

Figure 2. Small Signal Equivalent Circuit of Single Stage Transistor Amplifier with Resistive Load.

where C_{ob} is the capacitance measured between the collector and base with the emitter an open circuit to small signals. Routine analysis of this circuit yields the following results:[3]

$$\mathrm{GBW} = \frac{\omega_T R_s}{(1 + R_L C_{ob} \omega_T)(R_s + r_b')} \tag{1.5}$$

$$A_i(o) = \frac{i_o}{i_1} = \frac{-B_o R_s}{R_s + r_b' + B_o r_e'} \tag{1.6}$$

$$\omega_{3db} = \frac{\omega_\beta (R_s + r_b' + B_o r_e')}{(1 + R_L C_{ob} \omega_T)(R_s + r_b')} \tag{1.7}$$

where ω_T is the frequency at which $|h_{fe}| = 1$ and ω_β is the frequency at which $|h_{fe}| = \frac{B_o}{\sqrt{2}}$. For $R_L = R_s$ equation (1.8) gives the optimum value for R_s which maximizes the GBW.

$$R_s\Big|_{optimum} = \sqrt{\frac{r_b'}{C_{ob}\omega_T}} \tag{1.8}$$

A plot of GBW, normalized with respect to ω_T, versus ω_{3db}, normalized with respect to ω_β, has the form shown in Figure 3. With the above normalization the shape of the curve is more dependent on the load, or interstage, and less on the transistor parameters.

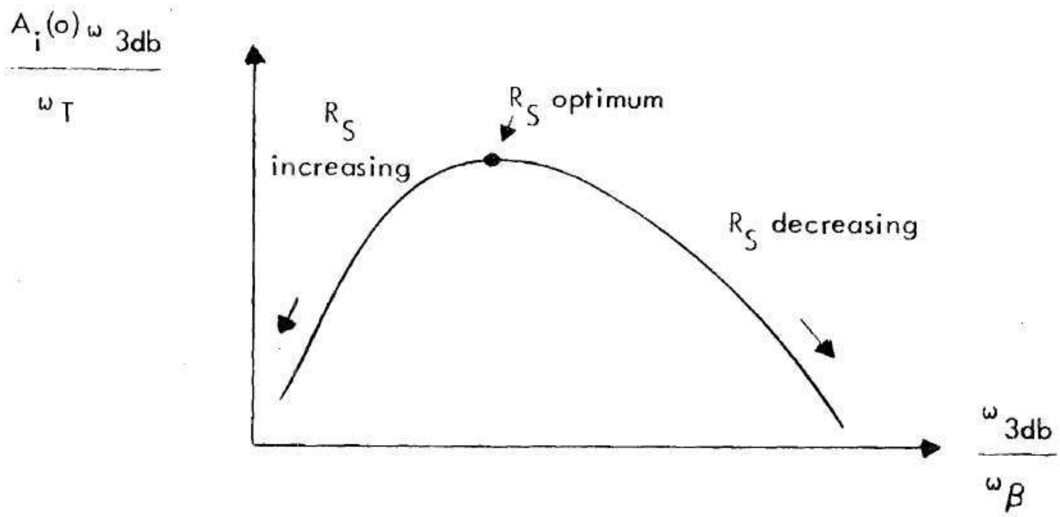

Figure 3. Normalized GBW of a Single Stage Transistor Amplifier with Resistive Load.

It is seen that, even for the simple stage with resistive load, GBW is not constant but is a function of the bandwidth of the stage. Thus there is no simple way to trade gain for bandwidth and in fact the GBW deteriorates greatly for either small or large bandwidths.

It is not useful therefore to define F for multiple-stage transistor amplifiers since neither the numerator, for a given broadbanding scheme, nor the denominator are constants. In an attempt to overcome this limitation, it is sometimes convenient to give a figure of merit, f_{max}, for the transistor which is the maximum frequency at which the device can be made to oscillate.

Since there are interaction effects and the limitations on frequency response are due to complex impedances and not simple capacitances, it is virtually impossible to derive the maximum possible GBW and the pole-zero configurations of the optimum interstages. Under certain restricted conditions one may use the resistance integral theorem together with network realizability requirements[4] to derive the following approximate expression for maximum GBW.

$$GBW_{max} \approx 2\varepsilon^{-n} \frac{1}{r_e' C_i} = 2\varepsilon^{-n} \frac{\omega_T}{1 + R_L C_{ob} \omega_T} \qquad (1.9)$$

The parameter n is greater than zero and is a function of β_o, r_e', C_i, and ω_{3db}; it is always chosen to maximize $A_i(0)$ while meeting necessary network realizability requirements. The necessary conditions for the derivation are the following: (1) Transistor behavior may be characterized by the unilateral model with Miller effect capacitance as shown in Figure 2. (2) r_b' in the model equals zero. (3) The interstage network is restricted to one-port networks.

Equation (1.9) is approximate and generally not very useful since the conditions used to derive it are unrealizable. That is, r_b' is not equal to zero and has a dominant effect on the frequency response in a broadband amplifier. The input is also not a simple RC parallel network because the load is not a simple resistance but a complex impedance.

To compare various broadbanding methods for transistor amplifiers, a curve of GBW normalized with respect to ω_T is usually plotted versus ω_{3db} normalized with respect to ω_β for an interior stage of an amplifier using the particular method of broadbanding. The calculation of GBW is made using the simplified unilateral hybrid-pi model with Miller effect capacitance. The comparison of the various broadbanding techniques is then made using a family of normalized curves where each curve is associated with a particular technique. A typical plot is shown in Figure 4.

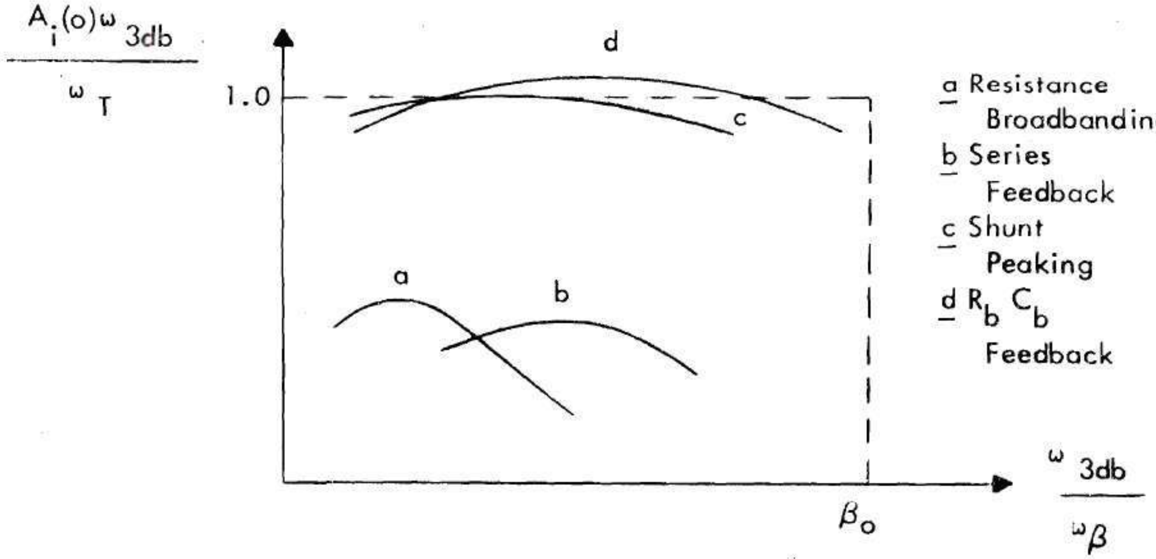

Figure 4. Comparison of Broadbanding Techniques for Transistor Amplifiers.

From Figure 4 it is apparent that curves <u>c</u> and <u>d</u> are much better than <u>a</u> and <u>b</u> and that <u>d</u> is best for large bandwidths. Several very important comments, however, must be made about the use of such curves. First, making use of the unilateral model is subject to considerable criticism. The unilateral model is derived assuming that the load impedance is a resistance, when in fact it is normally a complex impedance. The validity of using this approximation is very dependent upon the particular broadbanding technique. Second, these curves are not completely normalized curves. One assumes a set of typical values for f_T, β_o, $r_b{}'$, C_{ob}, $r_e{}'$ and plots a curve of $\frac{A_i(0)\omega_{3db}}{\omega_T}$ versus $\frac{\omega_{3db}}{\omega_\beta}$. If one assumes a different set of values the second curve will not have the exact shape as the first and may be somewhat different from the first curve. Although a family of curves for various broadbanding techniques is usually given as if it is a truly normalized and thus general plot, it is seen that the comparison is good only for particular sets of parameter values. To make general comparisons, one needs a set of families of normalized curves, each family of curves allowing a comparison of broadbanding techniques to be made for a given set of parameters. From a consideration of all the plots one could make judgements about which technique is best for most applications and which is best for a particular set of values. For example, consider the family of curves in Figure 4. If one reduces some parameter like C_{ob} by a factor of three, one would probably expect methods <u>c</u> and <u>d</u> still to be much better than <u>a</u> and <u>b</u> but <u>c</u> now might be better than <u>d</u> due to the parameter change.

Finally, even if the unilateral model were not used, the seven-element hybrid-pi model without excess phase shift is an approximation of the more exact ten-element model with the excess phase shift term. For large bandwidths the simpler model can introduce appreciable error. If one is using a feedback broadbanding technique, excess phase shift may cause instability.

Although it is difficult to compare broadband transistor amplifiers on GBW in general, this is not to imply that transistor amplifiers are incapable of as large a GBW as classical pentode amplifiers. In fact, f_{max}, the highest frequency at which the device can be used as an active two port, is much higher for transistors than pentodes and thus the GBW of transistor amplifiers can be much larger.

It can be seen from Figure 4 that the maximum GBW achievable with current transistor broadbanding techniques is about ω_T. Yet, the need often arises, as in digital test equipment, for amplifiers with MGBW greater than ω_T. In digital circuits, signal delays approach the nanosecond and sub-nanosecond region. Spacecraft landing systems with extremely small distance resolution will require amplifiers with MGBW greater than ω_T of the current transistors available. Too, there are research areas, such as oceanography, where amplifiers are used with such large bandwidths that only distributed amplification techniques can be used at the present time. From these examples it is seen that the development of transistor configurations having a MGBW greater than ω_T would be highly desirable.

As a means of achieving MGBW's greater than ω_T, it was decided to investigate a class of tunnel diode-common-base transistor combinations. Particular emphasis was placed on the gain, bandwidth, gain-bandwidth, and stability criteria for each configuration.

Tunnel diodes can be used as negative impedances over very wide bandwidths and are capable of low noise operation. The main disadvantage of tunnel diodes is the biasing and small signal stability problem.

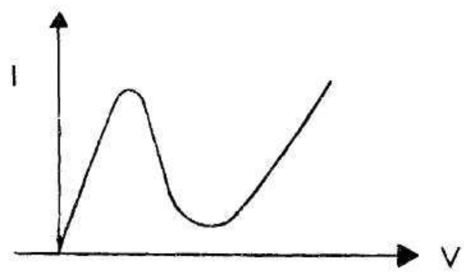

Figure 5. Tunnel Diode Volt-ampere Curve.

From Figure 5 it is obvious that the tunnel diode can be stably biased by a voltage source but not by a current source. The optimum point in the negative resistance region usually corresponds to a voltage across the device of 80 to 180 millivolts. Because of this, biasing a tunnel diode is usually difficult in the sense of, first, achieving a stable bias point and, secondly, achieving that point without adversely affecting the desired small signal response of the tunnel diode circuit.

The tunnel diode can be used in a low-pass amplifier in the simple series and parallel configurations as shown in Figure 6. The problem with these configurations is that if one stage does not provide sufficient gain there is no simple way to cascade stages. There can also be problems due to the dc voltage across R_L.

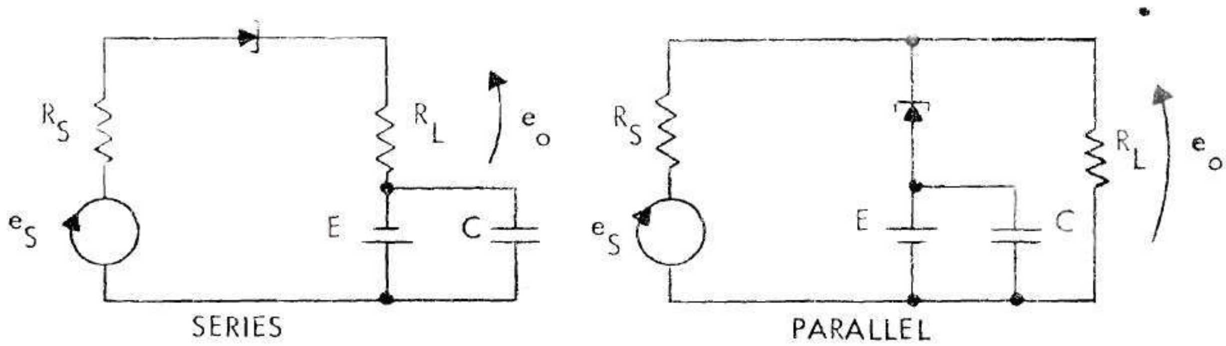

Figure 6. Simple Tunnel Diode Low-pass Amplifiers.

Attempts toward realizing multiple stage low-pass tunnel diode amplifiers have been directed towards either transmission or distributed amplifiers.[5,6] Such configurations have been impractical since they require exact values of the parameters for the different tunnel diodes and neglect the realization of the bias circuits which usually introduce many practical circuit limitations.

The common-base transistor configuration has an h_{21} current transfer function that is dominated by a pole at ω_α, the pole value for the dependent current generator in Figure 7. Now $\omega_\alpha \approx (1+m)\omega_T = (1+m)\beta_o\omega_\beta$ where m is a constant introduced by excess phase shift. Thus it

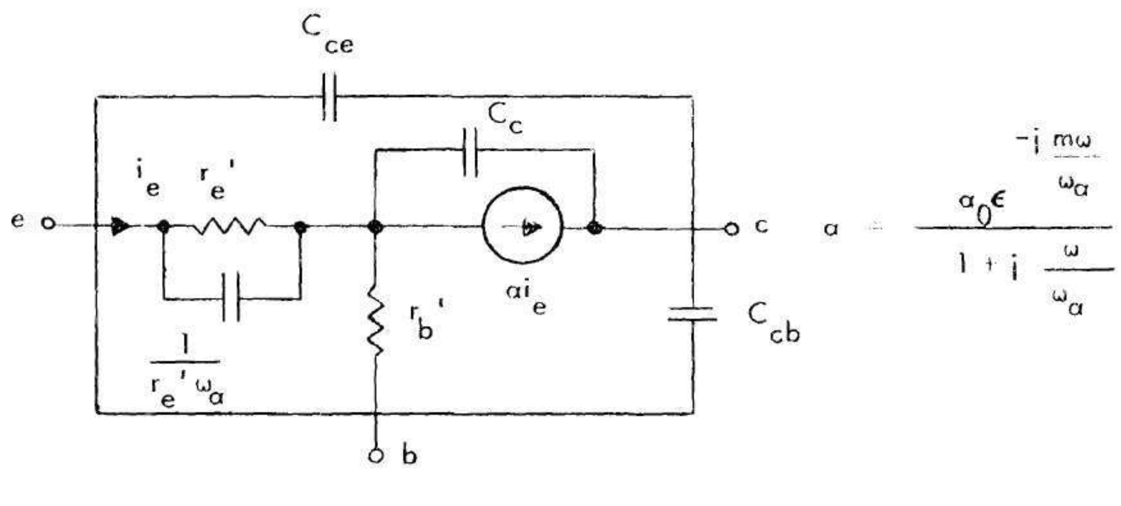

Figure 7. Small Signal Model for Transistor.

is seen that the dominant pole for the common-base current transfer is at least β_o times that for a common-emitter stage. Also, since normally $.6 \leq m \leq 1$ for a drift transistor, the dominant pole can be as much as $2\beta_o$ times the common-emitter dominant pole for a drift transistor common base stage.

Since the output impedance of a common-base stage is high and the input impedance is very low, some of the extrinsic elements, such as header capacitances, etc. can be more easily neglected in the common-base model than in the common-emitter model. The main disadvantage of the common-base stage is that, since the magnitude of the current gain is always less than one, one cannot achieve an overall voltage or current gain greater than one from an amplifier with cascaded common-base stages without using impedance transforming devices between stages. For a wideband amplifier the impedance converters must be very wideband, and standard converters such as transformers are unsatisfactory in that respect. As a solution to this problem, it was decided to use the tunnel diode as a very wideband impedance transforming device between common-base stages. This can be achieved by various series and parallel combinations of tunnel diodes and common-base transistor stages along with passive networks. Since both the poles of the tunnel diode impedance, and the pole on the current transfer function of the common-base stage occur at very high frequencies, it is reasonable to assume that such configurations are capable of providing very large gain-bandwidths as well as large bandwidths.

CHAPTER II

THE FORM OF THE TUNNEL DIODE-COMMON-BASE TRANSISTOR COMBINATIONS AND MODELING FOR THE ACTIVE ELEMENTS

The evolution of the form of the combinations can be illustrated with Figure 8. Assume that at low frequencies, the tunnel diode is to be used to provide current gain from a current source i_j to the current

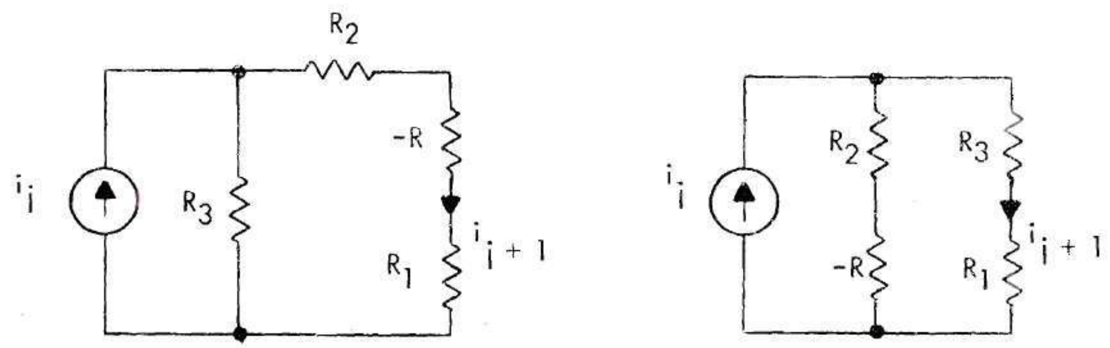

Figure 8. Tunnel Diode and Resistor Combinations to Provide Current Gain from i_j to i_{j+1}.

i_{j+1} flowing in a resistor R_1. The current source i_j represents the small signal output circuit of a common-base stage at low frequency. The resistor R_1 represents the low frequency small signal input impedance of a common-base stage. There are two ways of achieving the desired current gain. One is to place the tunnel diode in series with the common-base input as shown in the left half of Figure 8. The low frequency model for the tunnel diode biased in the negative resistance region is the resistor, -R. For this series combination along with R_2 and R_3 it is found

$$\frac{i_{j+1}}{i_j} = \frac{R_3}{R_1 + R_2 + R_3 - R} \tag{2.1}$$

For fixed R_1 and R it is seen that the current gain can be made to assume any value by the proper choice of R_2 and R_3.

The tunnel diode can also be placed in parallel with the common base input as shown in the right half of Figure 8. For the parallel combination which includes R_2 and R_3 it is found

$$\frac{i_{j+1}}{i_j} = \frac{-R + R_3}{R_1 + R_2 + R_3 - R} \tag{2.2}$$

For fixed R_1 and R, it is again seen that the current gain can be made to assume any value by the proper choice of R_2 and R_3. For wide bandwidths, the common base input and output and the tunnel diode have much more complex models. The resistors R_2 and R_3 may be part of more complex networks.

From a consideration of the requirements for low frequency current gain between common-base stages using the tunnel diode as an interstage element, bandwidth enhancement by the use of certain compensating networks, and sample calculations for a large number of tunnel diode-common-base combinations; the form of the combinations evolved to that given in Figure 9. Since the tunnel diode can provide current gain by being basically either in series or in parallel with the common base input, two forms of the combinations are given. The combination form given in the left half of Figure 9 is designated series since the tunnel diode along with associated N_i is basically in series with the common base input. The combination form given in the right half of Figure 9 is designated parallel since the tunnel diode along with associated N_i is basically in parallel with the

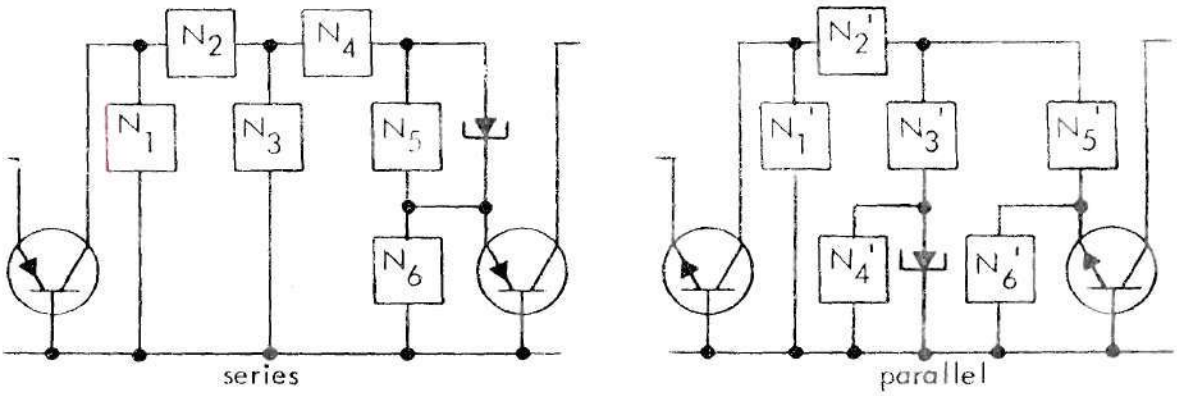

Figure 9. General Form of the Series and Parallel Combinations. Biasing Networks Omitted. Transistors Can Be NPN or PNP for Either Combination.

common base input.

The networks N_i are restricted to be RC one ports. The restriction to resistances and capacitances is due to the non-ideal behavior of actual inductors in wide bandwidth applications. Due to the nature of the transistor and tunnel diode models, the one port restriction allows one to combine various external and model elements into one element to reduce the number of variables for any given configuration. Since the simplest cases of the class of combinations have a relatively large number of variables and the amount of information to study a given configuration is a product function of the number of independent variables, this restriction is most useful.

Before any combination can be investigated, adequate models for the transistor in a common-base mode of operation and the tunnel diode must be derived. The modeling requirements are more stringent than normal in that the introduction of the tunnel diode as an interstage element between common-base stages creates stability problems that are non-existent for passive interstages.

The small signal model given in Figure 10 for the tunnel diode in the negative resistance region has been used from low frequency up through the lower range of microwave frequencies. Here R is the equivalent diode

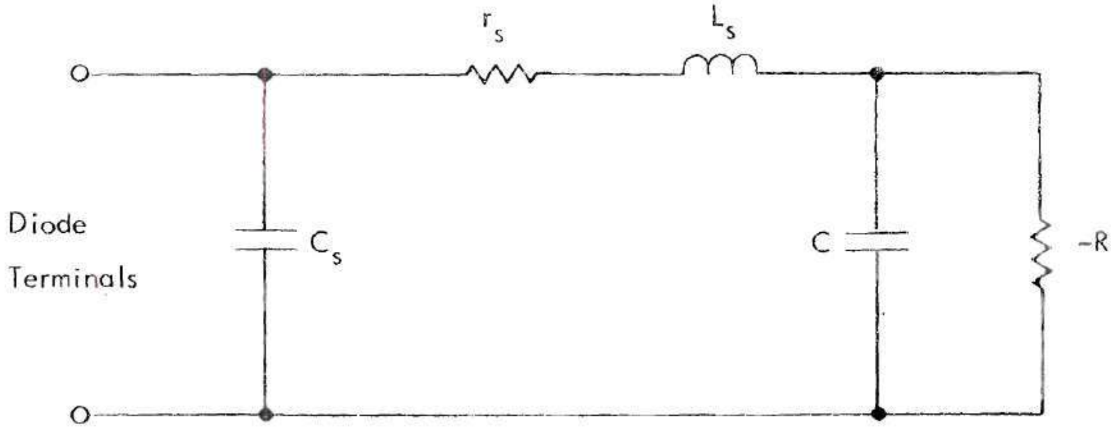

Figure 10. Equivalent Circuit for the Tunnel Diode.

resistance, C the junction capacitance, and r_s is the sum of the bulk resistance of the material and any lead contact resistance. L_s is the lead inductance and C_s the stray capacitance across the diode terminals. Since this model has been shown to be accurate over a wide range of frequencies, the remaining question is what simplifications can be made on the model in terms of the element values for currently available devices.

In Table 1 average or maximum values for the elements of the model of Figure 10 are given for tunnel diodes representing four different types of diode packages. Although the restrictions on the use of a given simplified model can be presented in a normalized fashion, the following question must now be considered. For what absolute range of frequencies are the modeling and methods of analysis to be valid? If the required conditions for the use of a simplified model are not met by actual devices in the desired frequency range, it would be imprudent to use the simplified

Table 1. Model Element Values for Four Differently Packaged Tunnel Diodes

Type	C_s pF	r_s max Ω	L_s avg nH	C max pF	R avg Ω	Comments
1N2969A	< 1	3	4	12	62.5	TO-18 package; general purpose use.
1N3715	< 1/2	3	0.5	8	53	miniature axial package; general purpose use.
TD-251A		7	1.5	.8	60	subminiature epoxy package; high speed logic and pulse circuits.
TD-405	0.1	6	0.1	.5	70	high performance microwave pill package.

model. The frequency range of interest is from dc up to frequencies where discrete element models are no longer valid. This upper frequency limit is largely a function of how small the circuit can be made and is about one to two GHz. for current technology.

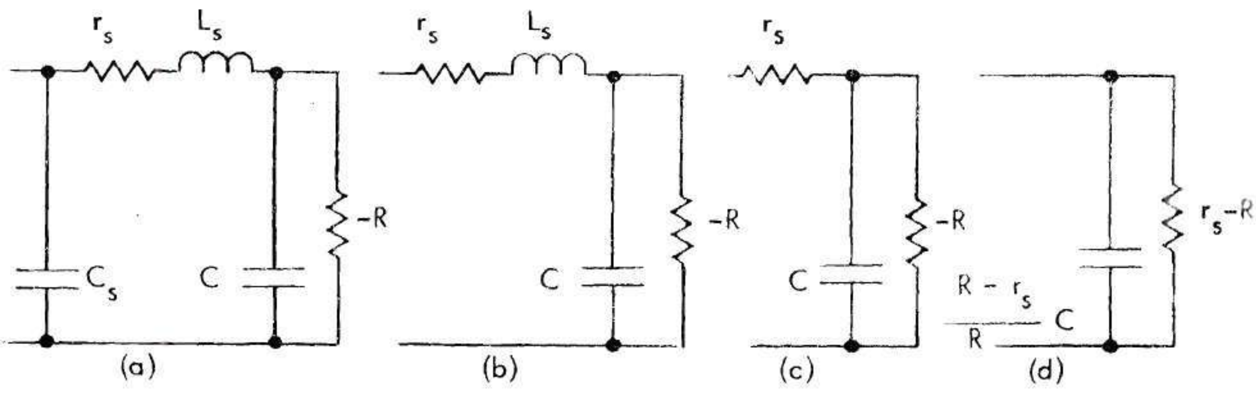

Figure 11. Set of Tunnel Diode Small Signal Models.

For the set of models in Figure 11, a computer program was used to compare the magnitudes and phases of the model impedances given the typical element values for many different tunnel diodes. For the frequency range of interest, it was found that there exist many tunnel diodes for which the simplified models (c) and (d) are quite adequate for frequencies up to 2/RC. Tunnel diodes in the TO-18 package are to be avoided since the above simplifications cannot be made for the majority of such diodes and there are other types of diode packages covering the same frequency range. In selecting a tunnel diode with a given R and C, one should choose the tunnel diode that has the smallest C_s and L_s consistent with other criteria such as cost, etc. An inexact way to estimate the sufficiency of models (c) and (d) for a given diode is to compare the magnitudes $1/C_s\omega$ and $L_s\omega$ with $\frac{R}{\sqrt{1 + (RC\omega)^2}}$ at the highest frequency of interest, ω_a. If $L\omega_a << \frac{R}{\sqrt{1+(RC\omega_a)^2}} << \frac{1}{C_s\omega_a}$ then model (c) should be adequate and if also $r_s << R$ then model (d) should be adequate. A more exact method would be the computer method previously discussed. It will be assumed in the following computer studies of various series and parallel combinations that model (c) or (d) is adequate for the tunnel diode for frequencies up to 2/RC. Such an assumption greatly aids in the reduction of the number of independent variables.

Basic modeling, model transformations, and simplifications for the transistor have been primarily in terms of common-emitter use up to some fraction of ω_T. The most common used model is the seven element hybrid-pi model given in Figure 12 which has been shown to conform fairly closely to measured behavior for $f \leq \frac{g_b' + g_\pi}{2\pi(C_\pi + C_\mu)} \equiv f_a$. Changing C_μ to C_{ob} in the model, where $C_{ob} = (C_\mu + C_{cb})$, for a transistor with relatively small r_b'

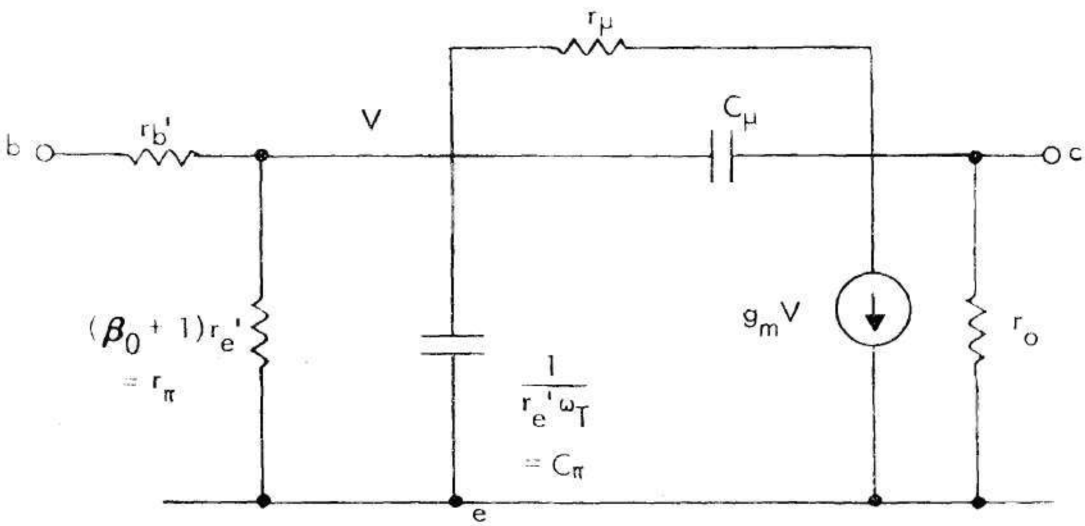

Figure 12. Seven Element Hybrid-pi Model for Transistor.

will increase somewhat its frequency range of use. The frequency f_T at which $|h_{fe}| = 1$, is normally at least five times f_a. For the transistor in a common-base mode of operation modeling for wideband operation should be accurate up to f_α, the pole frequency of the dependent current source in Figure 7. Since $f_\alpha \approx (1 + m)f_T$ where $.2 \leq m \leq 1$, it is seen that common-base models must be accurate over a much wider frequency range than their common-emitter counterparts. Because of the interest in achieving large amplifier bandwidths the transistor modeling in the common-base mode must also be good enough so that the previously mentioned stability problem may be accurately investigated. Excess phase shift, which has usually been neglected in the common-emitter models, must be included in the relatively wider bandwidth common-base models. Finally, model simplification in the common-base mode with regard to neglecting extrinsic elements can be expected to be somewhat different in that the intrinsic model impedance levels are different while the bandwidth of interest is larger.

For the reasons cited above it was decided to validate a common-base model for use up to ω_α and then effect some simplification on the model. For the transistor the model in Figure 13 can be derived from the physics of the device. Preliminary considerations in terms of inequalities

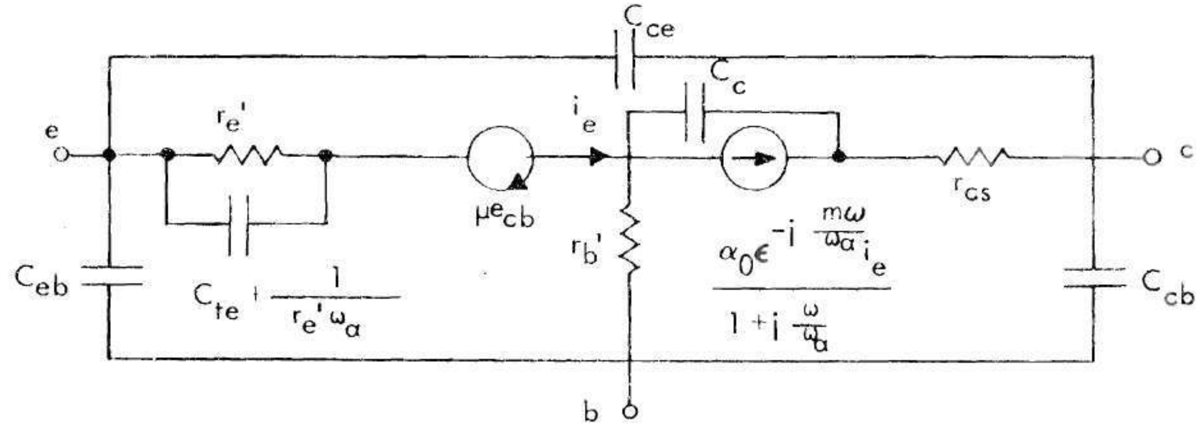

Figure 13. Small Signal Transistor Model $\omega \leq \omega_\alpha$.

derived from the physics showed that for a large class of transistors the slightly simplified model in Figure 14 should be accurate. To investigate the accuracy of the model in Figure 14 for $\omega \leq \omega_\alpha$ and hopefully make some simplifications the following study was conducted.

Due to the nature of the model it was decided to solve for the form of the h parameters and compare the theoretical variation of each h parameter with frequency to the measured variation for a set of actual devices. The measured data consisted of common-base y parameter measurements from dc to one gigahertz for several samples of both the 2N2415 and 2N918 type of transistor. For both of these f_α is around one GHz. These measured data were graciously provided by Texas Instruments Incorporated. Common-emitter y-parameter measured data over the same frequency range were available for several devices. Due to the presence of a fourth lead which is grounded according to the mode of operation, however, the common-emitter y-parameters cannot be transformed to the common-base y-parameters and the above measure-

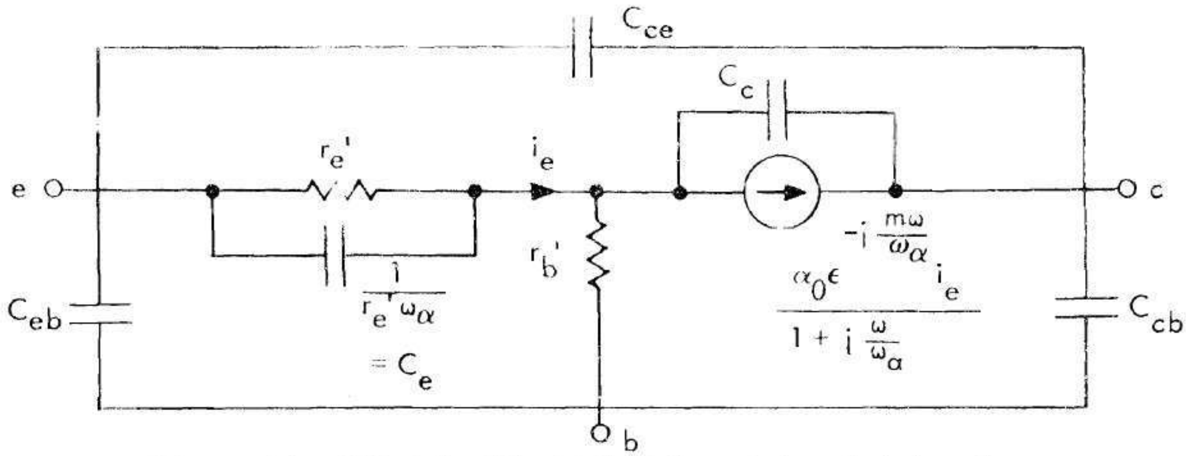

Figure 14. Slightly Simplified Transistor Model $\omega \leq \omega_\alpha$.

ments were requested. From the measured y-data the experimental values for each h-parameter were calculated.

To calculate the form of h_{11_b} from the model in Figure 13, $\varepsilon^{-j\frac{m\omega}{\omega_\alpha}}$ was approximated by the first two terms of its series expansion. From Table 2 it is seen that the approximation is fairly accurate to about $.6\,\frac{\omega_\alpha}{m}$. For a diffusion transistor $m = 0.2$ and for a drift transistor a typical value of m would be about 0.6. Thus the $(1 - j\,\frac{m\omega}{\omega_\alpha})$ approximation can be used for $\omega \leq \omega_\alpha$, the original frequency limit on the model.

Table 2. Comparison of Magnitude and Phase of $\varepsilon^{-j\frac{m\omega}{\omega_\alpha}}$ and $(1 - j\,\frac{m\omega}{\omega_\alpha})$

Frequency	Mag. $\varepsilon^{-j\frac{m\omega}{\omega_\alpha}}$	Mag. $1 - j\,\frac{m\omega}{\omega_\alpha}$	Angle-degrees $\varepsilon^{-j\frac{m\omega}{\omega_\alpha}}$	Angle-degrees $1 - j\,\frac{m\omega}{\omega_\alpha}$
$.1\ \omega_\alpha/m$	1	1.005	5.73	5.6
$.2\ \omega_\alpha/m$	1	1.02	11.46	11.3
$.5\ \omega_\alpha/m$	1	1.12	28.65	26.6
$.6\ \omega_\alpha/m$	1	1.17	34.4	31
$1\ \omega_\alpha/m$	1	1.415	57.3	45

For a large number of high frequency transistors it is found from the manufacturers' data sheets that $\frac{1}{r_b'C_c} >> \omega_\alpha$. If this condition is assumed, then the h_{11_b} expression is simplified and can be realized as a passive network. For the above reasons this inequality was used in the h parameter derivations. Its use also allowed simplifications in the form of the other three h-parameters.

Using these approximations one finds by routine analysis that

$$h_{11_b} = \frac{r_e' + (1-\alpha_o)r_b' + (1+\alpha_o m)r_e'C_e r_r's}{1 + r_e'C_e s} \quad \frac{1}{(C_{eb} + C_{ce})s} \tag{2.3}$$

The equivalent network for such a function is given in Figure 15.

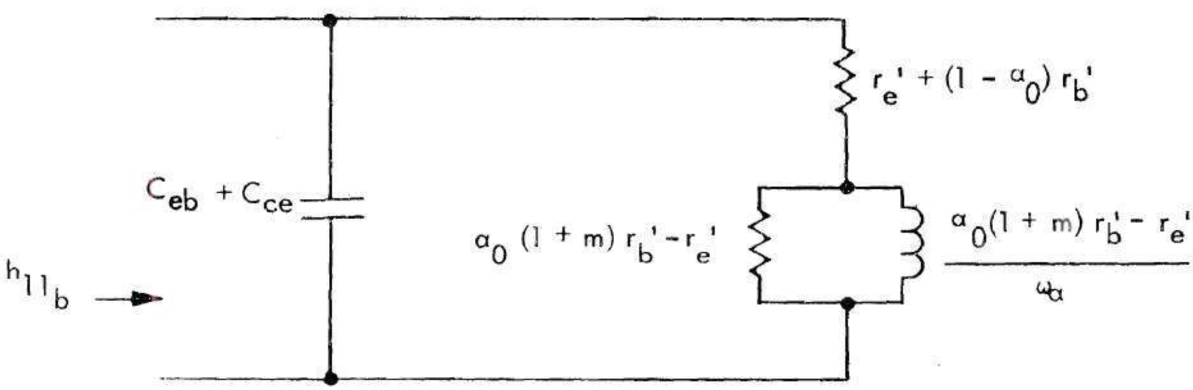

Figure 15. Network for Theoretical h_{11_b}.

For many transistors the element values in the above network will be such that one is able to neglect $C_{eb} + C_{ce}$ in the range $0 \leq \omega \leq \omega_a$. For the 2N2415 and 2N918 consideration of the data sheets indicate such an approximation should be valid.

If the equivalent circuit derived really corresponds to actual transistor behavior and if $C_{eb} + C_{ce}$ can be neglected in the desired frequency range, then one can add the real and imaginary parts of a parallel RC impedance to the actual values of h_{11_b} such that the real part of the series combination of the two impedances is constant and the imaginary part is zero over the given frequency range. This is illustrated in Figure 16.

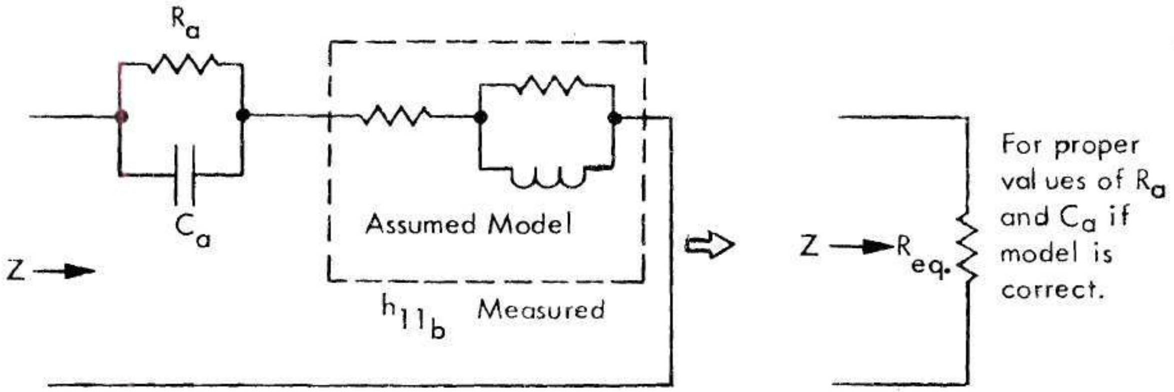

Figure 16. Illustration of Network Properties Used to Compare Experimental and Theoretical h_{11_b}.

The validity of the model for h_{11_b} was verified analytically using a computer program. For a set of values of R_a and C_a, the real and imaginary parts of the series combination of the RC network and the measured h_{11_b} for a given transistor were evaluated for a set of discrete frequencies. By varying R_a and C_a it was ascertained that there existed values of R_a and C_a for each transistor such that the combined series impedance was approximately a resistance for ω less than one GHz. for both the 2N2415 and the 2N918 transistors. The results for the best value of R_a and C_a for one of the 2N2415 transistors are given in Figure 17. Considering the accuracy of high frequency measured y-parameters and the fact that only discrete values of R_a and C_a were used, the correspondence between the predicted and calculated values of Z is within the tolerance of measurement

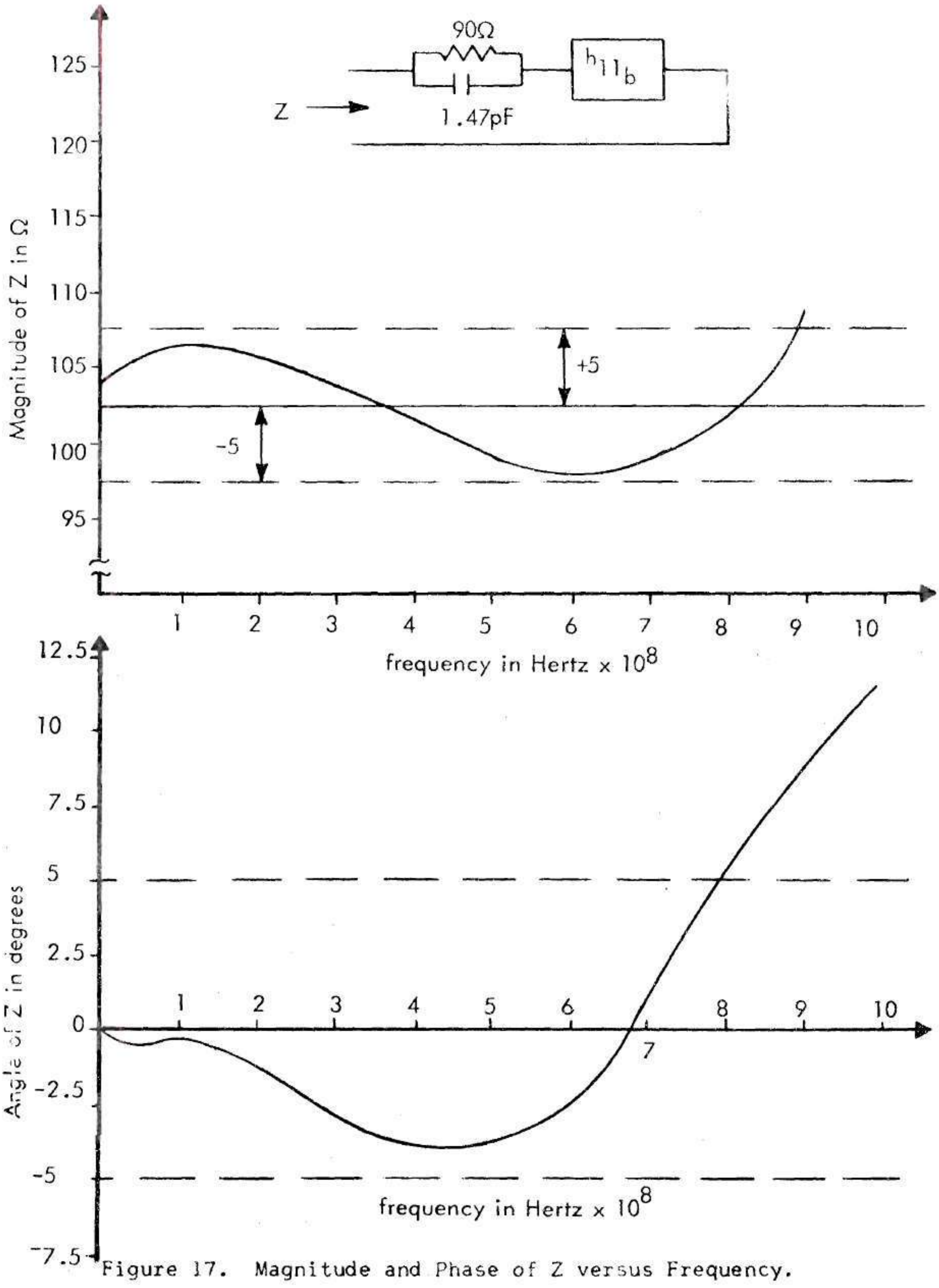

Figure 17. Magnitude and Phase of Z versus Frequency.

accuracy.

Again assuming $\frac{1}{r_b'C_c} > \omega_\alpha$ and $\varepsilon^{-j\frac{m\omega}{\omega_\alpha}} \approx 1 - j\frac{m\omega}{\omega_\alpha}$ it is found by standard analysis techniques that

$$h_{21} = \frac{-\alpha_o \varepsilon^{-j\frac{m\omega}{\omega_\alpha}}}{1 + (r_e'C_e + [r_e' + (1-\alpha_o)r_b']C_T)s + (1+\alpha_o m)r_e' r_b' C_e C_T s^2} \tag{2.4}$$

where

$$C_T = C_{eb} + C_{ce} \tag{2.5}$$

If

$$1 \gg \left| [r_e' + (1-\alpha_o)r_b']C_T\omega_\alpha + j(1+\alpha_o m)r_b'C_T\omega \right| \tag{2.6}$$

then for $\omega \leq \omega_\alpha$ equation (11) reduces to

$$h_{21} \approx \frac{-\alpha_o \varepsilon^{-j\frac{m\omega}{\omega_\alpha}}}{1 + \frac{s}{\omega_\alpha}} \tag{2.7}$$

The above inequality is dependent upon C_T and in essence states that if C_T is small enough then equation (2.7) is valid for h_{21}. The following values for C_{be} and C_{ce} have been given for the transistor in the commonly used TO-5 and TO-18 cans.[7] For a transistor in the TO-5 can $C_{eb} \approx 0.3$ pF and $C_{ce} \approx 0.6$ pF. For the TO-18 package $C_{eb} \approx 0.05$ pF and Cce $\approx$ 0.75 pF. Thus C_T approximately equals 0.85 pF for both types of package. Substitution of typical values in the inequality indicates that often equation

(2.7) can be used but that the inequality begins to fail as f_α approaches one GHz. It should be noted, however, that in order to use lumped element theory for an amplifier with a bandwidth approaching one GHz. that hybrid construction techniques would probably be required. The transistor chip would be bonded directly to the rest of the circuit without encapsulation. Thus C_T would be greatly reduced.

The correspondence between equation (2.7) and measured h_{21} for the 2N2415 and 2N918 transistors was found to be adequate. The main difficulty encountered was that $|h_{21}| = \frac{|Y_{21}|}{|Y_{11}|} \approx 1$ for frequencies much less than the ω_α break frequency. Since the experimental $|h_{21}|$ was found by the division of two nearly equal magnitudes, measurement inaccuracy can cause $|h_{21}|$ to vary above and below α_o at the lower frequencies. This is illustrated in Figure 18.

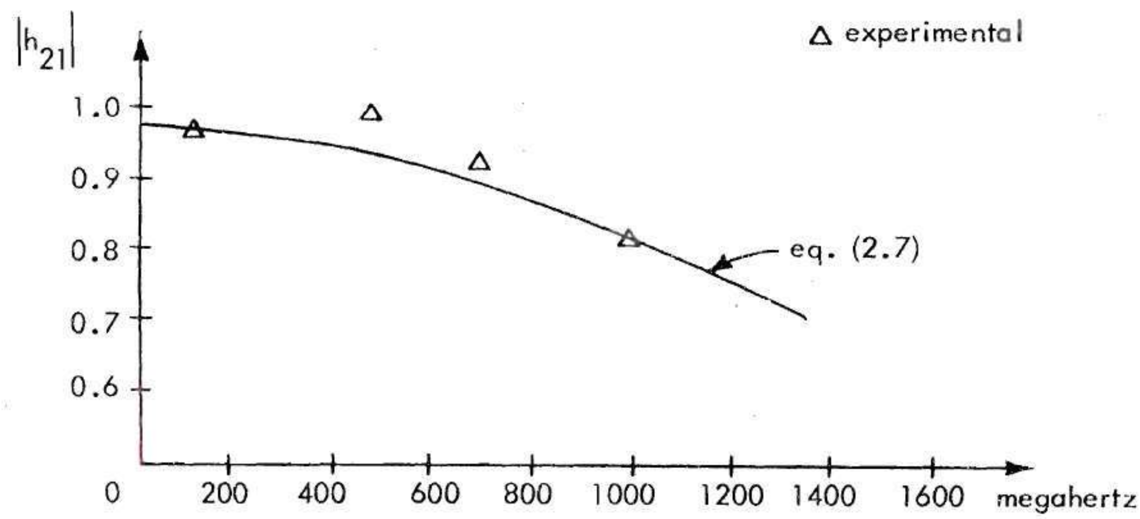

Figure 18. Comparison of Experimental and Theoretical $|h_{21}|$ for a 2N2415 Transistor.

To calculate h_{12} the simplified model in Figure 19 is used, in that the feedback current through C_{ce} is primarily determined by its own relatively large impedance. Standard analysis yields

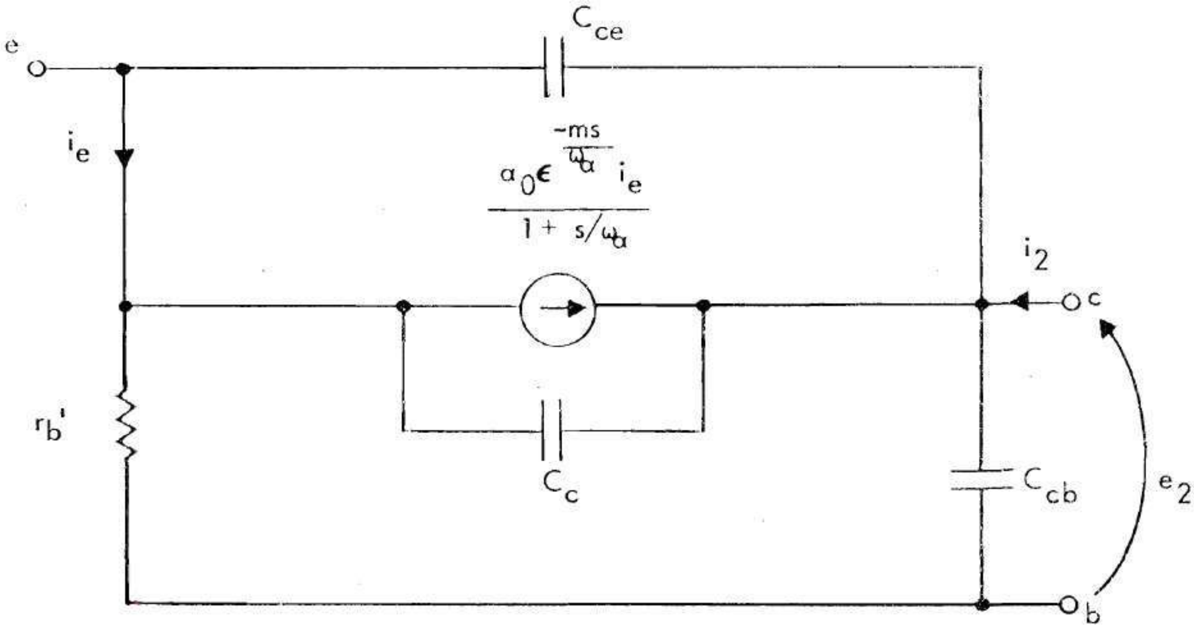

Figure 19. Simplified Model for h_{12} and h_{22} Calculation.

$$h_{12} \approx \frac{\left[\dfrac{(1-\alpha_o)C_{ce}\omega_\alpha s + (1+\alpha_o m)C_{ce}s^2}{s+\omega_\alpha}\right] + sC_c}{\left[\dfrac{(1-\alpha_o)C_{ce}\omega_\alpha s + (1+\alpha_o m)C_{ce}s^2}{s+\omega_\alpha}\right] + sC_c + g_b'} \tag{2.8}$$

The expression can be simplified by consideration of the term in brackets. For $\omega \leq (1-\alpha_o)\omega_\alpha$ the expression in brackets is approximately $(1-\alpha_o)C_{ce}s$ and equation (2.8) becomes

$$h_{12} \approx \frac{[1-\alpha_o)C_{ce} + C_c]s}{[(1+\alpha_o)C_{ce} + C_c]s + g_b'} \tag{2.9}$$

Now C_{ce} and C_c usually have values of about the same order of magnitude so that $C_c >> (1 - \alpha_o)C_{ce}$. Equation (2.9) then becomes

$$h_{12} \approx \frac{C_c s}{C_c s + g_b'} \tag{2.10}$$

and assuming $\frac{1}{r_b' C_c} >> \omega_\alpha$ this becomes

$$h_{12} \approx r_b' C_c s \tag{2.11}$$

Thus it is seen that for frequencies much less than ω_α the term in brackets in equation (2.8) can be completely neglected and h_{12} assumes a very simple form. Although this term increases with frequency, it should be verified whether the increase is slow enough so that the simplified expression of equation (2.11) can be used for $\omega \leq \omega_\alpha$. A typical plot of experimental h_{12} is shown in Figure 20. It is seen that the magnitude is approximately a linear function of frequency as predicted by equation (2.11) and that the phase is near the ninety degree value predicted by equation (2.11). Due to the small size of h_{12} experimental discrepancy is easily caused by measurement error. The correspondence between equation (2.11) and measured values of h_{12} is considered adequate for the set of transistors investigated.

To calculate h_{22} the model in Figure 19 is again used. Standard analysis techniques yield

$$h_{22} = \frac{(A + sC_c)g_b'}{A + g_b' + sC_c} + C_{cb}s \tag{2.12}$$

where

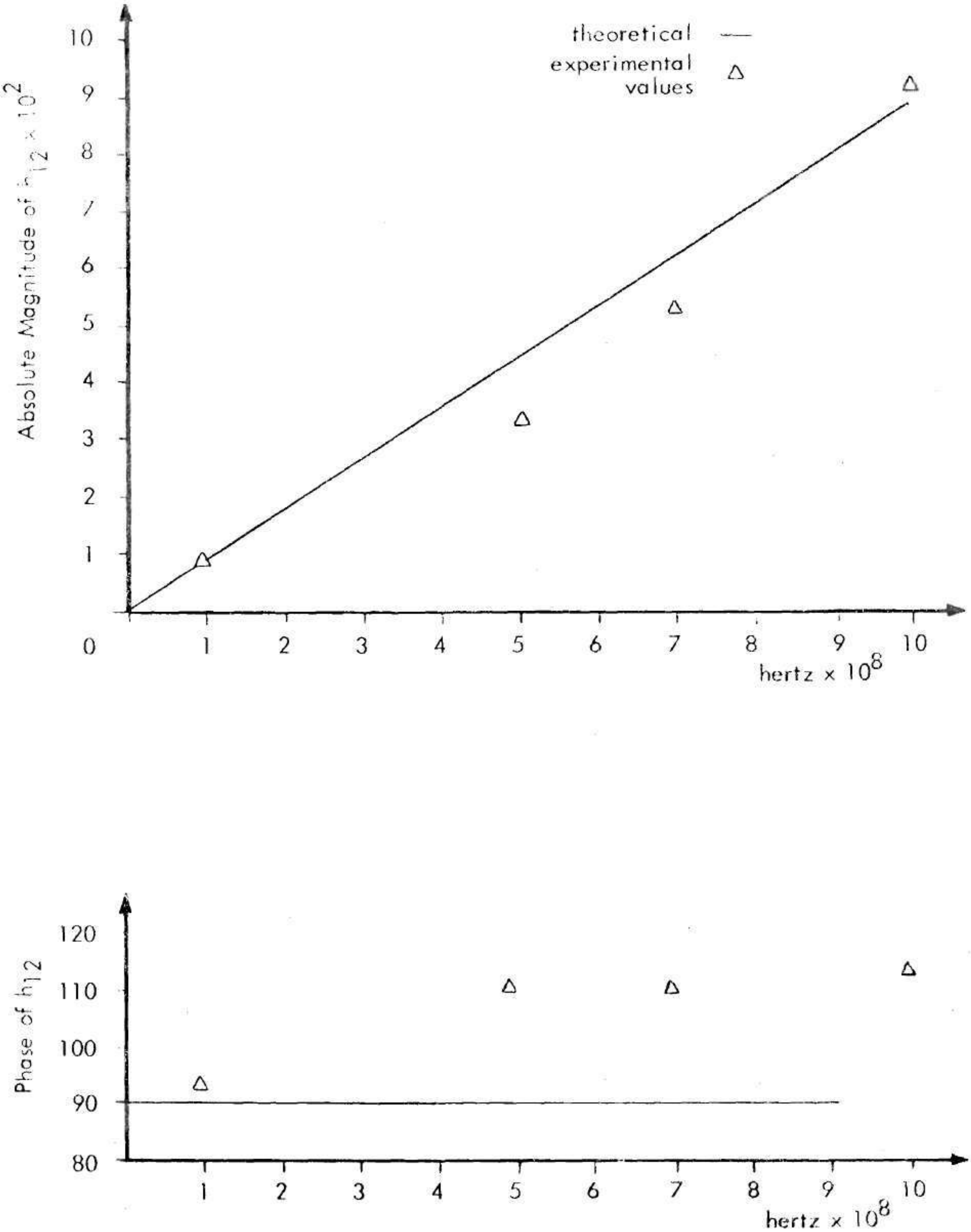

Figure 20. Comparison of Experimental h_{12} and Equation (2.11) for a 2N2415 Transistor.

$$A = \frac{(1 - \alpha_o)C_{ce}\omega_\alpha s + (1 + \alpha_o m)C_{ce}s^2}{s + \omega_\alpha} \tag{2.13}$$

is the same term appearing in brackets in the h_{12} expressions. As previously discussed, A can be neglected at the lower frequencies. Equation (2.12) then reduces to

$$h_{22} \approx \frac{g_b' C_c s}{g_b' + C_c s} + C_{cb}s \tag{2.14}$$

Again assuming $\frac{1}{r_b' C_c} >> \omega_\alpha$ equation (2.14) becomes

$$h_{22} \approx (C_c + C_{cb})s \tag{2.15}$$

A typical plot of h_{22} is given in Figure 21. It is seen that the imaginary part of h_{22} is essentially of the form $A\omega$ as predicted by equation (2.15).

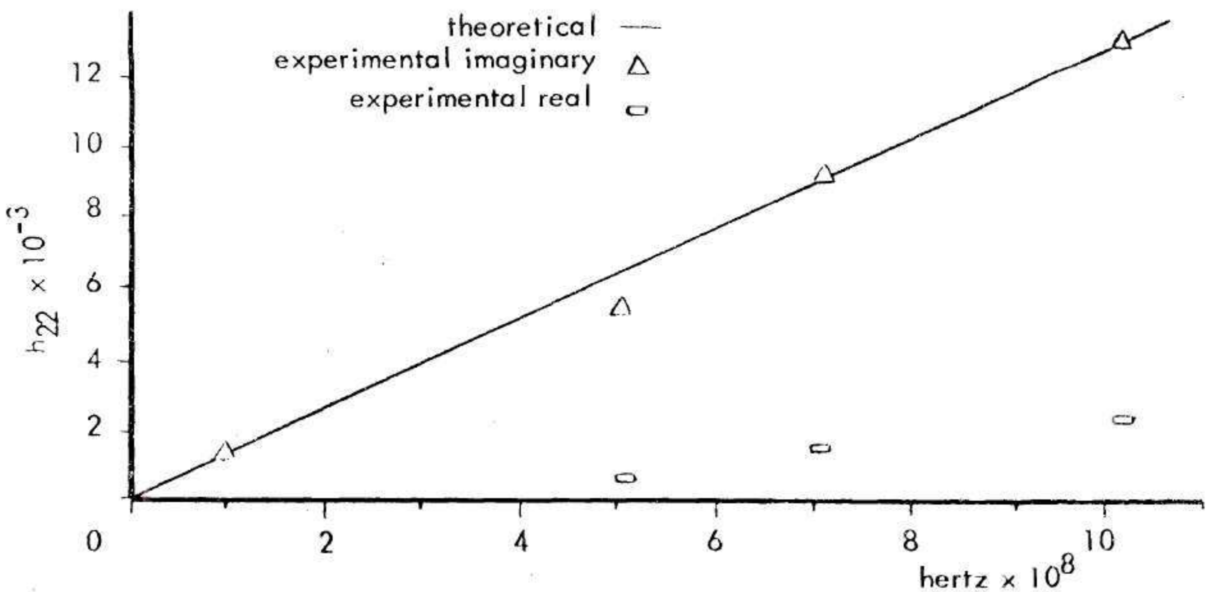

Figure 21. Measured h_{22} for a 2N2415 Transistor.

There is, however, a small real part. In terms of typical admittances that would be in parallel with h_{22} in a circuit it was ascertained that the expression given by equation (2.15) for h_{22} should be adequate. It should be noted that the real part is probably caused by the collector bulk resistance, r_{cs}, of Figure 13. If this real part is significant then r_{cs} must be included in the model.

By comparison of experimental data with theoretical expressions incorporating various simplifications it is seen that the model given in Figure 14 should be adequate for $\omega \leq \omega_\alpha$. The model in h-parameter form is given in Figure 22 for the inequalities listed. This form of the model will be seen to be of significant value.

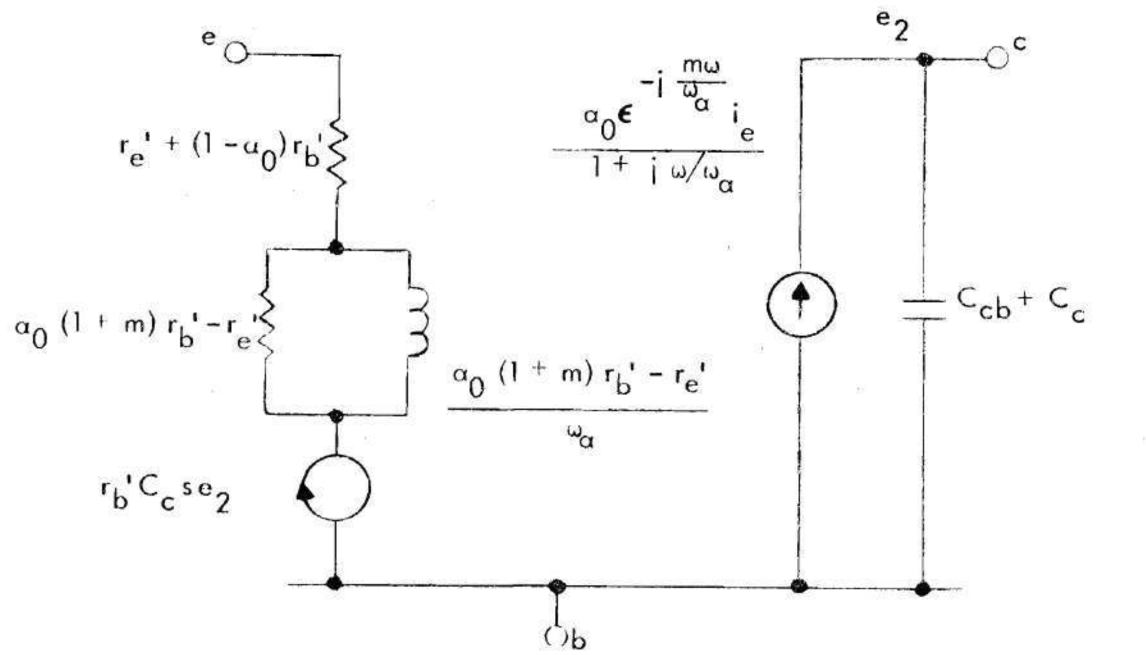

$$\frac{1}{r_b' C_c} >> \omega_\alpha \qquad 1 > \left| \left[r_e' + (1 - \alpha_0) r_b' \right] C_T \omega_\alpha + j \, (1 + \alpha_0 m) \, r_b' C_T \omega \right| \qquad \omega \leq \omega_\alpha$$

Figure 22. Common Base h Model.

CHAPTER III

THEORETICAL INVESTIGATION OF TUNNEL DIODE-COMMON-BASE TRANSISTOR COMBINATION BEHAVIOR

A method for theoretically investigating the class of combinations delineated in Chapter II will now be presented. For any combination one can predict what values of normalized bandwidth and gain-bandwidth are possible and the variance of these with the independent variables. Stability is also predicted. The ranges of the independent variables are restricted in order to meet biasing requirements and stability considerations.

Model Choice, Simplification, and Unilateralization

For the tunnel diode, the simplified models (c) and (d) in Figure 10 were found to be accurate to about $\frac{2}{RC}$ for a large class of tunnel diodes. These models are repeated in Figure 23. It will be assumed in the theoretical investigation that the tunnel diode will be chosen such that model (c) or

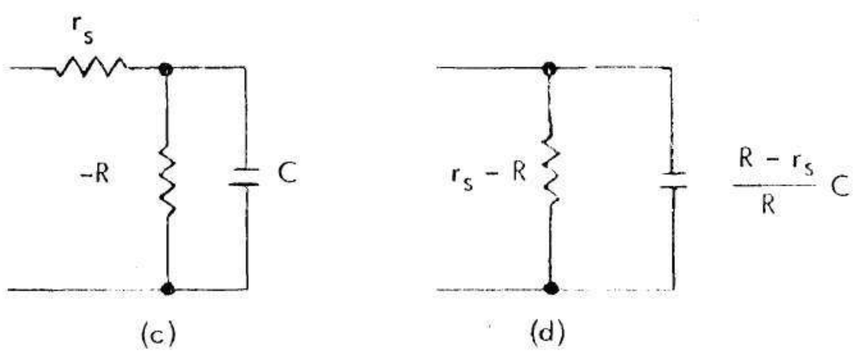

Figure 23. Simplified Tunnel Diode Small Signal Models.

(d) can be used for the tunnel diode.

Comparison of experimental and theoretical h-parameter behavior in Chapter II indicated that the model given in Figure 14 should be adequate for the transistor. For convenience this model is repeated in Figure 24. To investigate the effects of a broadbanding technique on a two port active

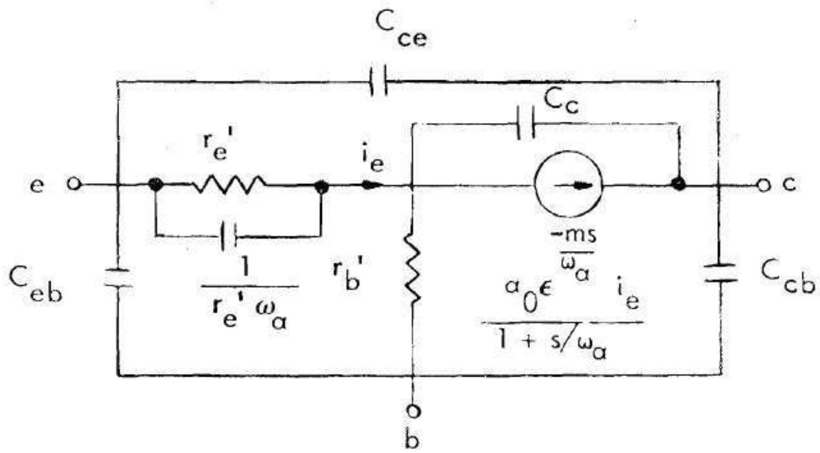

Figure 24. Common-base Transistor Model $\omega \leq \omega_\alpha$.

device, one is normally forced to unilateralize the device model. The feedback is a function of the load impedance which can assume many forms. To estimate the circuit behavior for any load, it is standard procedure to either omit the feedback elements in the model, assume the load has a constant form, or derive a unilateral model incorporating the effects of feedback for the form of the load at low frequencies. The first method is illustrated in Figure 25. For the common-emitter-common-base combination shown, the form and element values of the small signal models are such that the effects of feedback through the combination can be neglected. One uses a unilateral model for the combination.

The second method is illustrated in Figure 26. The effect of the

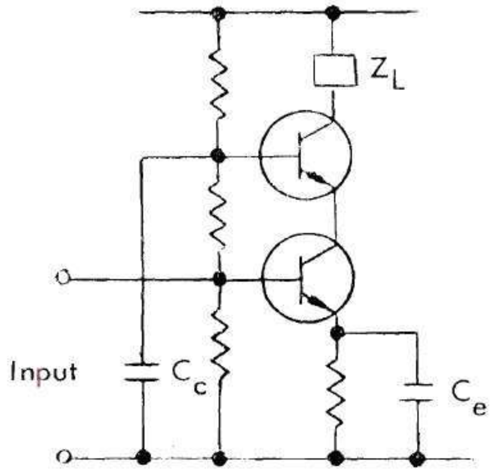

C_c and C_e large. The impedance of both may be considered a short circuit at moderate frequencies.

Figure 25. Common-emitter-common-base Transistor Combination.

resistive shunt feedback is to greatly reduce the input impedance of each stage. Although this impedance is a complex function of frequency, it is small enough in comparison to the impedance of the parallel combination of R_b and C_b that the load is considered to be this combination. The analysis for the gain equations of an interior stage is thereby greatly simplified.

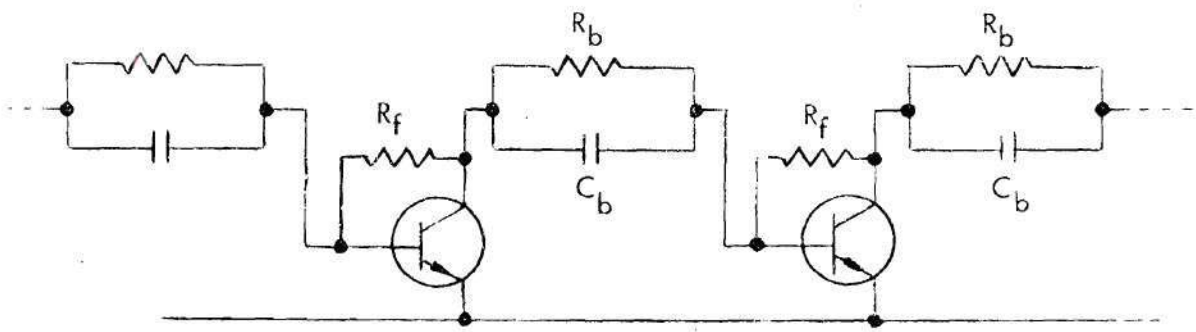

The third method is illustrated in Figure 27. For common-emitter stages a Miller effect model is formed by considering what resistive value the load assumes as $\omega \rightarrow 0$. Coupling capacitors and emitter bypass capacitors are assumed to be short circuits for this calculation. This

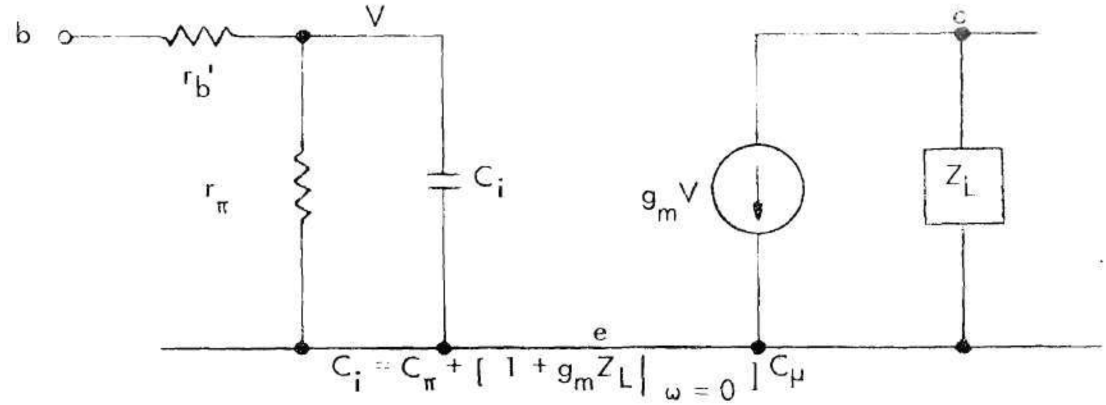

Figure 27. Unilateral Hybrid-π Model for Transistor.

model is then used to study the particular broadbanding technique. This is the most commonly used method and several limitations on its accuracy have already been discussed in Chapter I. To derive general gain equations, however, one is forced to use method three if methods one or two do not apply.

For the model in Figure 24, it is seen that C_{ce} and r_b' provide feedback from the output to the input terminals. The model in this form does not easily allow conversion to an approximate unilateral model. In Figure 28 it is seen that unbypassed emitter resistance in a common-emitter stage can be absorbed into the h-π model without any loss of frequency range. This is accomplished by finding the normal-π model for the circuit in dashed

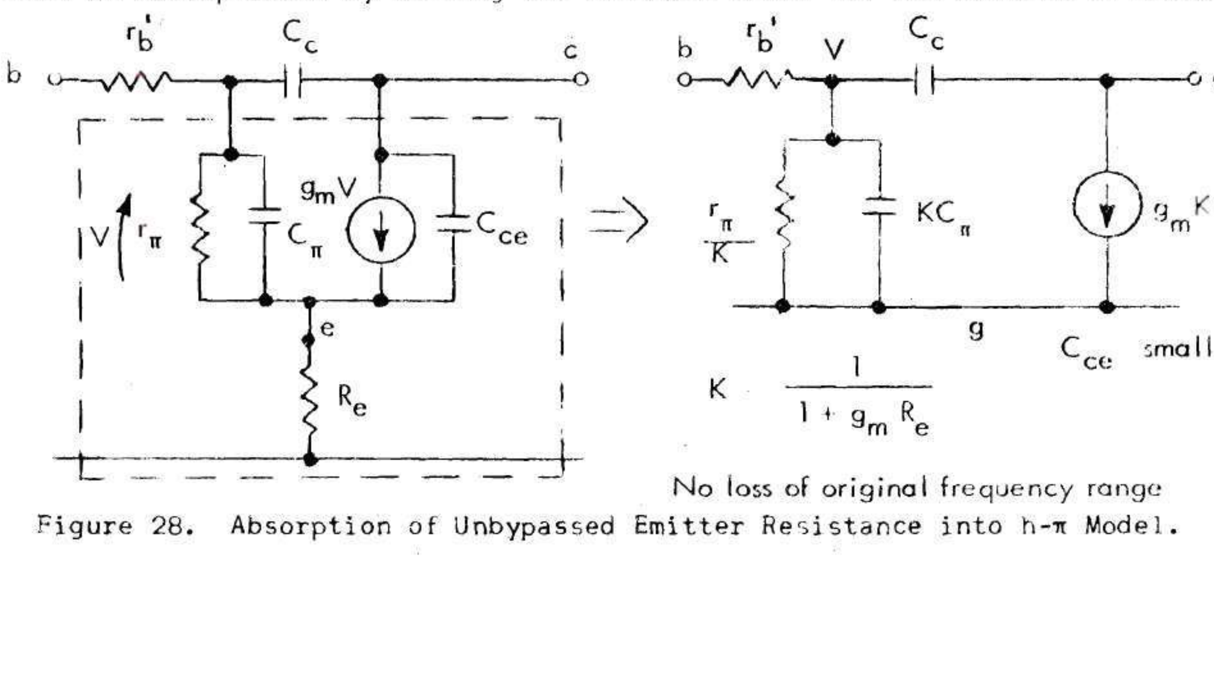

Figure 28. Absorption of Unbypassed Emitter Resistance into h-π Model.

lines. The large similarity between the circuit in the dashed lines and the model in Figure 24, when C_{be}, C_{ce}, and C_{cb} are neglected, would tend to imply that such a procedure would be useful for this model. The model is redrawn in Figure 29 to illustrate this similarity. The only difference is in the dependent current generator. The results of such an

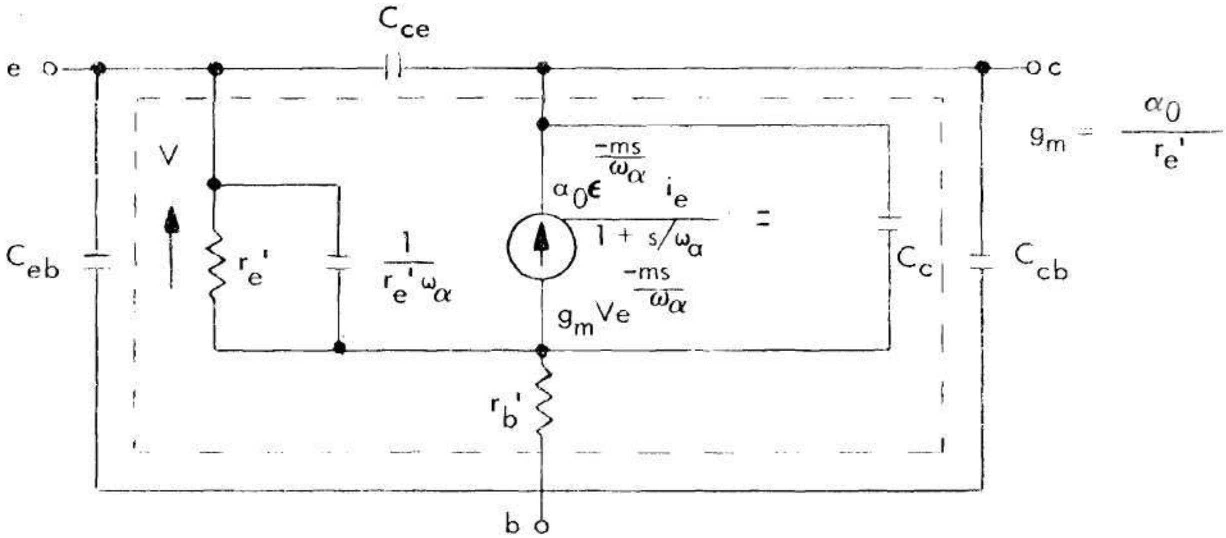

Figure 29. Common-base Model Redrawn to Illustrate Similarity with Part of Figure 28.

analysis, however, are disappointing. The parameter r_b' cannot be absorbed into a unilateral form unless the model frequency range is greatly reduced.

After the application of other such transformations, it was ascertained that a unilateral model could be most easily obtained from the model in h-parameter form. This model was given in Figure 22 and required that the transistor parameters meet two inequalities. These inequalities were imposed to avoid undue complexity in the model and to make the model have a realizable network form. Since a large class of transistors meet these conditions, it will be assumed in the theoretical studies that the transistor parameters satisfy these inequalities.

In Figure 30 the h model is given with a load Z_L. If an approximate equivalent passive circuit can be derived for $r_b'C_c s e_2$, the model will be

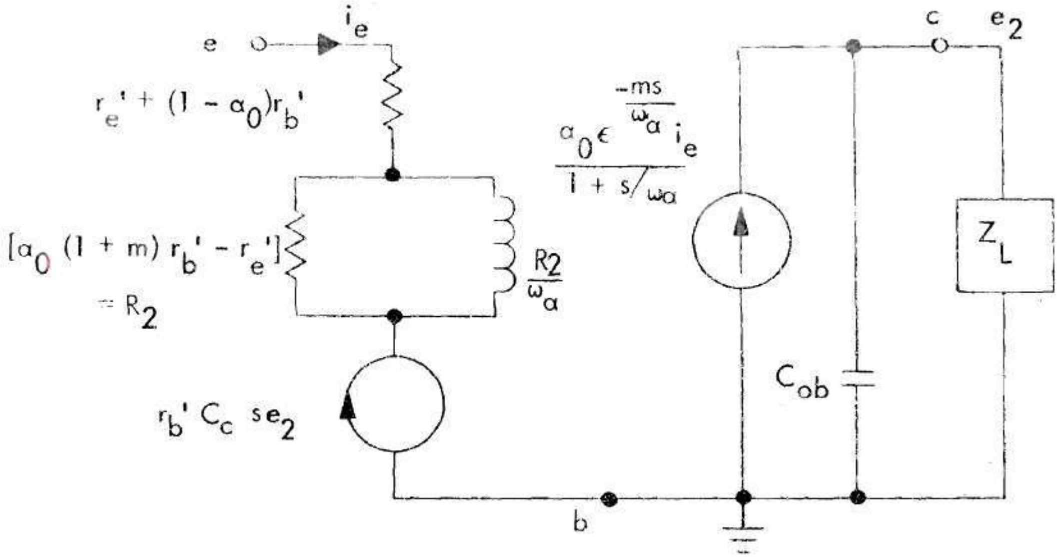

Figure 30. Common-base h Model with Load Z_L.

unilateralized. This is done by application of method three previously discussed. As ω approaches zero, Z_L approaches some resistive value R. For this condition

$$e_2 = \frac{\alpha_o \epsilon^{-\frac{ms}{\omega_\alpha}} R}{1 + s/\omega_\alpha} i_e \tag{3.1}$$

The equivalent impedance Z_{eq} which is reflected into the input equals $\frac{r_b' C_c s e_2}{i_e}$ and for this case

$$Z_{eq} = \frac{\alpha_o R r_b' C_c s \epsilon^{-\frac{ms}{\omega_\alpha}}}{1 + s/\omega_\alpha} \tag{3.2}$$

The right side of equation (3.2) is not realizable as a passive network. Since the expression is exact only at the lower frequencies, the equation is simplified by omitting the excess phase shift term. Now

$$Z_{eq} \approx \frac{\alpha_o R r_b' C_c s}{1 + s/\omega_\alpha} \tag{3.3}$$

which has the equivalent network shown in Figure 31.

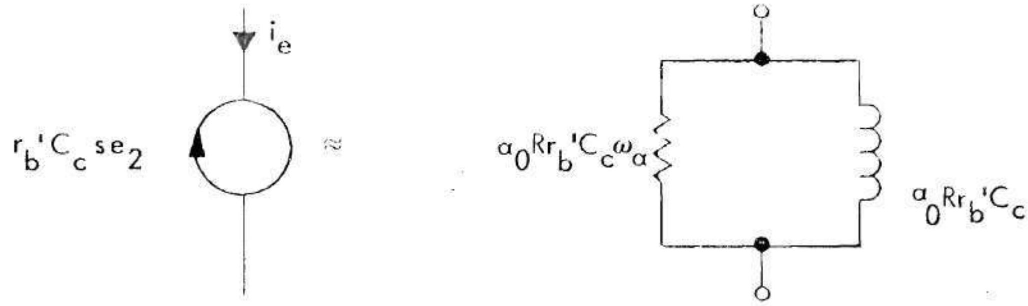

Figure 31. Approximate Equivalent Network for $h_{12}e_{12}$.

The time constant of this parallel RL combination is $1/\omega_\alpha$, which is the same as the parallel combination in the equivalent circuit for h_{11}. Thus the unilateral h model assumes the form of Figure 32, where the transistor conditions for validity are restated. This model will be used for the transistor in the theoretical investigation of the class of combinations. This model has acceptable accuracy for the following reasons: First, only those transistors are being considered for which $\frac{1}{r_b'C_c} \gg \omega_\alpha$. The magnitude of h_{12} approximately equals $r_b'C_c\omega$ so that at ω_α, the upper frequency limit on the model, $|h_{12}| \approx r_b'C_c\omega_\alpha \ll 1$. Second, unilateralization for the common-base mode should cause less error than for the common-emitter mode. The effect of h_{12} for a two-port network is to produce an input current change if the source impedance is finite. The input current change, ΔI, appears in the output multiplied by h_{fe} for a common-emitter stage and by h_{fb} for a common-base stage. The large difference in the magnitudes of h_{fe} and h_{fb} over most of the frequency range indicates that feedback can be more easily neglected for a common-base stage for ΔI's of the same order of magnitudes. For typical values of source impedance and h_{12} for each configuration, the ΔI's are usually of the same order of magnitude.

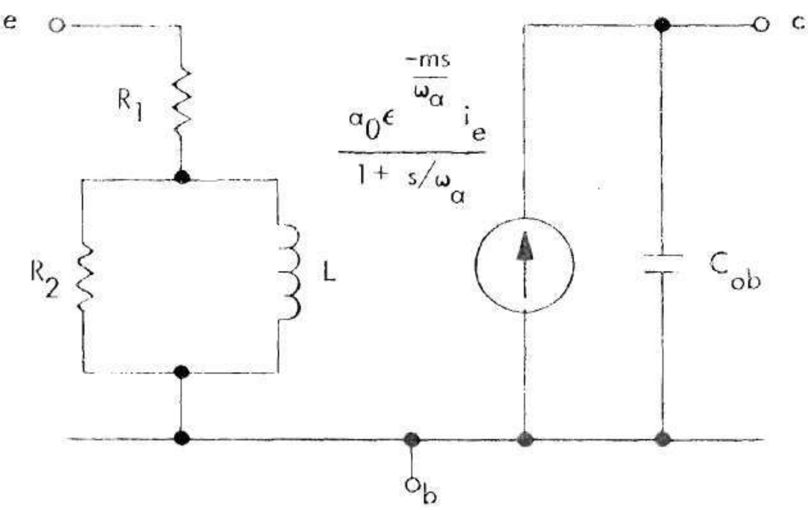

$$R_1 = r_e' + (1 - \alpha_o) r_b' \qquad R_2 = \alpha_o(1 + m) r_b' + \alpha_o R_L r_b' C_c \omega_\alpha - r_e'$$

$$L = \frac{\alpha_o(1 + m) r_b' - r_e'}{\omega_\alpha} + \alpha_o R_L r_b' C_c \qquad C_T = C_{eb} + C_{ce}$$

$$R_L = Z_L \big|_{\omega \to 0}$$

Conditions

$$\frac{1}{r_b' C_c} >> \omega_\alpha$$

$$1 > \Big| [r_e' + (1 - \alpha_o) r_b'] C_T \omega_\alpha + j(1 + \alpha_o m) r_b' C_T \omega \Big|$$

$$\omega \leq \omega_\alpha$$

Figure 32. Unilateral h Model for Common-base Transistor.

Gain Equations of a Combination

Now that unilateral models are available for the active devices, gain equations can be written for any particular configuration. The gain equations for a particular parallel and series combination will be given to illustrate the procedure. In Figure 33 the circuit and small signal network for a series combination is shown. This is the simplest possible series combination and yet there are nine independent network variables. These are R_3, C_3, $-R$, C, R_1', R_2, L, m, and α_0 (note $\omega_\alpha = R_2/L$). Model (c) of Figure 23 is used for the tunnel diode since r_s can be added to $r_e' + (1 - \alpha_0)r_b'$ of the unilateral model. It is seen from Figure 33

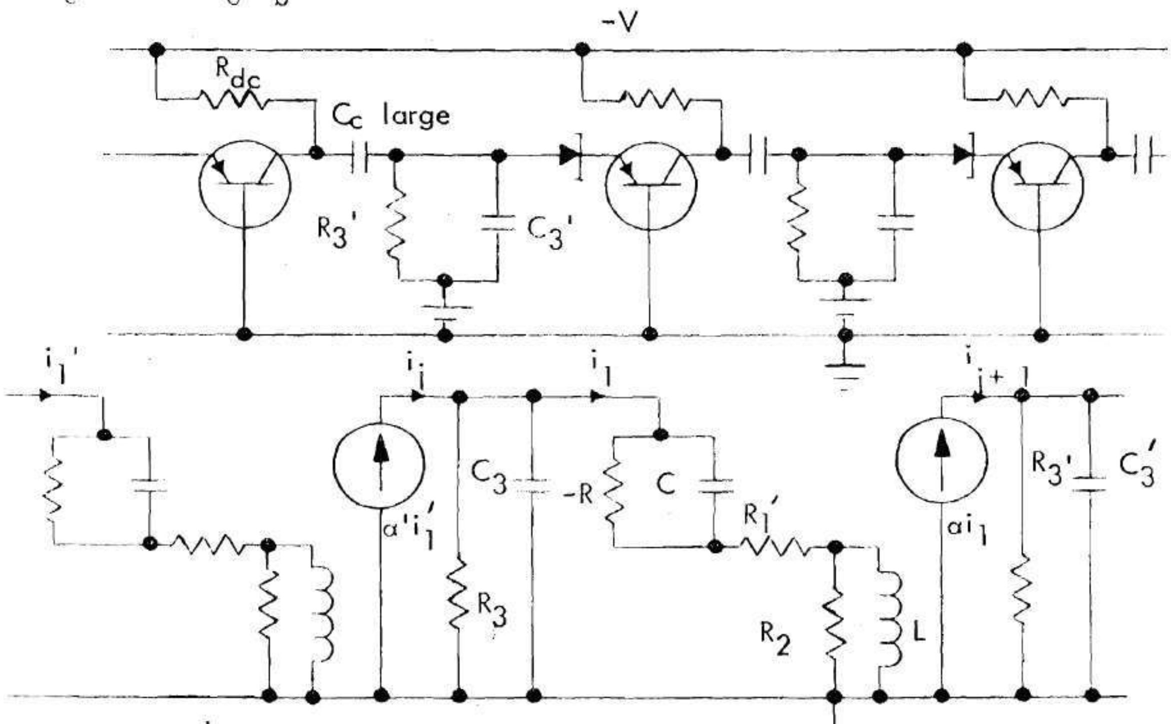

$$\alpha' = \frac{\alpha_0' \epsilon^{-m's/\omega_\alpha'}}{1 + s/\omega_\alpha'} \qquad R_3 = R_3' \| R_{dc} \qquad C_3 = C_3' + C_{ob} \qquad \alpha = \frac{\alpha_0 \epsilon^{-ms/\omega_\alpha}}{1 + s/\omega_\alpha}$$

$$R_1' = r_s + r_e' + (1 - \alpha_0) r_b' = r_s + R_1$$

Figure 33. Circuit and Small Signal Network for a Series Combination.

that the total current or voltage gain of an N-stage amplifier can be expressed in terms of the current gains i_{j+1}/i_j. It is found by standard analysis that

$$\frac{i_{j+1}}{i_j} = \frac{K(1 + es)\varepsilon^{-\frac{ms}{\omega_\alpha}}}{a + bs + cs^2 + ds^3} \tag{3.4}$$

where

$$k = \alpha_o R_3 \tag{3.5}$$

$$a = R_1' + R_3 - R \tag{3.6}$$

$$b = (R_1' - R)R_3C_3 + (R_1' + R_2 + R_3 - R)\frac{L}{R_2} - (R_1' + R_3)RC \tag{3.7}$$

$$c = \left[(R_1' + R_2 - R)\frac{L}{R_2} - R_1'RC\right]R_3C_3 - (R_1' + R_2 + R_3)R\frac{L}{R_2}C \tag{3.8}$$

$$d = -(R_1' + R_2)RR_3\frac{L}{R_2}CC_3 \tag{3.9}$$

$$e = -RC \tag{3.10}$$

In Figure 34 the circuit and small signal network for a parallel combination is given. This is the simplest possible parallel combination with the exception of letting $C_3 = 0$. Model (d) is used for the tunnel diode since the use of model (c) would create three additional independent variables. There are nine independent network variables for this combination. These are R', C', R_1, R_2, R_3, C_3, L, m, and α_0. Any total transfer gain for an N-stage amplifier can be easily given in terms of the current gain i_{j+1}/i_j for each stage. Standard analysis techniques yield

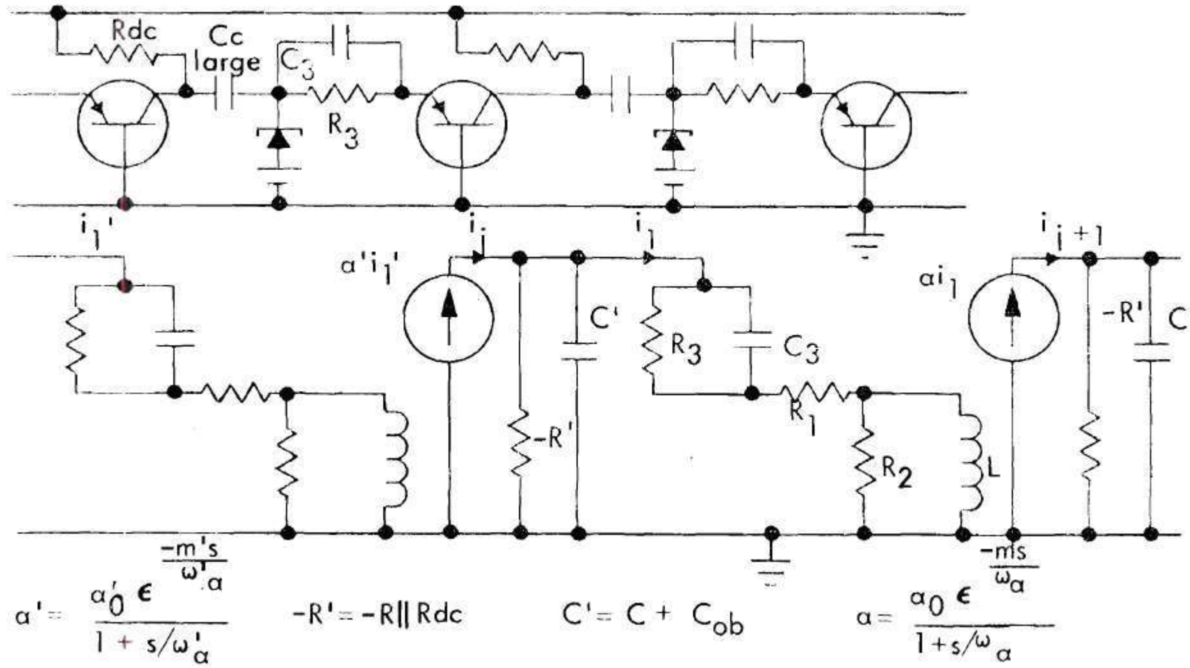

Figure 34. Circuit and Small Signal Network for a Parallel Combination.

$$\frac{i_{j+1}}{i_j} = \frac{K(1 + es)\varepsilon^{-\frac{ms}{\omega_\alpha}}}{a + bs + cs^2 + ds^3} \tag{3.11}$$

where

$$K = - R'\alpha_0 \tag{3.12}$$

$$a = (R_1 + R_3 - R') \tag{3.13}$$

$$b = (R_1 + R_2 + R_3 - R')\frac{L}{R_2} + (R_1 - R')R_3C_3 \tag{3.14}$$

$$-R'C'(R_1 + R_3)$$

$$c = (R_1 + R_2 - R')R_3 \frac{L}{R_2} C_3 - (R_1 + R_2 + R_3)R' \frac{L}{R_2} C' \tag{3.15}$$
$$-R_1 R_3 R' C_3 C'$$

$$d = -(R_1 + R_2)R_3 R' \frac{L}{R_2} C_3 C' \tag{3.16}$$

$$e = R_3 C_3 \tag{3.17}$$

Normalization and Simplification of Gain Equations

After obtaining gain equations for a given combination, it is useful to investigate whether the number of independent network variables can be reduced. For the two combinations given, each has the term $\alpha_o \varepsilon^{-\frac{ms}{\omega_\alpha}}$ appearing in the numerator of its gain equation. For all transistors, α_o is very close to unity. It is seen from the gain equations that α_o, as a network variable, only affects the low frequency gain and not the frequency response. The excess phase shift term $\varepsilon^{-\frac{ms}{\omega_\alpha}}$ will only affect the phase of the gain expression. Thus the gain expressions can be normalized with respect to $\alpha_o \varepsilon^{-\frac{ms}{\omega_\alpha}}$ since $\varepsilon^{-\frac{ms}{\omega_\alpha}}$ will not affect the gain magnitude, bandwidth, or gain-bandwidth and the effect of α_o on the low frequency gain or the gain-bandwidth can be added back later by simple multiplication.

For the remaining variables, the question arises of how to write or transform these so that the theoretical studies are as general as possible. The most profitable way is to write the circuit time constants normalized with respect to ω_α. Then gain-bandwidth will be normalized with respect to ω_α; that is, a normalized gain-bandwidth of 2 means the actual gain-bandwidth is $2\,\omega_\alpha$. In almost all gain-bandwidth studies for the transistor in a common-emitter configuration, the gain-bandwidth has been normalized with respect to ω_T. Since $\omega_\alpha \approx (1 + m)\,\omega_T$, normalization with respect to ω_α allows gain-bandwidth comparisons between the class of combinations and ordinary transistor configurations to be easily made. This normalization also aids the process of variable range restriction for stability considerations which will be discussed in the next section. To illustrate normalization of the network time constants with respect to ω_α, this process will be presented for the series and parallel combination already discussed.

Consider the series combination. Inspection of the unilateral transistor model in Figure 32 yields

$$\frac{L}{R_2} = \frac{1}{\omega_\alpha} \tag{3.18}$$

The tunnel diode time constant is normalized by setting

$$RC = \frac{K_1}{\omega_\alpha} \tag{3.19}$$

The third and final network time constant is normalized by setting

$$R_3C_3 = \frac{K_2}{\omega_\alpha} \tag{3.20}$$

Since R_3 is stepped to vary the dc gain, the question arises of whether K_2 should be calculated for each R_3 with $C_3\omega_\alpha$ at a discrete value. This means

$$K_2 = R_3[C_3\omega_\alpha] \tag{3.21}$$

where R_3 and $C_3\omega_\alpha$ are stepped through possible ranges of values. For a particular set of normalized values for the other network variables, R_3 is normally stepped through a set of values to vary the low frequency gain over some desired range. The procedure allows one to make a plot of normalized gain-bandwidth versus normalized 3 db frequency for the set of values. If K_2 is held constant while R_3 is varied, then C_3 must change each time R_3 changes. Since C_3 equals C_3', an external capacitance, plus the C_{ob} of the transistor to the left of the tunnel diode, C_{ob} places a lower limit on the variance of C_3.

A more natural arrangement is to have C_3 remain at a particular value while R_3 is varied as above. To accomplish this arrangement a factor P is defined such that

$$P = [C_3\omega_\alpha] \tag{3.22}$$

then

$$K_2 = R_3 P \tag{3.23}$$

In the theoretical studies P is stepped through a range of possible values. For each P and a set of the other variables, R_3 is varied to produce a curve as described above. K_2 is not held constant for this curve but varies with R_3.

Substitution of equations (3.18), (3.19), and (3.20) into the previous equations giving the coefficients of the gain equation yield

$$a = R_1' + R_3 - R \tag{3.24}$$

$$b = [K_2(R_1' - R) - K_1(R_1 + R_3) + (R_1' + R_2 + R_3 - R)] \frac{1}{\omega_\alpha} \tag{3.25}$$

$$c = \left[(R_1' + R_2 - R)K_2 - (R_1' + R_2 + R_3)K_1 - R_1'K_1K_2\right] \frac{1}{\omega_\alpha^2} \tag{3.26}$$

$$d = \left[-(R_1' + R_2)K_1K_2\right] \frac{1}{\omega_\alpha^3} \tag{3.27}$$

$$e = K_1/\omega_\alpha \tag{3.28}$$

To frequency scale gain equation (3.4), s is replaced by $(\omega_\alpha s)$ in this expression. A bandwidth of one now corresponds to a bandwidth of ω_α for the original gain expression. The expression is now normalized with respect to ω_α. The coefficients of the normalized gain expression are

$$a = R_1' + R_3 - R \tag{3.29}$$

$$b = K_2(R_1' - R) - K_1(R_1' + R_3) + (R_1' + R_2 + R_3 - R) \tag{3.30}$$

$$c = (R_1' + R_2 - R)K_2 - (R_1' + R_2 + R_3)K_1 - R_1'K_1K_2 \tag{3.31}$$

$$d = -(R_1' + R_2)K_1K_2 \tag{3.32}$$

$$e = -K_1 \tag{3.33}$$

This general normalized gain expression is used to study gain-bandwidth for the combination. There are now six independent variables. These are R, R_1', R_2, R_3, K_1, and P.

For the parallel combination it is seen from the transistor model that

$$\frac{L}{R_2} = \frac{1}{\omega_\alpha} \tag{3.34}$$

The $R'C'$ time is normalized by setting

$$R'C' = \frac{K_1}{\omega_\alpha} \tag{3.35}$$

The remaining network time constant R_3C_3 is normalized by setting

$$R_3C_3 = \frac{K_2}{\omega_\alpha} \tag{3.36}$$

Since C_3 is an external capacitor, there is no need to fix it when R_3 is stepped to vary the low frequency gain. Thus K_2 can assume a set of discrete values and C_3 changes whenever R_3 is changed. Substitution of equations (3.34), (3.35), and (3.36) into the previous equations giving the coefficients yields

$$a = R_1 + R_3 - R' \tag{3.37}$$

$$b = (R_1 + R_2 + R_3 - R')\frac{1}{\omega_\alpha} + (R_1 - R')\frac{K_2}{\omega_\alpha} - (R_1 + R_3)\frac{K_1}{\omega_\alpha} \tag{3.38}$$

$$c = (R_1 + R_2 - R')\frac{K_2}{\omega_\alpha^2} - [(R_1 + R_2 + R_3) + R_1K_2]\frac{K_1}{\omega_\alpha^2} \tag{3.39}$$

$$d = -(R_1 + R_2)\frac{K_1K_2}{\omega_\alpha^3} \tag{3.40}$$

$$e = \frac{K_2}{\omega_\alpha} \tag{3.41}$$

The gain equation is frequency scaled by replacing s with $(\omega_\alpha s)$. Since all time constants have been given relative to ω_α, the new gain equation is normalized with respect to ω_α. The coefficients of the normalized gain expression are

$$a = R_1 + R_3 - R' \tag{3.42}$$

$$b = (R_1 + R_2 + R_3 - R') + (R_1 - R')K_2 - (R_1 + R_3)K_1 \tag{3.43}$$

$$c = (R_1 + R_2 - R')K_2 - (R_1 + R_2 + R_3)K_1 - R_1K_1K_2 \tag{3.44}$$

$$d = -(R_1 + R_2)K_1K_2 \tag{3.45}$$

$$e = K_2 \tag{3.46}$$

This normalized gain expression is used to study gain-bandwidth for this combination. The number of independent variables is now six. These are R', R_1, R_2, R_3, K_1 and K_2. Restrictions on the range of possible values for the network variables must now be considered.

Restrictions on the Normalized Variable Values

The network variables are functions of the transistor model parameters, tunnel diode model parameters, and elements of the N_i one-port networks. The first and most obvious restriction on the range of values for the network variables is that those variables involving active device parameters have ranges corresponding to actual devices. For example, in the series combination discussed in this chapter one network variable is R, the junction incremental resistance of the tunnel diode. Actual tunnel diodes normally have mean values for R of 150, 55, 25, etc. ohms with some variance about each mean value. Thus one is restricted to certain ranges of values for the network variable R.

Second, restrictions are imposed on the range of possible values for the normalized time constants in order to predict stability as well as study achievable gain-bandwidths and bandwidths. For $K_1 \leq 1$ the tunnel diode is still an appreciable negative impedance when ω reaches ω_α and the circuit can be unstable. The common-base transistor model, however, is valid only to ω_α. Therefore stability, or corresponding instability, cannot be predicted analytically since stability may easily depend upon network behavior beyond ω_α. For the frequency range of interest, the investigation of common-base modeling for $\omega \geq \omega_\alpha$ did not yield useful results. The number of variables that must be included in such a model is so large that analytical stability predictions are virtually impossible. Therefore, the normalized tunnel diode time constant K_1 is constrained to be greater than or equal to one. As $K_1 \rightarrow 1$ it should be noted that, depending upon the particular form of the combination, stability may still depend somewhat upon network behavior beyond ω_α. For the theoretical studies, K_1's as small as one are allowed with the understanding that stability predictions can be in error as $K \rightarrow 1$. For the two combinations presented in this chapter, experimental verification of theoretical results has indicated that stability predictions seem adequate for K_1's as small as one.

Finally, restrictions are placed on R_3, the low frequency gain determining element for both configurations. The smallest value of R_3 allowed in either combination is that which produces an $A_i(0) \equiv i_{j+1}/i_j\big|_{\omega=0}$ of $\pm$ 2. Two represents an approximate lower limit on gain due to signal to noise degradation. The largest value of R_3 allowed is that which produces an $A_i(0)$ of $\pm$ 20. The upper limit is due to biasing limitations. It will be seen in the next chapter that as the passband gain increases, biasing becomes more difficult. For both combinations maximum gain-bandwidths occur at large $A_i(0)$. Letting R_3 increase indiscriminately can produce very large gain-bandwidths. Imprudent choice of other network variables can also produce unusually large gain-bandwidths. The purpose of the theoretical investigation, however, is to predict what values of gain-bandwidth and bandwidth are possible for those values of the network variables which correspond to actual devices, allow stability predictions to be made, and are practical from biasing considerations.

Gain-Bandwidth Definitions

The concept of gain-bandwidth has been used and misused in many ways. Normally this concept is identified with the area or an estimate of the area under the curve of some function of a transfer gain versus frequency. For low-pass product amplifiers, the following three formulas are normally used to define or estimate that gain-bandwidth product, (GBW):

$$GBW = \int_0^\infty |H(j\omega)|d\omega \qquad (3.47)$$

$$GBW = \int_0^\infty \ln|H(j\omega)|d\omega \qquad (3.48)$$

$$GBW = |H(j\omega = 0)|\omega_{3db} \qquad (3.49)$$

where $H(j\omega)$ is the transfer gain expression for $s = j\omega$. The first of these is sometimes considered to be the most basic. It should be noted that this expression is bounded only if there are at least two more poles than zeros. Obviously for more zeros than poles $|H(j\omega)| \to \infty$ as $\omega \to \infty$ and the integral is unbounded. For an equal number of poles and zeros, $|H(j\omega)|$ becomes constant for $\omega > K$ where K is a positive number. Therefore the integral is unbounded.

To illustrate the case of one more pole than zero, consider Figure 35. For this passive network, standard analysis yields

$$\frac{i_1}{i} = \frac{R}{(R_1 + R) + R_1 RCs} \tag{3.50}$$

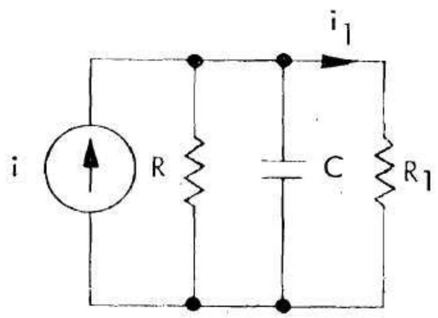

Figure 35. Transfer Gain Having One Pole and No Zeros.

Solving for $|H(j\omega)| = \left| \frac{i_1}{i}(j\omega) \right|$ yields

$$|H(j\omega)| = \frac{R}{\sqrt{(R_1 + R)^2 + R_1{}^2 R^2 C^2 \omega^2}} \tag{3.51}$$

Substitution of the right side of equation (3.51) into equation (3.47) yields

$$\int_0^{\infty} \frac{R}{\sqrt{(R_1 + R)^2 + R_1{}^2 R^2 C^2 \omega^2}}\, d\omega = \infty \tag{3.52}$$

Therefore the gain-bandwidth is unbounded, a result which may be explained as follows: For any $H(\omega)$ with one more pole than zero, $H(j\omega) \geq \frac{K}{\omega}$ for ω greater than some ω_a. Therefore equation (3.47) may be written

$$GBW = \int_0^{\infty} |H(j\omega)|d\omega \geq \int_0^{\omega_a} |H(j\omega)|d\omega + \int_{\omega_a}^{\infty} \frac{K}{\omega}\, d\omega \tag{3.53}$$

Now

$$\int_{\omega_a}^{\infty} \frac{K}{\omega}\, d\omega = K \ln \omega \Big|_{\omega_a}^{\infty} = \infty \tag{3.54}$$

Thus GBW using this definition will always be unbounded for this case. For $H(j\omega)$ with at least two more poles than zeros, the integral normally converges.

Equation (3.48) would appear to be of great value since amplifier responses are often plotted in decibels. For N_z, the number of zeros, not equal to N_p, the number of poles, the magnitude of $H(j\omega)$ approaches $+\infty$ or 0 as $\omega \rightarrow \infty$. Therefore $\ln|H(j\omega)|$ approaches $+\infty$ or $-\infty$ as $\omega \rightarrow \infty$, and the integral is unbounded. Thus only for $N_z = N_p$ can this equation be used and then only if $|H(j\omega)| \rightarrow 1$ for $\omega > \omega_b$. The last condition is required since $|H(j\omega)| \rightarrow C$ for ω greater than some K, when $N_z = N_p$. Thus, equation (3.48) may be written

$$GBW \approx \int_0^{K} \ln|H(j\omega)|d\omega + \int_K^{\infty} \ln C\, d\omega \tag{3.55}$$

For $C \neq 1$ the second integral is obviously unbounded. Thus, the use of this definition for GBW is highly restricted. The main advantage of this definition is that, where it applies, one may use the resistance integral theorem to obtain

$$\int_0^{\infty} \ln|H(j\omega)|d\omega = \frac{\pi}{2} \lim_{\omega \to \infty} \omega \, \phi\,(\omega) \tag{3.56}$$

where

$$H(j\omega) = |H(j\omega)| \angle \phi(\omega) \tag{3.57}$$

Thus $(\lim_{\omega \to \infty} \omega\, \phi(\omega))$ can be found in terms of the coefficients of the $H(s)$ gain expression and one has a method to easily evaluate the integral. Due to the restrictions on its use, this GBW definition cannot be used for the class of tunnel diode-common-base transistor combinations. In fact it has only been used in the study of all pass equalizers.

Equation (3.49) is probably the most commonly used GBW factor. It can be considered as a definition for gain-bandwidth or as an estimate of the area defined by the integral of equation (3.47). Since equation (3.47) can be used only when $|H(j\omega)|$ is decreasing at least as $\frac{1}{\omega^2}$ for large ω, $|H(j\omega)|\omega_{3db}$ is normally a reasonable estimate of the integral. Equation (3.49) will be taken as the GBW definition in the theoretical studies for the following reasons. First, this definition will yield a bounded value for the case where $N_p = N_z + 1$. Second, one normally plots normalized GBW versus normalized ω_{3db}. The use of this definition allows one to infer $|H(j\omega = 0)|$ from a given GBW and ω_{3db}. Thus, more information is contained in the curves. Third, for complex gain expressions, this GBW is easier to evaluate than the others. Fourth, most gain-bandwidth studies for ordinary transistor product amplifiers have been in terms of this definition. Thus comparisons can be easily made.

Computer Method for Studying Gain-Bandwidth

The technique of using the digital computer to study gain-bandwidth for the class of combinations is illustrated for the two combinations discussed in this chapter. Both are of the normalized form

$$H(s) = \frac{K(1 + es)}{a + bs + cs^2 + ds^3} \tag{3.58}$$

As discussed gain-bandwidth, GBW, is chosen to be

$$GBW = |H(j\omega = 0)|\omega_{3db} \tag{3.59}$$

Now

$$|H(j\omega = 0)| = \frac{K}{a} \equiv A_i(0) \tag{3.60}$$

Standard analysis techniques yield that $(\omega_{3db})^2$ is the positive real root of the equation

$$Fx^3 + Gx^2 + Hx + M = 0 \tag{3.61}$$

where

$$F = d^2 \tag{3.62}$$

$$G = c^2 - 2bd \tag{3.63}$$

$$H = b^2 - (2ac + 2a^2e^2) \tag{3.64}$$

$$M = -a^2 \tag{3.65}$$

To predict stability a Routh-Hurwitz criterion is used. For $H(s)$ of the form of equation (3.58), $H(s)$ is stable if $a > 0$, $c > 0$, $d > 0$, and

$bc - ad > 0$ or if $a < 0$, $c < 0$, $d < 0$, and $bc - ad > 0$.

The computer program is discussed in general terms below. The exact program for both the series and the parallel configuration discussed in this chapter is given in Appendix II. One sets up a series of loops which step the normalized network variables through respective ranges of values. The parameter R_3 which varies the DC gain is in the innermost loop. The set of R_3 values are always chosen so that $A_i(0)$ is stepped in a 20, 10, 8, 6, 4, 3, 2 sequence. Once the computer picks a particular set of values for the network variables, the coefficients a, b, c, d, and e of H(s) are calculated for that set of values. Using these coefficients, stability is checked. If instability is predicted, the coefficients a, b, c, and d are printed out. If stability is predicted, then the coefficients F, G, H, and M of equation (3.61) are calculated in terms of the values for a, b, c, d, and e. Then the computer uses a modified Muller procedure to find the roots of equation (3.61). The real and imaginary parts of each root are printed out. The positive square root of the absolute value of the real part of each root is calculated and printed out. Finally K/a is calculated for the particular set of network values and is multiplied by the above square root of the real part of each root. This value is also printed out and for the positive real root represents the desired gain-bandwidth.

The following question could be posed at this point. Why not have the computer find the positive real root of equation (3.61) and only print out K/a times the square root of this root? Thus only the desired gain-bandwidth would be printed out instead of three values. The reason for printing all three is that due to round off error the positive real root may be given with a very small imaginary part. The other two complex roots could also have a positive real part. Thus it would be extremely difficult for the computer to decide which is the positive real root for this case. Therefore, three values are given and the person analyzing the data can easily tell which is the actual gain-bandwidth.

To illustrate the format of the data printout, consider the following typical replica of one page of data printout for the previously discussed series configuration.

FIXING THE FOLLOWING PARAMETERS AT

$R_1 = 20$ $R = 150$ $R_2 = 150$ $K_1 = 1$ $P = 0.005$

AND VARYING R_3 AS FOLLOWS, ONE OBTAINS

R_3	Y	IM(X)	RE(X)	GBW
124	0.2282	0.00	-0.0521	4.564
	0.1001	0.00	0.0100	2.00
	2.4918	0.00	-6.2091	49.836
118.2	0.1939	0.00	-0.0376	1.939
	0.2338	0.00	0.0546	2.338
	2.5915	0.00	-6.716	25.915
115.5	0.1943	0.00	-0.0377	1.554
	0.2879	0.00	0.0829	2.303
	2.6406	0.00	-6.972[illegible]	2.112
111.5	0.2009	0.00	-0.0404	1.205
	0.3576	0.00	0.1279	2.146
	2.7166	0.00	-7.3801	15.299
104	0.21942	0.00	-0.0481	.8776
	0.4669	0.00	0.2180	1.868
	2.8719	0.00	-8.2477	11.488
97	0.2365	0.00	-0.0560	0.710
	0.5486	0.00	0.3009	1.646
	3.0222	0.00	-9.1339	9.067
86.7	0.2645	0.00	-0.0699	0.529
	0.6704	0.00	0.4494	1.341
	3.3141	0.00	-10.9832	6.668

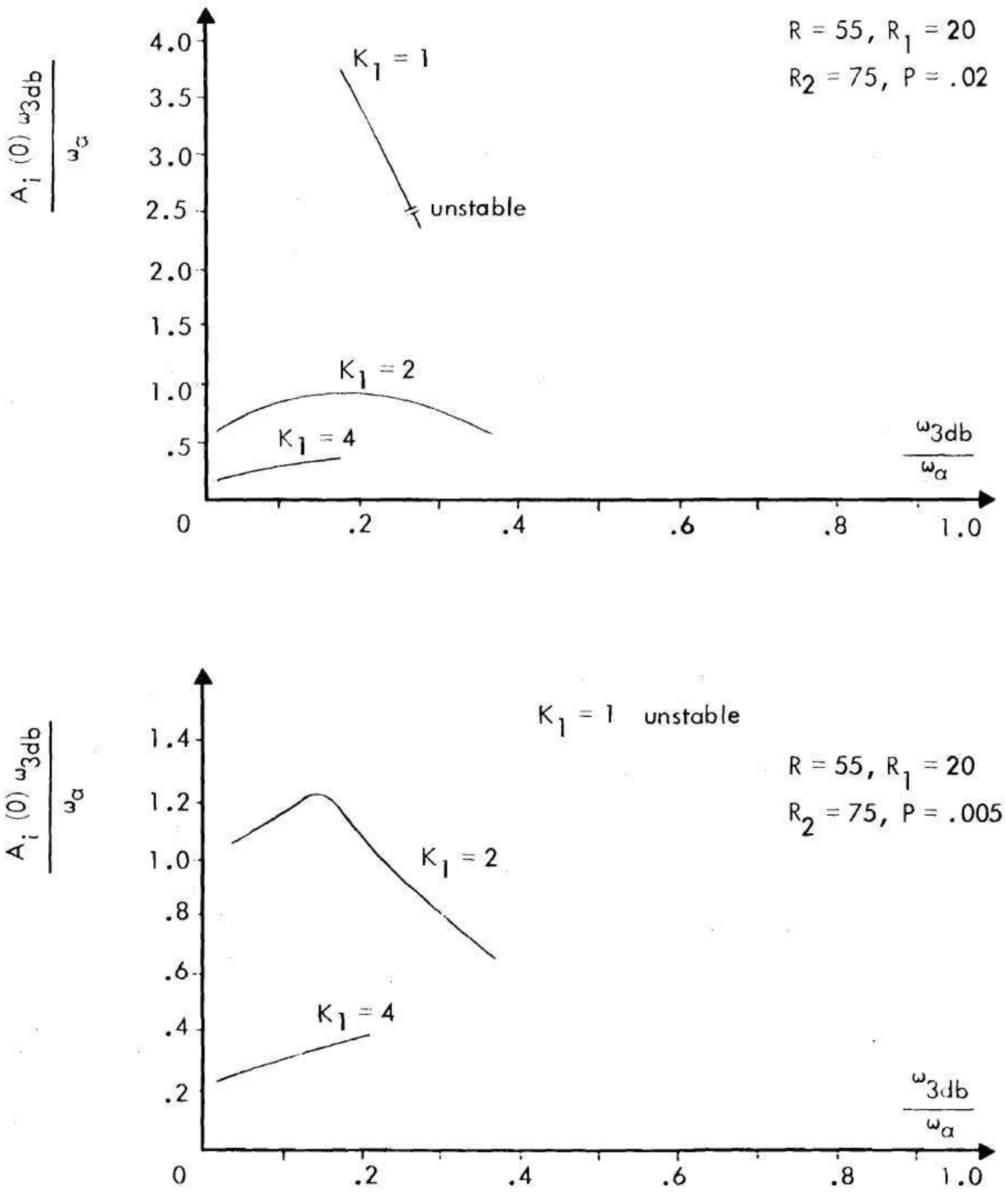

Figure 36. Normalized Gain-bandwidth versus Normalized Bandwidth for Series Combination of Figure 33.

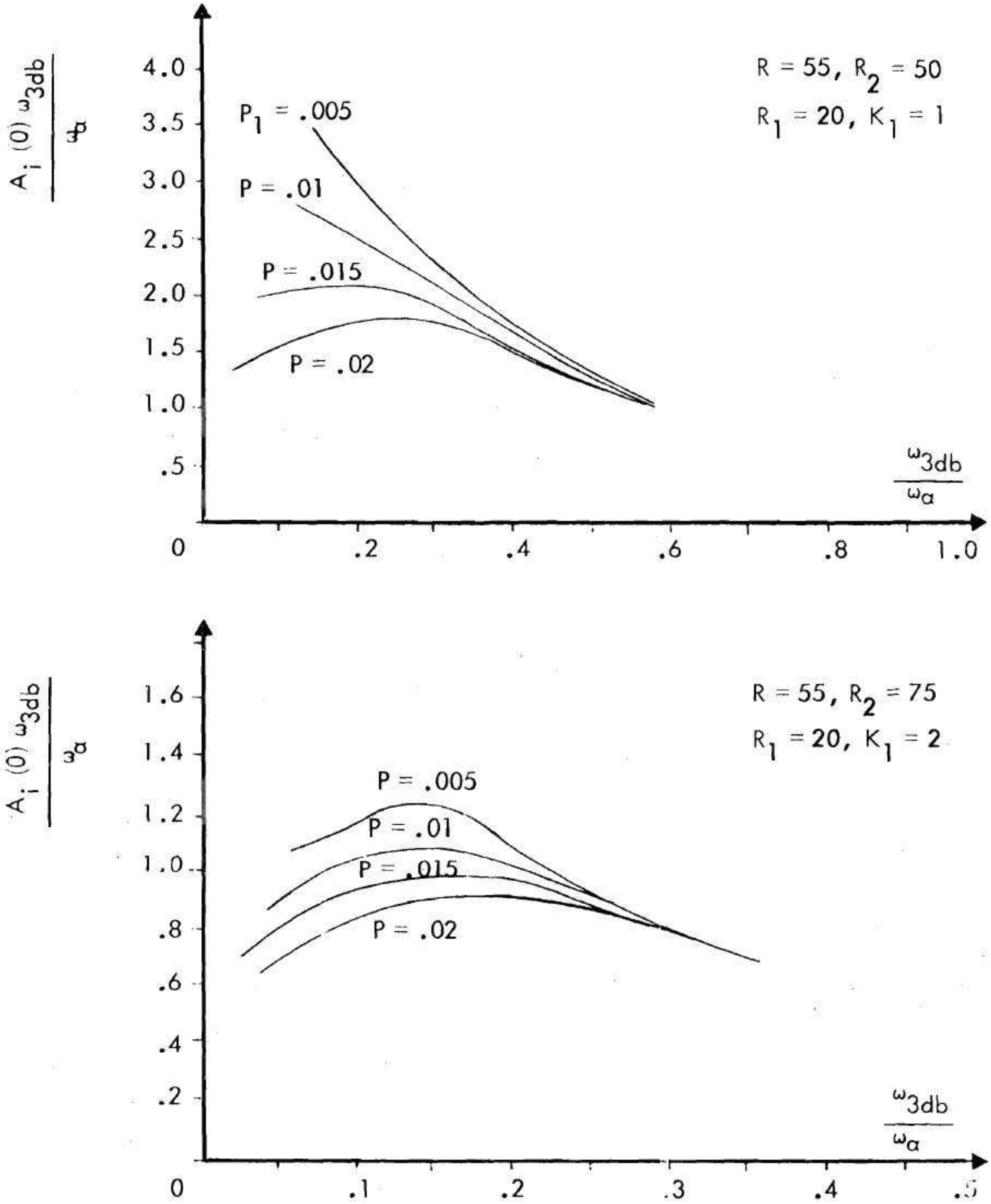

Figure 37. Normalized Gain-bandwidth versus Normalized Bandwidth for Series Combination of Figure 33.

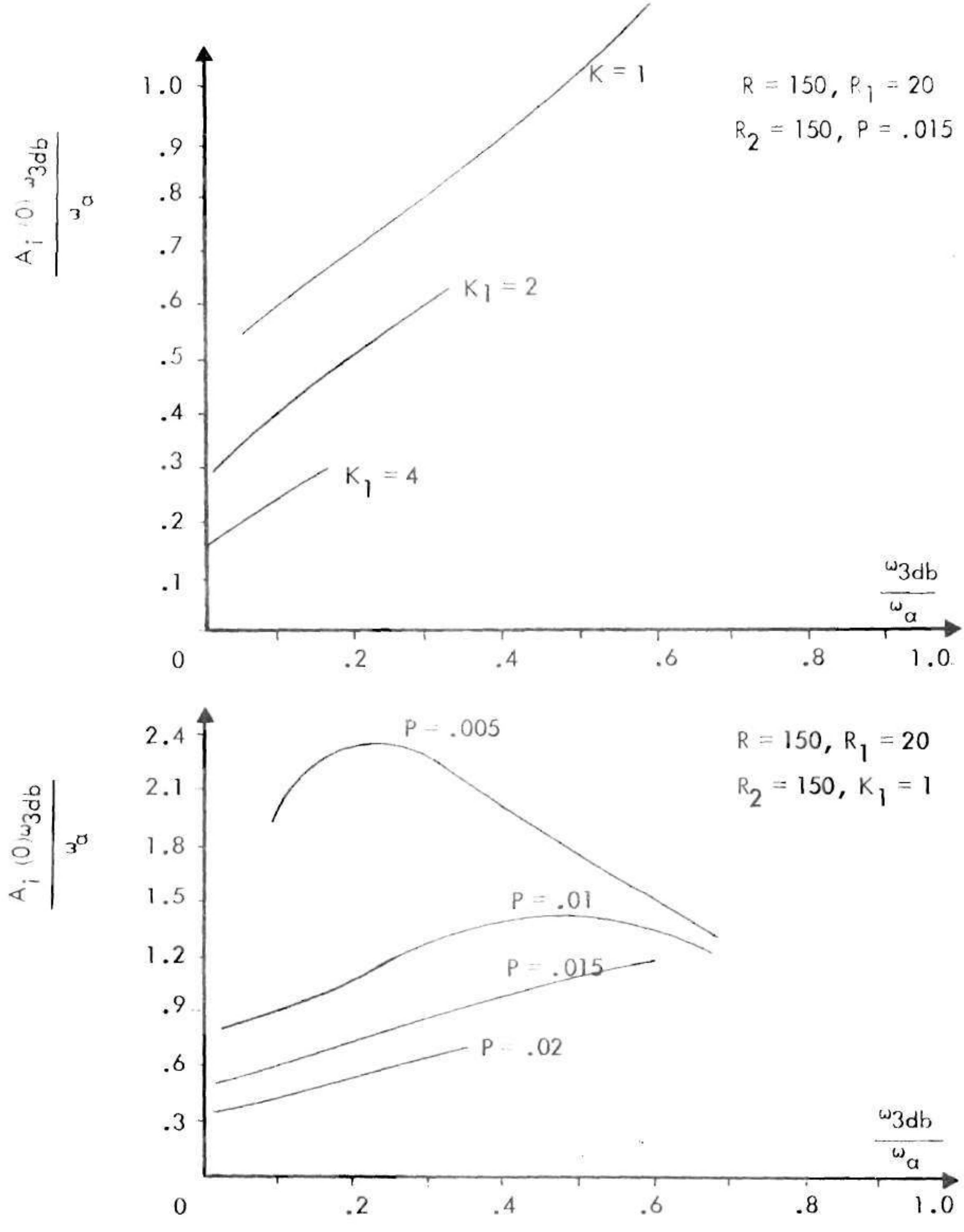

Figure 38. Normalized Gain-bandwidth versus Normalized Bandwidth for Series Combination of Figure 33.

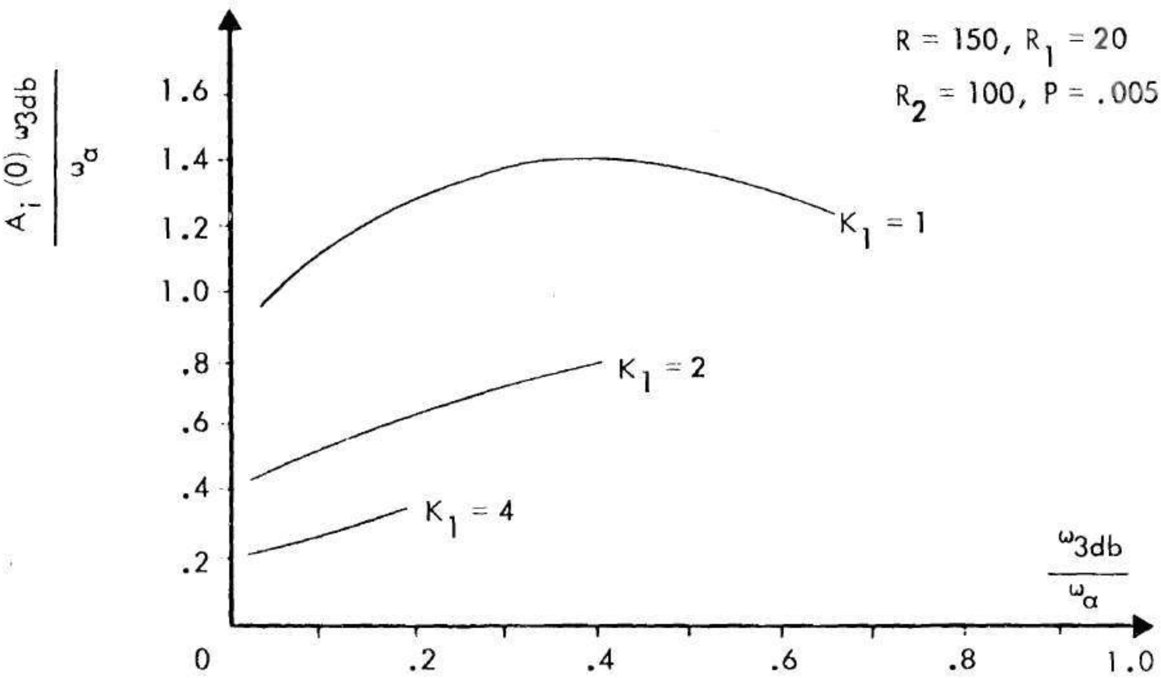

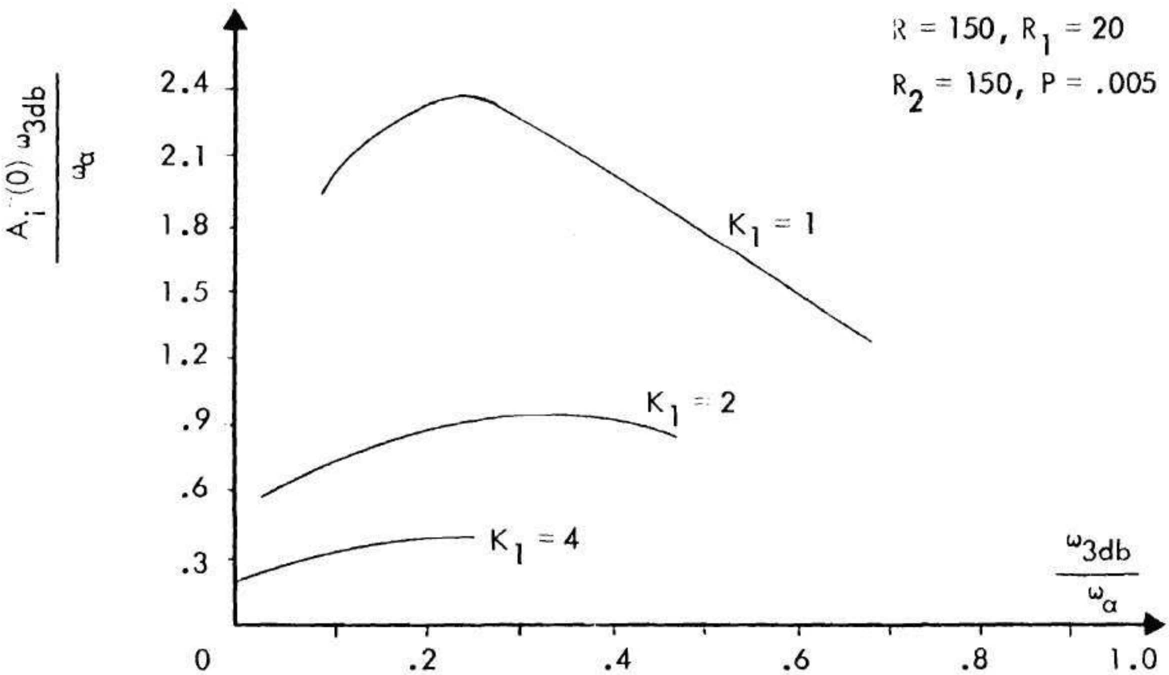

Figure 39. Normalized Gain-bandwidth versus Normalized Bandwidth for Series Combination of Figure 33.

One sees that values for the other five network variables are chosen and then R_3 is stepped through its set of values. As previously stated, the set of values for R_3 is chosen such that $2 \leq A_i(0) \leq 20$. The above format is very useful in that each page of printout generates a curve of normalized gain-bandwidth versus normalized bandwidth. For the curve the values of the five normalized network variables at the top of the page should be given. It is unnecessary to give the values of R_3. For a given value of normalized GBW and normalized bandwidth lying on the curve, $A_i(0)$ is easily calculated. One can then easily find R_3 in terms of $A_i(0)$ and some of the given network values.

Various curves of normalized gain-bandwidth versus normalized frequency for the series combination discussed in this chapter are given in Figures 36, 37, 38, and 39. For a 1 ma peak current tunnel diode $R \approx 150$ ohms and for a 2 ma peak current $R \approx 55$ ohms. Consideration of a large number of such curves allows one to infer somewhat the topology of the N space. To include all situations, the criteria vary enough that generalizations are practically impossible with regard to the optimum region of the N space. In any giver situation design criteria and the initial choices of certain variables due to bandwidth, biasing, or other constraints lead one to a subspace of the N space. The use of the computer method and associated curves then allow one to ascertain whether the desired criteria can be met and the values of the network variables meeting these criteria. Once the ranges of the network variables are chosen, then the ranges of the circuit element values can be chosen. An example illustrating a practical use of the combinations and the theoretical investigation methods

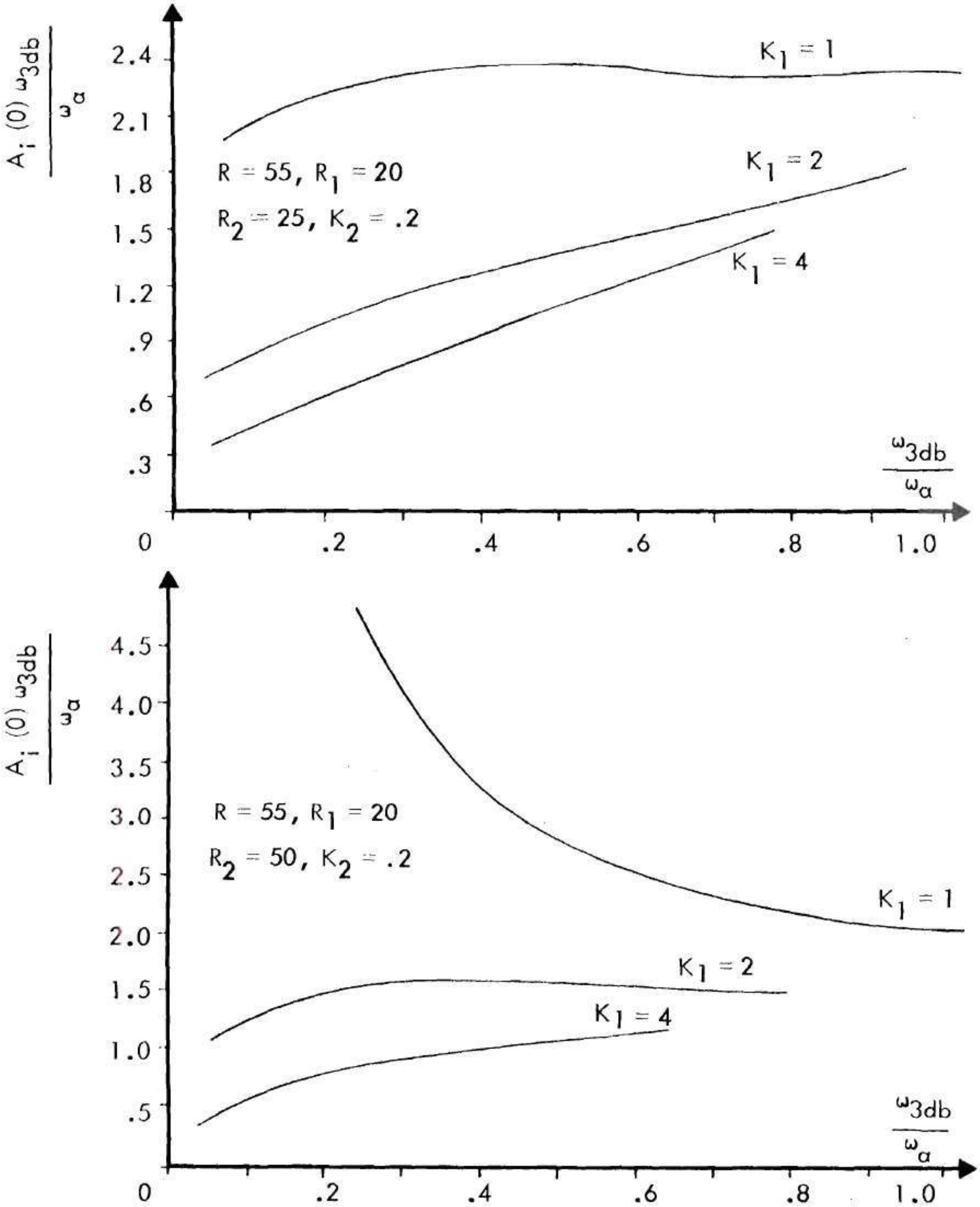

Figure 40. Normalized Gain-bandwidth versus Normalized Bandwidth for Parallel Combination of Figure 34.

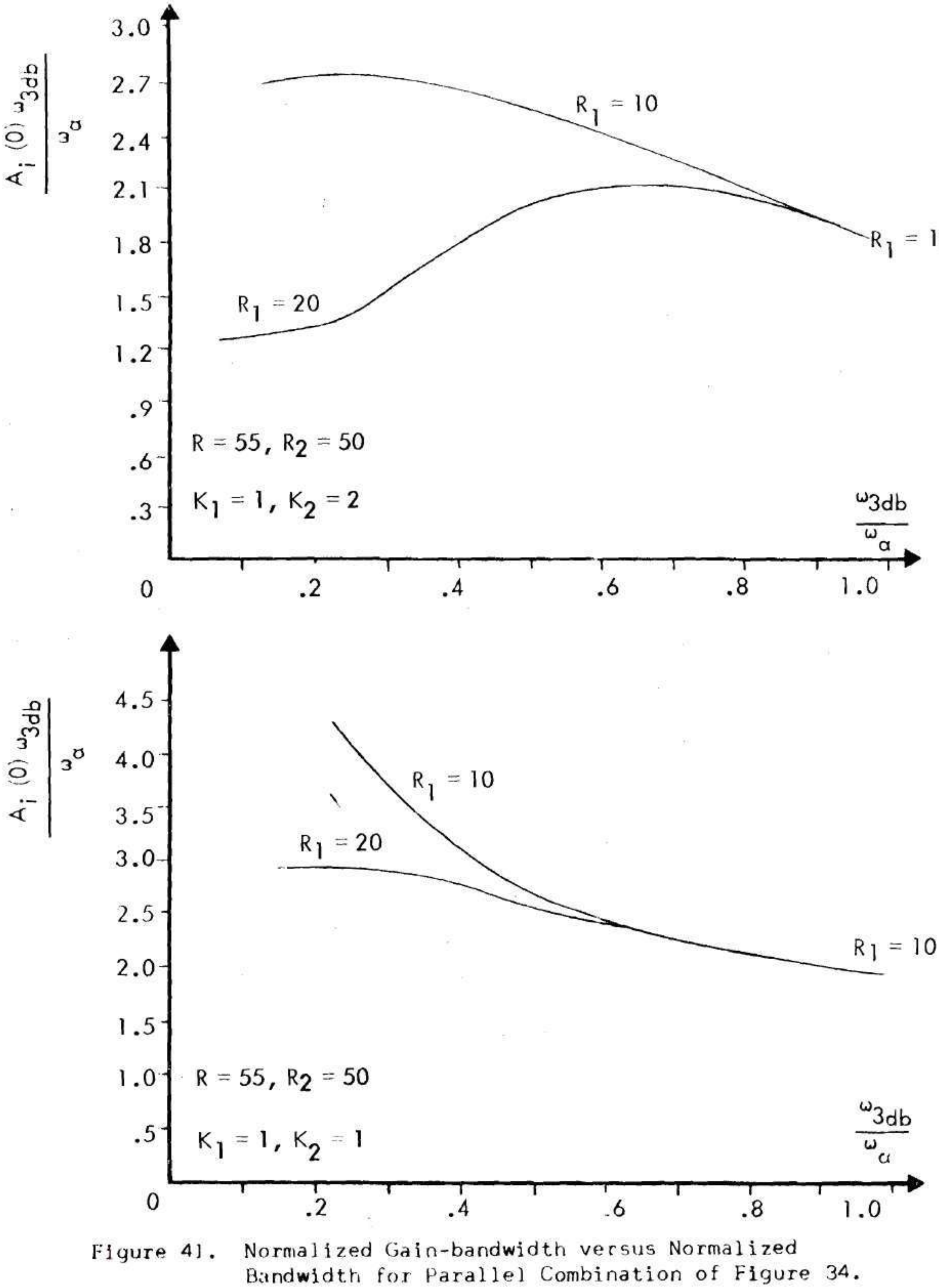

Figure 41. Normalized Gain-bandwidth versus Normalized Bandwidth for Parallel Combination of Figure 34.

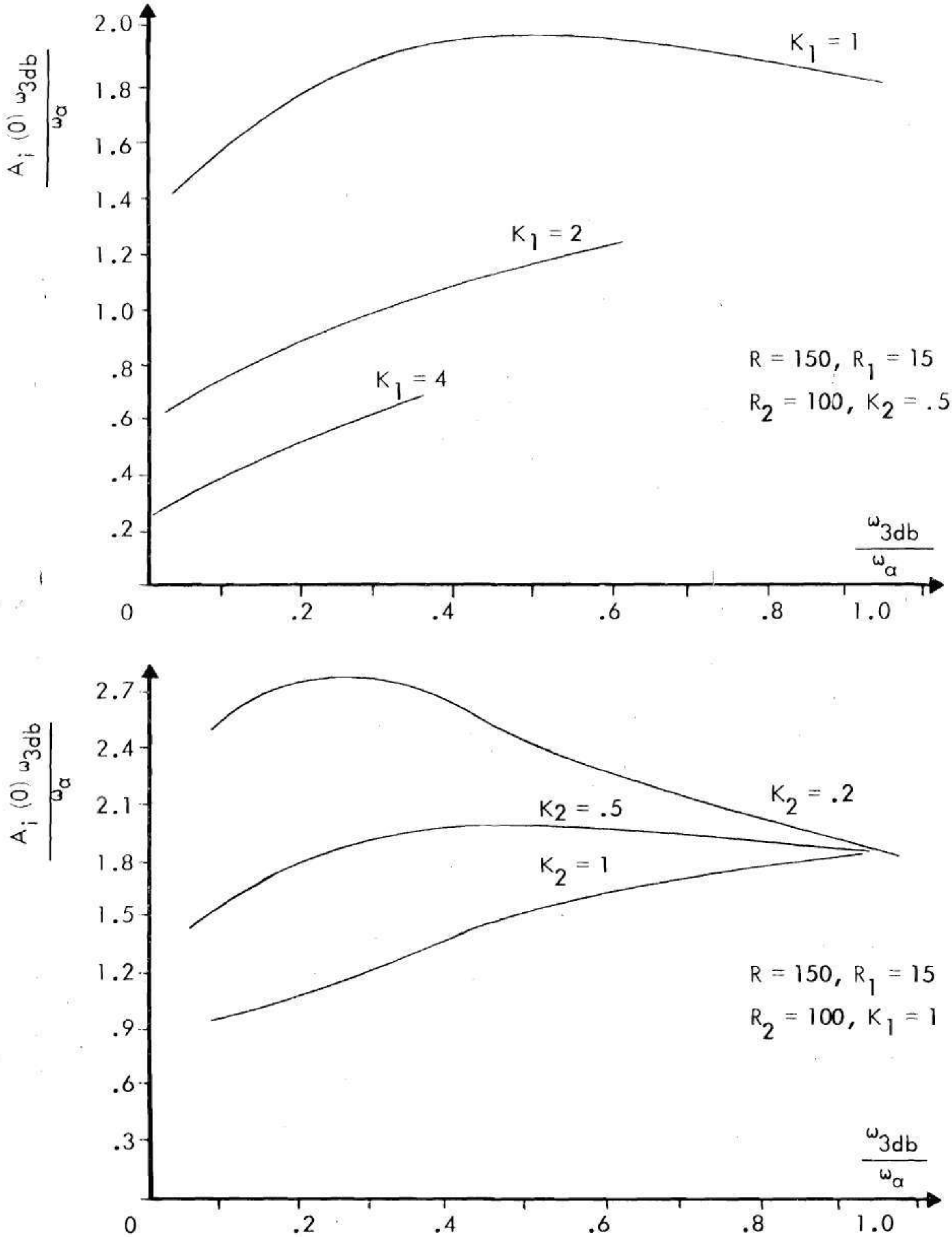

Figure 42. Normalized Gain-bandwidth versus Normalized Bandwidth for Parallel Combination of Figure 34.

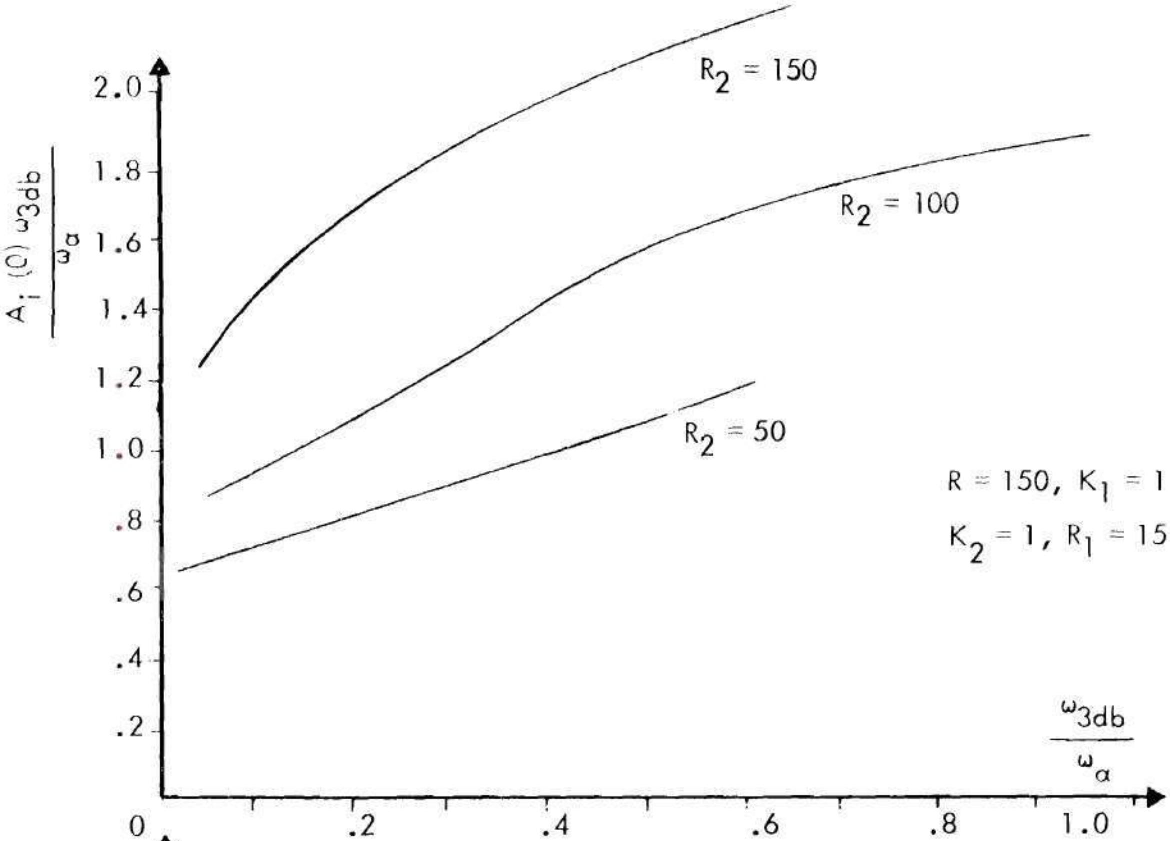

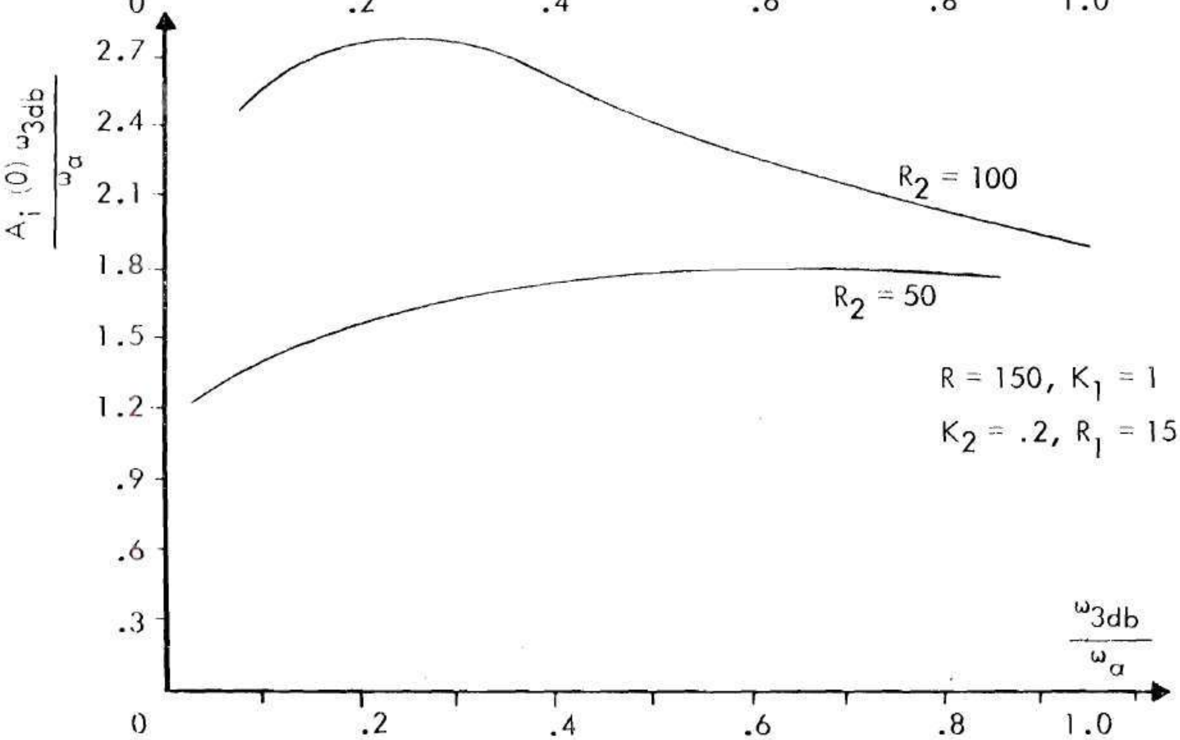

Figure 43. Normalized Gain-bandwidth versus Normalized Bandwidth for Parallel Combination of Figure 34.

will be given in a later chapter.

For the preceding series combination inspection of a large number of curves reveals that practical gain-bandwidths as large as five times ω_α are possible. In Figures 40, 41, 42, and 43 some curves of normalized gain-bandwidth versus normalized frequency are given for the parallel combination discussed in this chapter. Inspection of a large number of such curves reveals that gain-bandwidths as large as five ω_α are also possible for this combination. Since $\omega_\alpha \approx (1 + m)\omega_T$ and $0.2 \leq m \leq 1$, it is seen that gain-bandwidths as large as ten times ω_T, the present upper bound, are possible.

CHAPTER IV

BIASING

For the class of tunnel diode-common-base transistor combinations to be useful, stable biasing techniques must be available. As a worst case, assume that each N_i of Figure 8 has a DC resistive value. The class of combinations then assumes at zero frequency the form of Figure 44. Both transistors are assumed to be PNP transistors for comparison purposes. The voltage source E_1 is used to reverse bias the collector-base

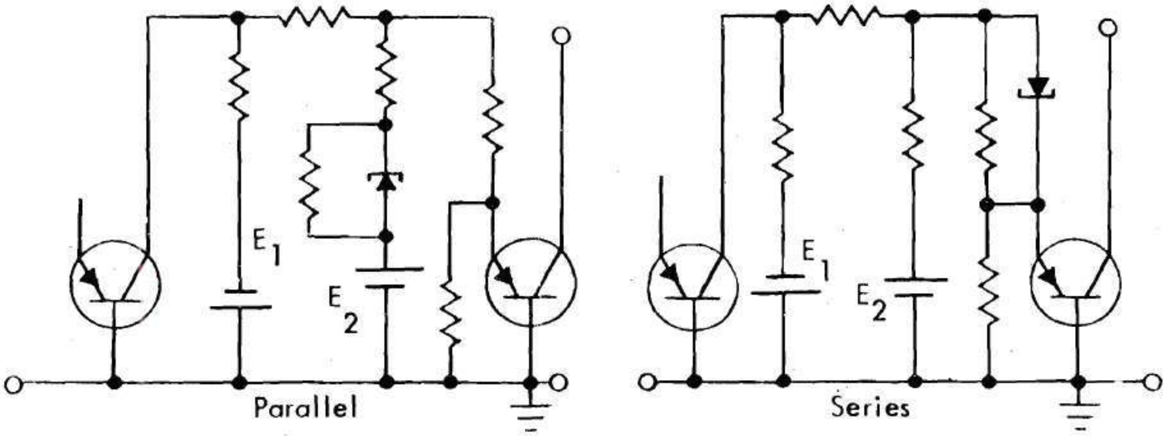

Figure 44. Worst Case DC Form for Class of Tunnel Diode-Common-Base Transistor Combinations.

junction of the transistor for both the series and parallel combinations. The voltage source E_2 is used to bias the tunnel diode in the negative resistance region and to forward bias the transistor emitter-base junction in both combinations. For typical circuit element values, the establishment of the proper polarities and magnitudes of the voltages at the collector-base junction, across the tunnel diode, and across the emitter-base junction is exceedingly difficult with direct coupling. To eliminate this difficulty and avoid the large DC drift problems associated with single ended direct-coupled product type amplifier stages, the stages are capacitive coupled. The previously defined $A_i(0)$ is now actually the current gain at a frequency somewhat greater than zero, where the coupling capacitor can be considered a short circuit. The combinations at DC now assume the form of Figure 45. The collector-base junction voltage is now set by simple load line techniques. The circuits for biasing the tunnel diode and emitter-base junction are seen to be identical in form. Combining like elements, this form is given in Figure 46.

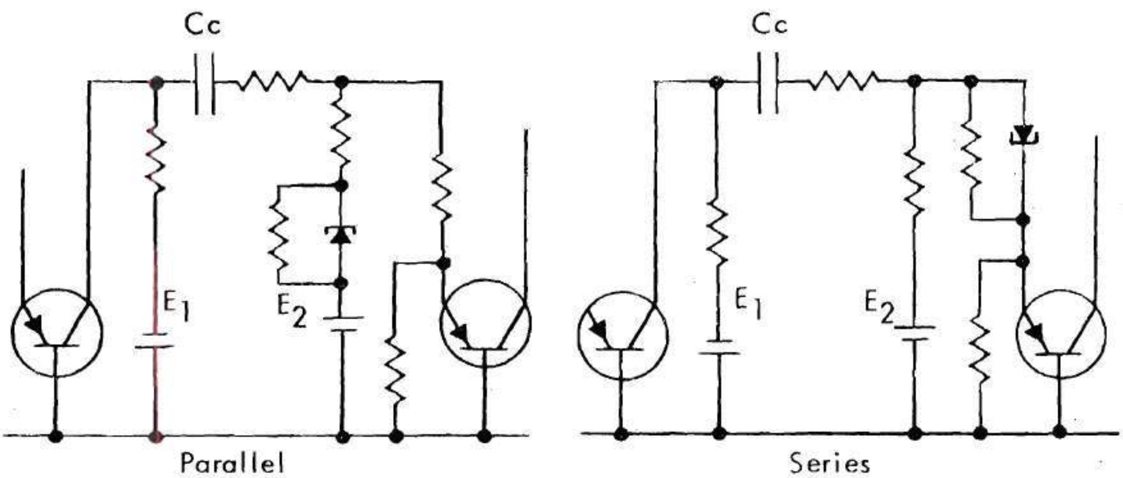

Figure 45. Worst Case dc Form for Class of Combinations Using Capacitor Coupling

R_A is the total equivalent resistance in series with the tunnel diode and emitter-base junction. R_B is the equivalent resistance in parallel with the tunnel diode and R_C is the equivalent resistance in parallel with the emitter-base junction.

Biasing is now possible if the volt ampere curve of the circuit to the right of E_2 is voltage source stable. This means that there is only

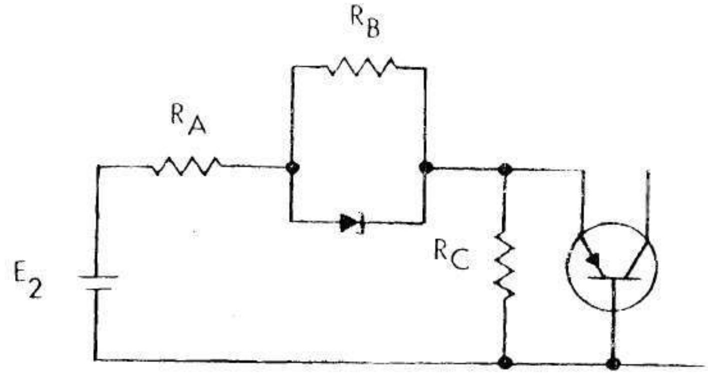

Figure 46. General Form of Bias Circuit for Tunnel Diode and Emitter Base Junction.

one point of possible operation corresponding to each value of E_2 voltage. Consider, for example, the typical tunnel diode volt ampere curve in Figure 47. Obviously, the device can be stably biased by a voltage source

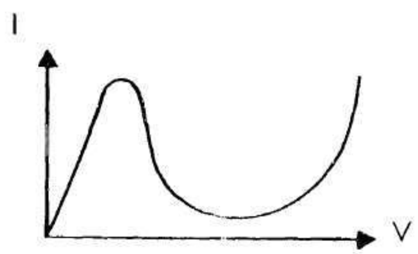

Figure 47. Tunnel Diode Volt Ampere Curve.

but not by a current source. If the voltage source has source resistance R_s, then, for stable biasing, R_s must be less than $|-R|$, where $-R$ is the slope in the negative resistance region. For the class of tunnel diode-common-base combinations, the circuit to the right of the bias source E_2 will normally have a negative resistance region. Thus there can be a bias stability problem.

Two ways of producing an E_2 with a small source resistance are now

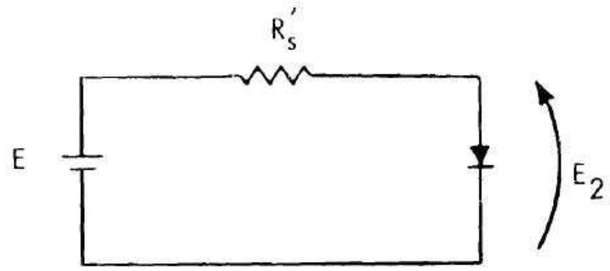

Figure 48. Approximation of Small Value Voltage Source by Forward Biased Diode Junction.

discussed. In Figure 48 the voltage source E_2 is approximated by a forward biased diode junction. Since diode voltage is a logarithmic function of the current through the diode, the voltage E_2 will hardly vary if the circuit to the right of E_2 requires a reasonably small amount of current. Inexpensive transistor emitter-base junctions can be used as diodes by shorting the collector-base junction. Different materials and manufacturing techniques produce different average diode voltages.

In Figure 49 the voltage source E_2 is realized by using feedback around an operational amplifier. The voltage E_2 equals $-\frac{R_2}{R_1} V_z$ where V_z is the Zener diode voltage. There is a constant load on the Zener diode

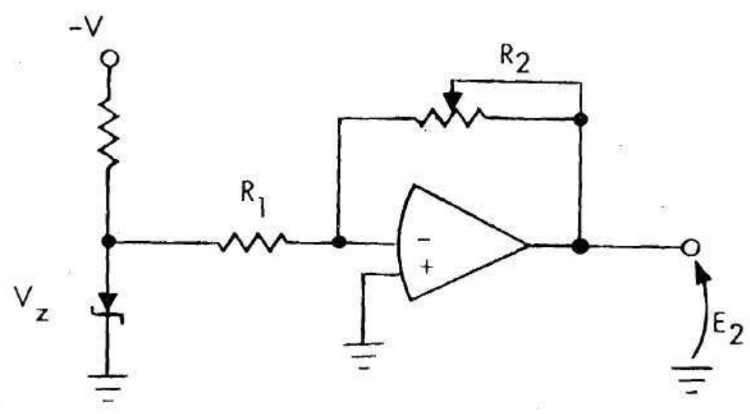

Figure 49. Voltage Source E_2 Realization Using Operational Amplifier.

since the amplifier negative input is always close to zero volts. The effect of the feedback is to greatly reduce the output impedance. To increase the output current capability, one can add an emitter follower as in Figure 50. With the increased availability of low cost high performance integrated circuit operational amplifiers, this method is

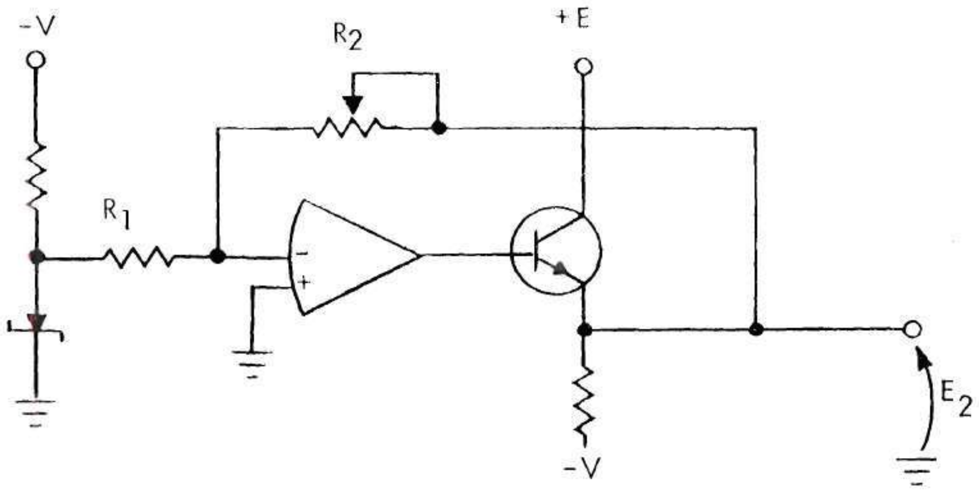

Figure 50. Voltage Source E_2 Realization Using Operational Amplifier and Emitter Follower.

attractive since the output closely approximates a voltage source.

To illustrate the biasing techniques and associated problems, we consider the series and parallel combinations discussed in Chapter III. In both Figures 33 and 34, capacitive coupling was used in the circuit defining the combination. For both combinations the DC bias circuit for the tunnel diode and emitter base junction reduces to the form of Figure 51. Comparing this to the general form given in Figure 46, it is seen that they are identical if $R_B = R_C = \infty$. It is informative to choose a particular tunnel diode, transistor, and R_A value and solve for the volt-ampere characteristic of the series combination. The volt ampere curves for a

1N3713 tunnel diode, 2N2189 transistor, and R_A equal to 80 ohms are given respectively in Figures 52, 53, and 54.

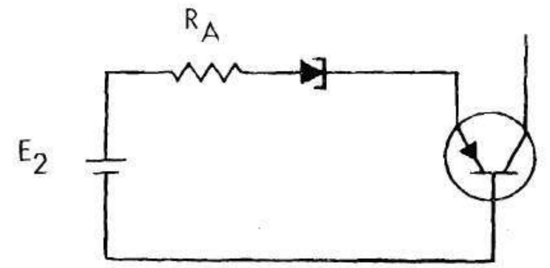

Figure 51. Form of Bias Circuit for Tunnel Diode and Emitter-Base Junction for Series Combination of Figure 33 and Parallel Combination of Figure 34.

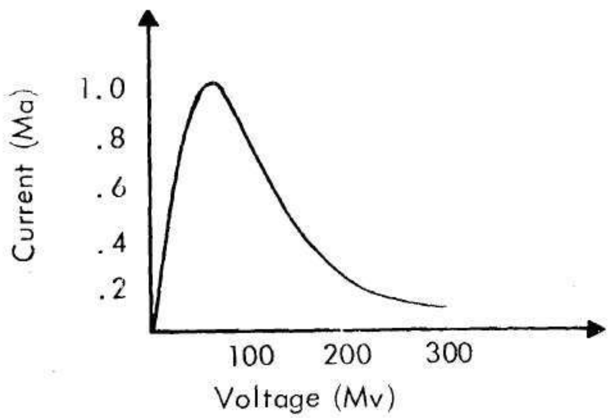

Figure 52. Volt-ampere Characteristic for a 1N3713 Tunnel Diode.

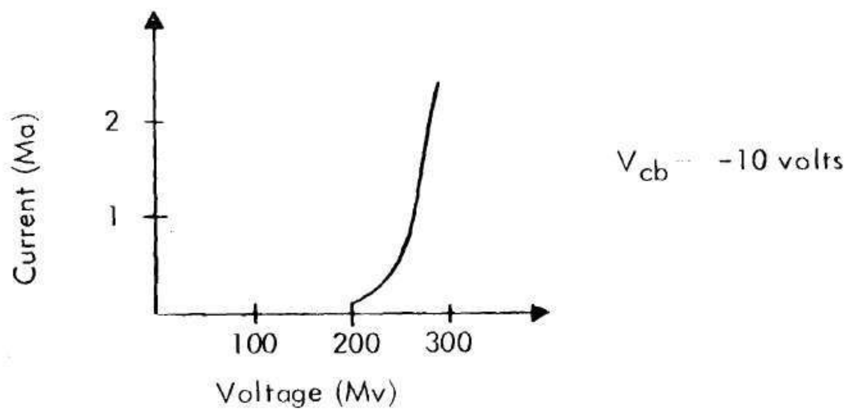

Figure 53. Volt-ampere Characteristic for Emitter-base Junction of 2N2189 Transistor.

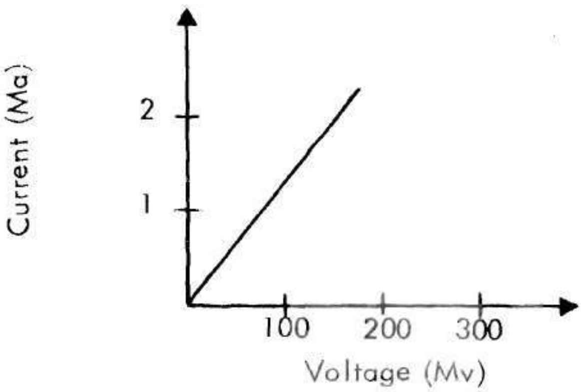

Figure 54. Volt-ampere Characteristic of 80 ohm Resistor.

The volt-ampere characteristic of the series combination is given in Figure 55. It is seen that the slope of the curve in the negative resistance region is quite steep. The achievement of small signal current gains greater than one requires that the tunnel diode operate in its negative resistance region. This condition is equivalent to biasing the series combination somewhere in its negative resistance region. For this condition, the given value of R_A corresponds to a small signal current gain of approximately -3 in the series combination and +5 in the parallel combination. The steepness of the slope increases as the small signal gain

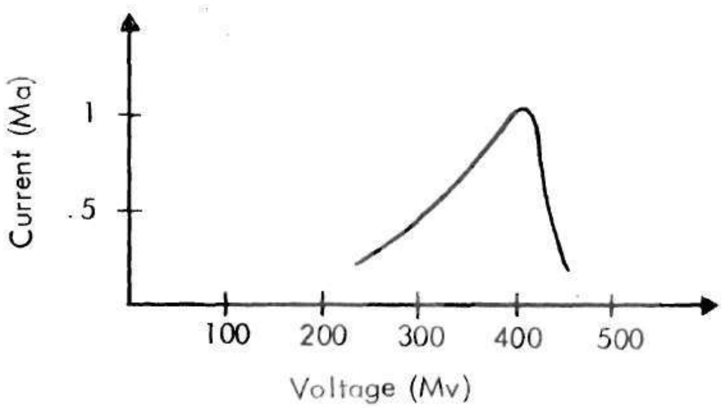

Figure 55. Volt-ampere Characteristic of Series Combination of 80 ohm Resistor, 1N3713, and 2N2189 Emitter base Junction.

increases. Therefore the inverse of the slope, $-R$, is quite small.

Since R_s must be less than $|-R|$ in order that the bias point in the negative resistance region is a stable equilibrium point, the bias source must be carefully designed to provide the required small R_s in a given case. The range of voltages over which the series combination exhibits a negative resistance ia also seen to be small. Therefore, E_2 must also be capable of fine voltage adjustment and exhibit good stability with regard to environmental changes and time.

Both proposed methods of realizing E_2 meet these requirements if properly designed. These stringent requirements on the bias source E_2 were found to be more of a limiting factor on the practical use of the combinations than small signal stability or other considerations. The increase in gain-bandwidth must be worth the increased complexity of biasing.

CHAPTER V

PROCEDURE AND INSTRUMENTATION

To evaluate the theoretical methods of Chapter III by comparing predicted behavior with the actual behavior of experimental amplifiers, several pieces of equipment were designed. The first was an apparatus to accurately measure the volt-ampere characteristic of tunnel diodes. This characteristic is difficult to measure due to the inherent instability of the tunnel diode in the negative resistance region. A simplified schematic of the circuit used is given in Figure 56. A resistance of value R_4 is placed in parallel with the tunnel diode to make the combination a small signal stable network. Admittance measurements on actual resistors were

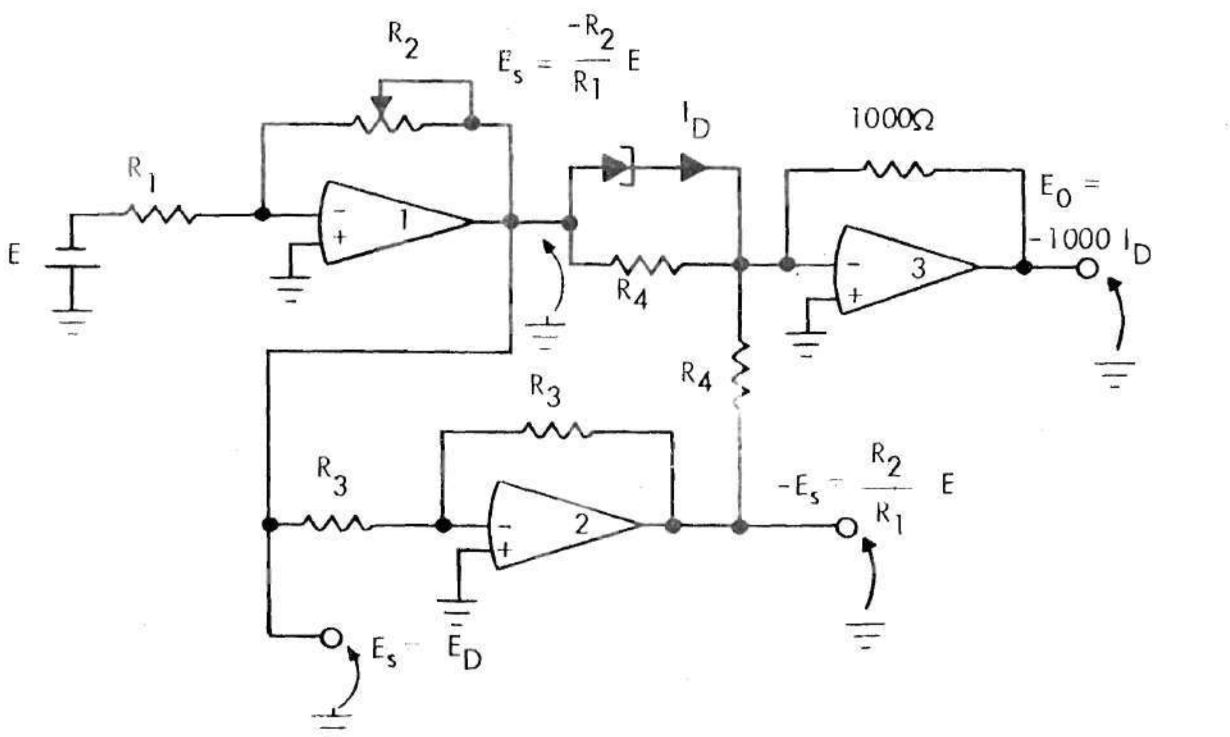

Figure 56. Simplified Schematic of Tunnel Diode Measurement Circuit.

made for frequencies as high as one GHz. For thin film resistors it was ascertained that the DC resistance in series with a small inductance represented an adequate network model. The small signal network for a thin film resistor and a tunnel diode in the negative resistance region is given in Figure 57. Sufficient conditions for this network to have all poles and zeros in the left half of the complex frequency plane are:

$$R_4 < R - r_s \tag{5.1}$$

$$\frac{L}{R_4} < RC \tag{5.2}$$

$$L_s < r_s RC \tag{5.3}$$

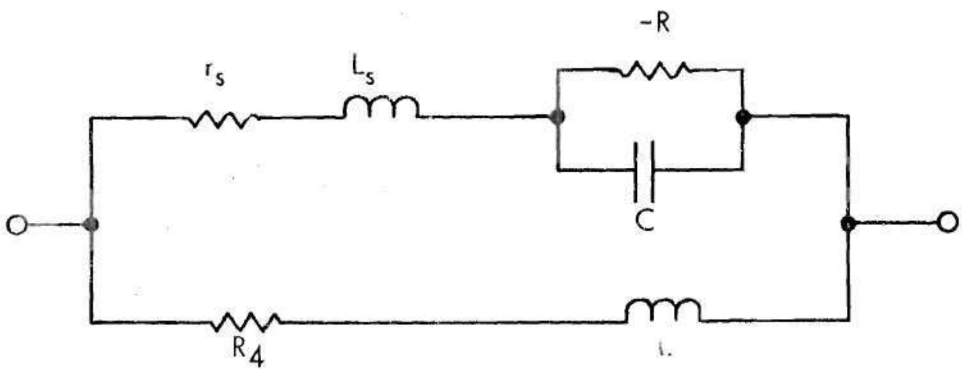

Figure 57. Small Signal Network for Thin Film Resistor and Tunnel Diode in Negative Resistance Region.

The inequality given in equation (5.3) is dependent only on the tunnel diode model parameters. Therefore, if the parameters of the tunnel diode model have values such that this inequality does not hold, then a stable network might be unattainable by paralleling the tunnel diode with any value of thin film resistor. The DC resistance of R_4 can be easily chosen from inequality (5.1). Inequality (5.2), however, places a limit on the time constant of the actual resistor. Since the tunnel diode RC time constant can be quite small, it is seen that the lead inductance of the resistor must be minimized. For this reason, the test jig containing the tunnel diode and thin film resistor must be carefully designed and constructed for low values of the above inductances.

The DC operation of the measurement circuit of Figure 56 is as follows. The output voltage E_s of operational amplifier 1 equals $-\frac{R_2}{R_1}E$, where E is a constant reference voltage. Since E is a negative voltage, E_s is positive. R_2 is variable and can be set at any value between zero and R_{2max}. Thus E_s has a range from zero to $-\frac{R_{2max.}}{R_1}E$. The output of operational amplifier 2 is $-E_s$. For a high gain operational amplifier with feedback, the amplifier input voltage is virtually zero. Therefore, the total current, I_T, flowing into the negative input of operational amplifier 3 is easily calculated, and

$$I_T = I_D + \frac{E_s}{R_4} - \frac{E_s}{R_4} \tag{5.4}$$

Thus the current in R_4, the stabilizing resistance, is subtracted out by the operational amplifier 2 circuit. For an ideal operational amplifier with feedback to the negative input, all the input current flows through the feedback resistor. Therefore, the output voltage of operational amplifier 3 is $-1000\ I_D$.

By connecting the outputs of operational amplifiers 1 and 3 to an xy recorder, one can easily generate the tunnel diode volt-ampere characteristic by varying R_2 from zero to its maximum value. The tunnel diode voltage is the output voltage of amplifier 1 and 1000 times the tunnel diode current is the output voltage of amplifier 3. This method produces an accurate repeatable curve. The schematic of the actual measurement circuit is given in Figure 58. After plotting the volt-ampere curve for a particular diode, one uses this curve to choose the bias point in the negative resistance region and to calculate R for the region around this point. Since the tunnel diode negative resistance $(-R)$ is only constant over a relatively small voltage region, a large accurate curve, as can be generated by this circuit, is most useful.

Accurate wide band y-parameter measurements were required for a particular transistor. From these measurements, the parameter values of the common base model for the transistor could be calculated. This transistor would be then used in the experimental amplifiers to compare the predicted and actual behavior. There was no equipment available in the School of Electrical Engineering that was adequate for these measurements. Radiation Inc., however, had the capability to make such measurements and graciously provided these measurements. The transistor chosen for the measurements was a 2N2189 which has an f_α of approximately 150 MHz. This choice was based upon the discrete nature of the components in the experimental amplifiers. With discrete elements and the available construction techniques, 200 MHz seemed an appropriate upper bound for measurements on the experimental amplifiers. Lumped element circuit theory analysis above this frequency would be inaccurate due to the size of the circuit. The availability of hybrid or integrated circuit facilities would have greatly increased this upper bound. For the measured transistor, the model parameter values producing the closest correspondence between the model behavior

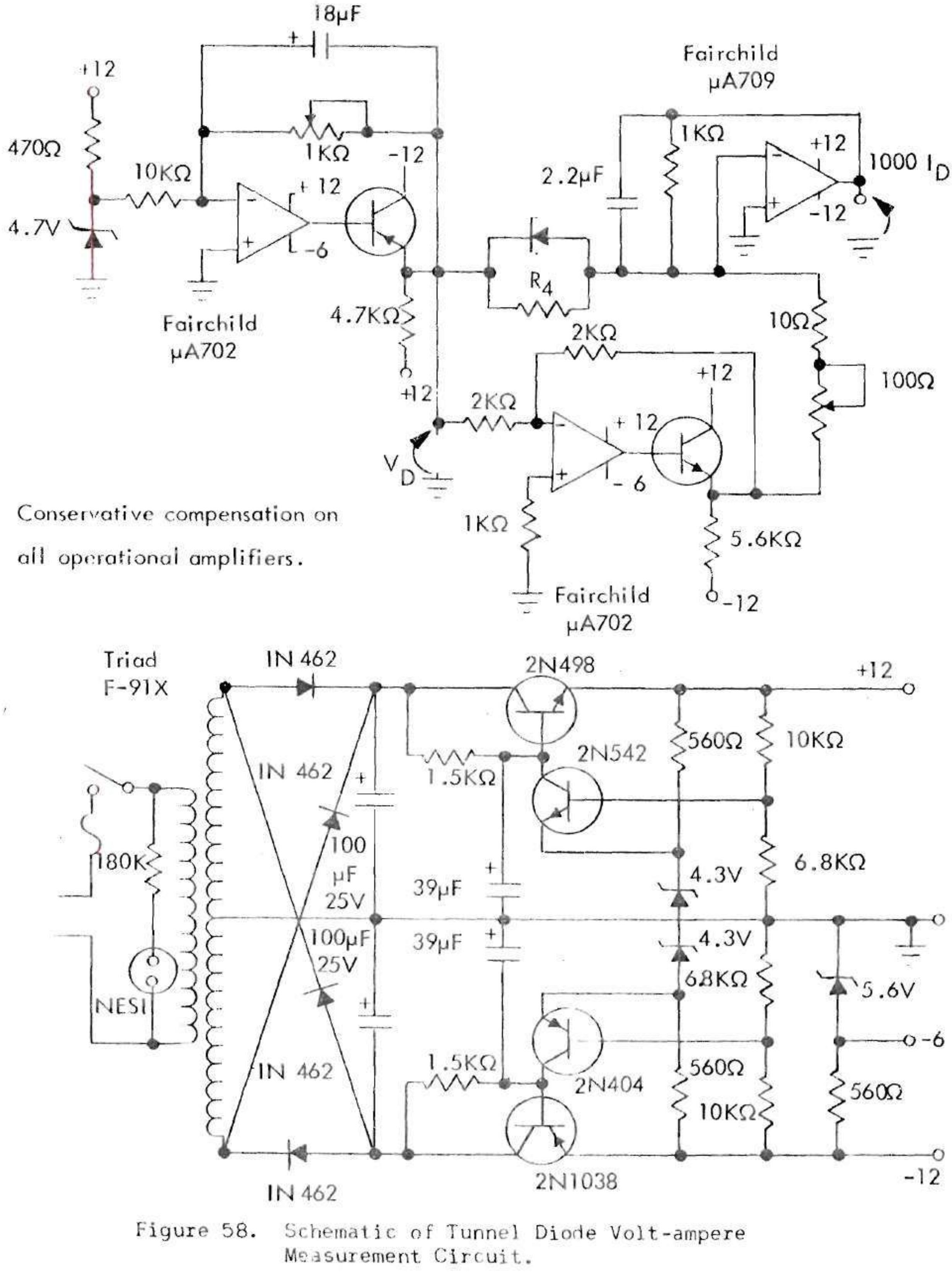

Figure 58. Schematic of Tunnel Diode Volt-ampere Measurement Circuit.

and the transistor measurements were chosen. The unilateral model for this transistor, with the load impedance at low frequency equal to 50 ohms, is given in Figure 59.

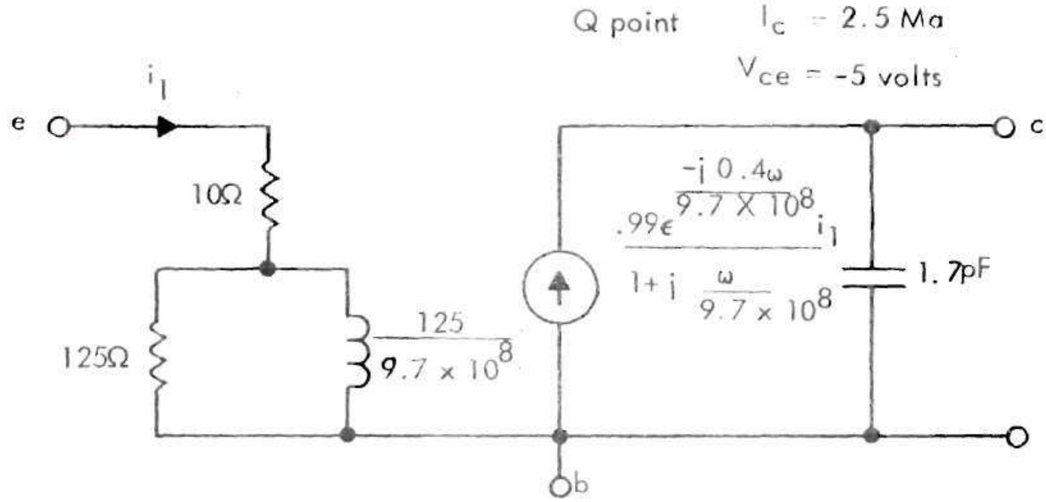

Figure 59. Unilateral Common Base Model for a 2N2189 Transistor.

Since each point on a curve of gain-bandwidth versus ω_{3db} represents the behavior of a particular amplifier, a general experimental amplifier apparatus was desired in which any particular amplifier could be easily realized. Inspection of Figures 33 and 34 reveals that the gain i_{j+1}/i_j is from one dependent current source to the next. The oscillator used in the research had a calibrated output if its load was 50 ohms. For these reasons a two transistor circuit was designed. The first transistor was used to match the oscillator output and to provide a current source input for the network containing the tunnel diode and the common-base input of the second transistor. Its f_α should be much greater than the second transistor so that its current transfer function is constant over the frequency range of interest. The second transistor is the test transistor. Its output was connected to a standard 50 ohm load for measurement ease.

A simplified small signal circuit for the configuration is given in Figure 60. The common-base input of the first transistor and a compensation network presents a 50 ohm load to the oscillator. Therefore e_1 can be read

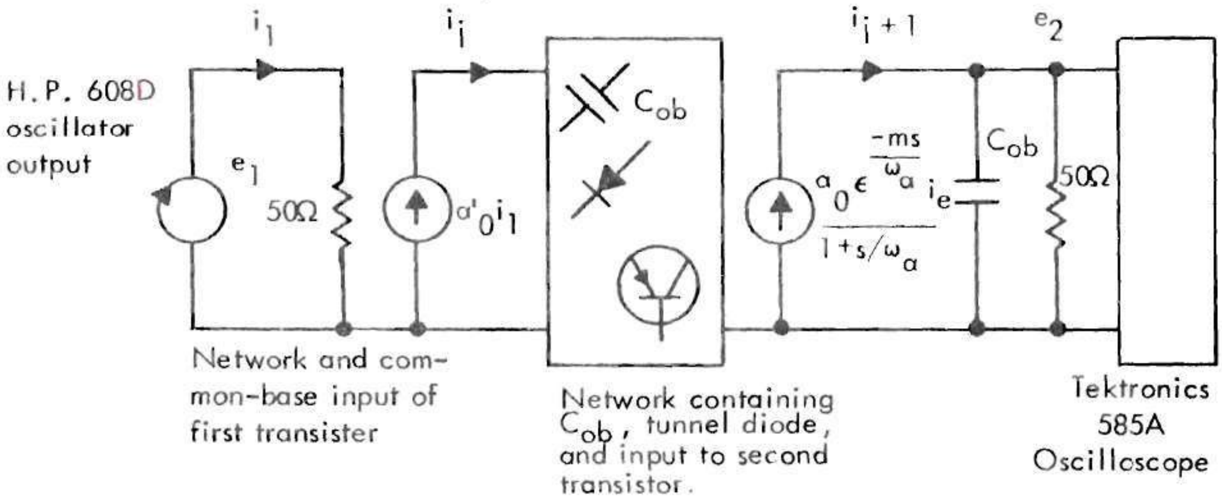

Figure 60. Simplified Small Signal Circuit of General Amplifier Configuration.

from the oscillator's calibrated output. The input current i_1 equals $\frac{e_1}{50\Omega}$ and i_j equals $\alpha_o' \frac{e_1}{50\Omega}$. The current i_{j+1} flows into the parallel combination of the C_{ob} of the second transistor, the standard 50 ohm load, and the input impedance of the Tektronix 585 oscilloscope. For the frequency range of interest this parallel combination can be made to equal approximately 50 ohms. For this condition $e_2 = i_{j+1}$ (50) or $i_{j+1} = \frac{e_2}{50}$. The voltage e_2 is measured by the oscilloscope. Therefore one has the relation

$$\frac{i_{j+1}}{i_j} = \frac{\frac{e_2}{50}}{\alpha_o' \frac{e_1}{50}} = \frac{1}{\alpha_o'} \frac{e_2}{e_1} \approx \frac{e_2}{e_1} \tag{5.5}$$

The first transistor's beta is chosen such that α_o' is very close to one. The complete schematic for the general amplifier design is given in Figure 61. The input transistor is a selected 2N2415 which has an f_α of approximately 1.3 GHz. Due to the previously discussed problems associated with biasing, the bias source has a ten turn potentiometer as the feedback resistor for the operational amplifier. This allows very fine adjustment of the bias voltage. The series combination of Chapter III is produced by connecting R_3', C_3' and the tunnel diode to terminals A, B, and C as shown in Figure 62. The parallel combination is produced by connecting R_3, C_3 and the tunnel diode to terminals A, B, C as shown in Figure 63. For particular tunnel diodes, the measured 2N2189, and various values of the other network variables, the general amplifier apparatus was used to measure actual behavior of the series and parallel combinations of Figures 33 and 34.

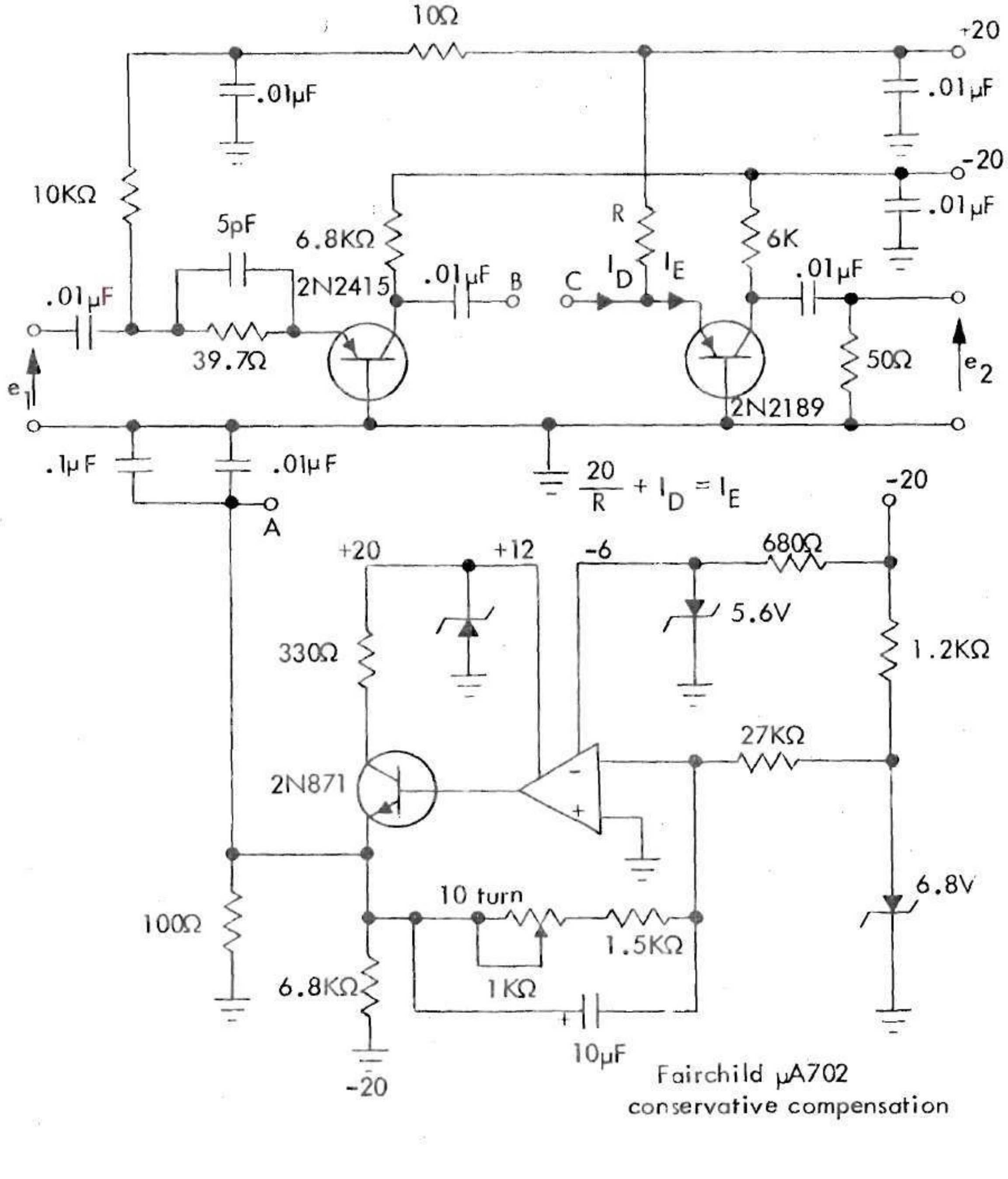

Figure 61. Schematic of General Amplifier Apparatus Used to Generate Particular Amplifiers.

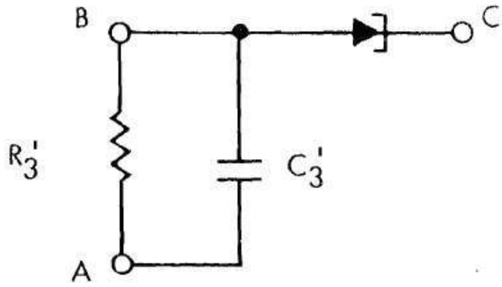

Figure 62. Network Connections to Terminals A, B, C of General Amplifier Apparatus to Produce Series Combination of Figure 33.

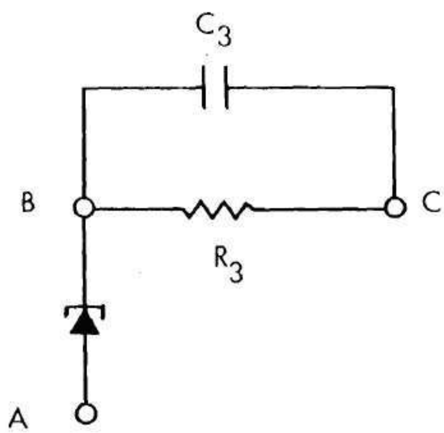

Figure 63. Network Connections to Terminals A, B, C of General Amplifier Apparatus to Produce Parallel Combination of Figure 34.

CHAPTER VI

DISCUSSION OF RESULTS

Predicted versus Experimental Performance for a Set of Amplifiers

Using the general amplifier apparatus of Chapter V, a number of experimental amplifiers were built. The behavior of the current gain i_{j+1}/i_j versus frequency was measured for each amplifier. The tunnel diodes were JEDEC numbers 1N3712, 1N3713, 1N3714, and 1N3715. The 1N3712 and 1N3713 are 1 ma peak current tunnel diodes with R in the range from about 125 ohms to 150 ohms. The 1N3714 and 1N3715 are 2.2 ma peak current tunnel diodes with R in the range from about 45 ohms to 65 ohms. These tunnel diodes are general purpose types in the miniature axial package.

To evaluate the correspondence between predicted and experimental amplifier behavior for the 1 ma peak current tunnel diodes, consider Figure 64. Here, the predicted behavior for the network variables corresponding to the actual devices is plotted for both the series combination of Figure 33 and the parallel combination of Figure 34. The experimentally derived behavior of the amplifiers is given in the form of triangles on the graphs. It is seen that the correspondence between the predicted and actual behavior is quite good, especially considering the accuracy of high frequency measurements.

For the 2.2 ma peak current tunnel diodes the stability criterion built into the computer program predicted that the amplifiers of both the series and parallel combination should be unstable. This was found to be

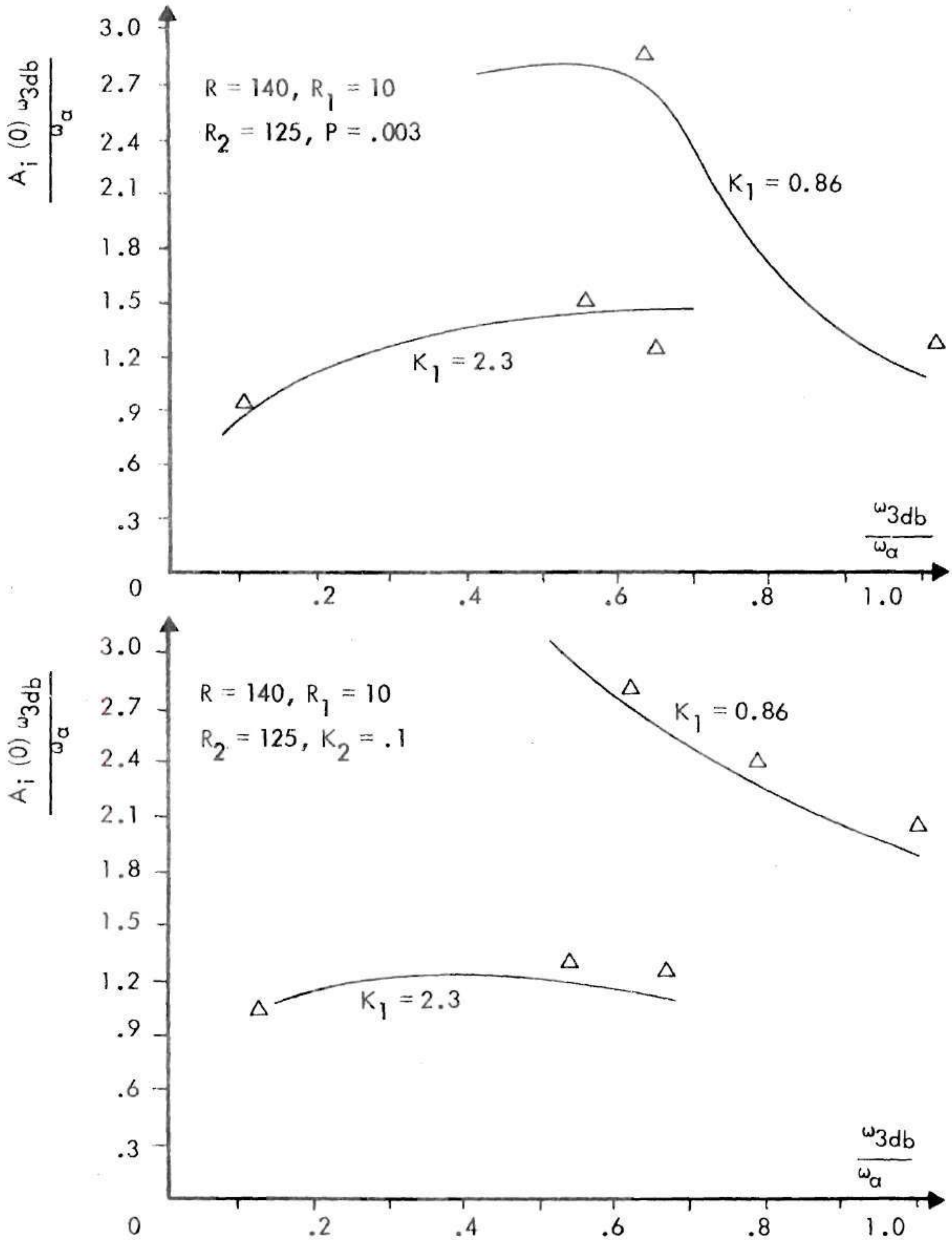

Figure 64. Predicted Versus Measured Performance for a Set of Amplifiers.

correct experimentally. Thus the methods of Chapter III also seem to be adequate for stability predictions.

In summary, the experimental studies indicated that the methods developed to theoretically investigate the behavior of the combinations are reasonably accurate. The main difficulty encountered in the experimental studies was with biasing. This was due to the steepness of the slope in the negative resistance region of the volt-ampere characteristic of the series combination of the emitter-base junction, tunnel diode, and external resistance. Therefore, as previously discussed, the bias source must have very low internal impedance and be capable of fine voltage adjustments. Stability problems due to stray capacitance, lead inductance, etc. were not encountered. It was noted earlier that for the network variable K_1 as small as one, stability predictions could be in error. For the amplifiers built, however, no problems of this nature were encountered. It should be noted that each triangle in Figure 64 represents the results of building a particular amplifier, achieving a stable bias point, and then measuring i_{j+1}/i_j for that amplifier over a wide bandwidth. For illustration purposes, a picture of the general amplifier apparatus is given in Figure 65. A picture of the experimental setup is given in Figure 66.

A Design Example

To illustrate the use of the combinations and the methods of theoretically investigating combination behavior, the following design example is presented. Assume that the transistors to be used are 2N2189's. The specifications for each amplifier stage are that $A_i(0)$, the low frequency current gain, should be at least three due to signal to noise considerations

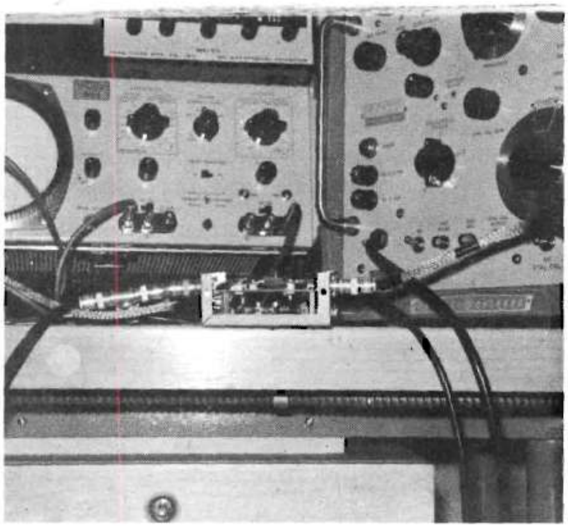

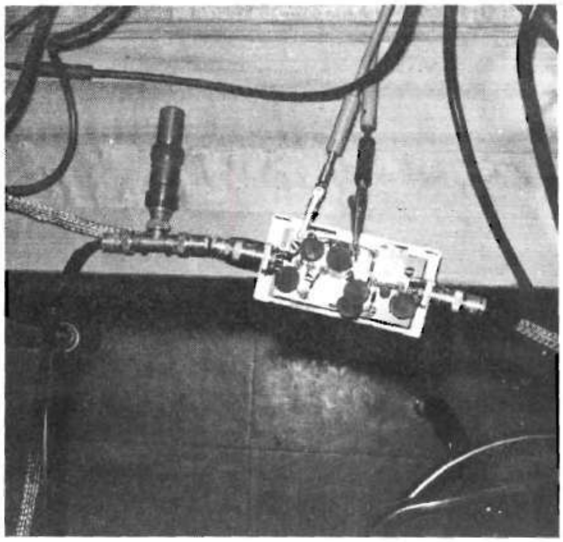

Figure 65. General Amplifier Apparatus.

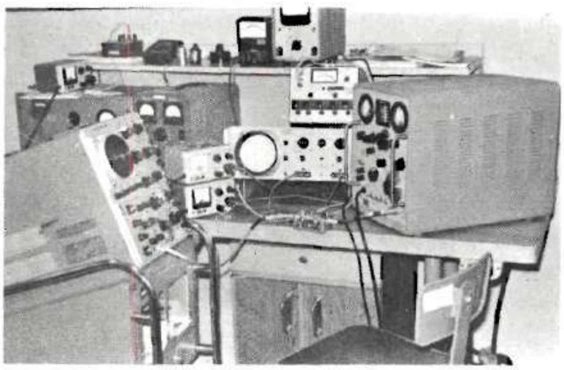

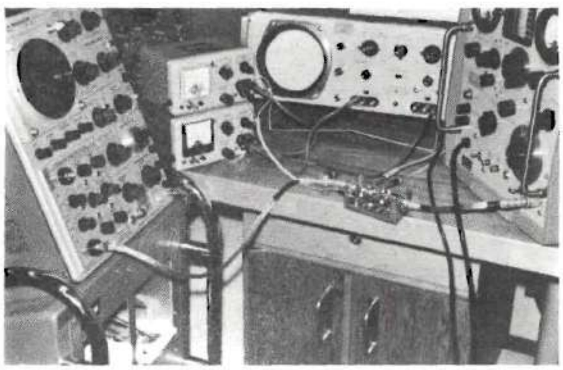

Figure 66. Experimental Setup for Measuring Combination Performance.

and that ω_{3db} should be greater than or equal to 75 MHz. Combining $A_i(0) \geq 3$ and $\omega_{3db} \geq 75$ MHz, it is seen that gain-bandwidth must be greater or equal to 225 MHz. The load impedance is given as 50 ohms.

In the previous experimental work, the transistor used had extensive measurements made on it in order to compare predicted and experimental behavior. In a practical design situation, however, one is normally interested in meeting the design objectives with any transistor of the given type in the circuit and therefore takes a worst case approach to the design problem. This approach is taken here. Since the gain equations, stability criteria, etc. have already been given for the series combination of Figure 33 and the parallel combination of Figure 34, the amplifier configuration will be chosen from these two combinations. For given network variables, $A_i(0)$ is larger for the parallel combination. Thus a given gain can be realized with a smaller R_A in the parallel combination. This aids biasing in that the slope of the negative resistance region of the dc series combination is smaller. Therefore the parallel configuration is chosen.

Using the 2N2189 data sheet, the ranges on the parameters of the unilateral common-base hybrid model of Figure 32 are found. This model with the possible range of parameter values for the 2N2189 is given in Figure 67. The method of obtaining these parameter ranges using the data sheet and some additional information is given in Appendix I.

Preliminary investigation using the computer revealed that for 2.2 ma and greater peak current tunnel diodes, the amplifier should be unstable. This is primarily due to the magnitude of R_2 in the model in relation to the negative resistances of the tunnel diodes. The next lowest

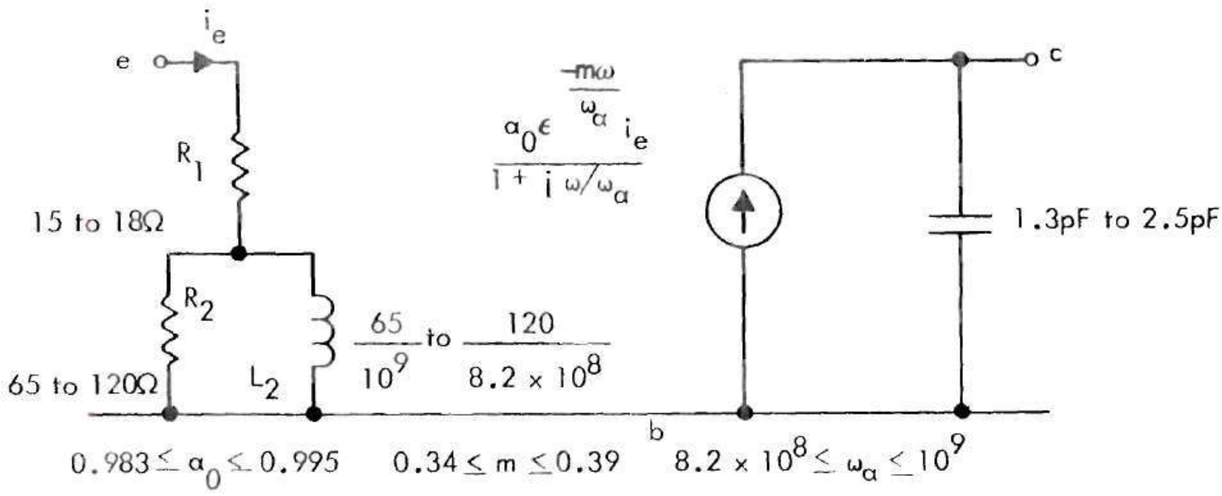

Figure 67. Range of Model Parameter Values for 2N2189 Unilateral Hybrid Common-base Model. Quiescient Point: -1.5 ma, -9 volts.

peak current is about 1 ma. Therefore a 1 ma peak current tunnel diode was chosen for the amplifier stage. Consideration of various tunnel diodes revealed that a 1N3713 should be adequate in that its model parameters had reasonably small variance and its 1/RC was greater than ω_α of the 2N2189. With $\frac{1}{RC} > \omega_\alpha$ the addition of external capacitance can trim the resultant 1/RC to the desired fraction of ω_α.

Using these values in the computer program, it was found that K_1 and K_2 as small as possible gave maximum gain-bandwidth. For stability reasons one has already been given as a lower limit for K_1. Therefore choose $K_1 = 1$. Since there will be a small amount of stray capacitance across R_3, K_2 is chosen as 0.2 instead of 0. Since $\frac{1}{R_3C_3}$ is now five times ω_α, the effect of this time constant is quite small and is effectively zero.

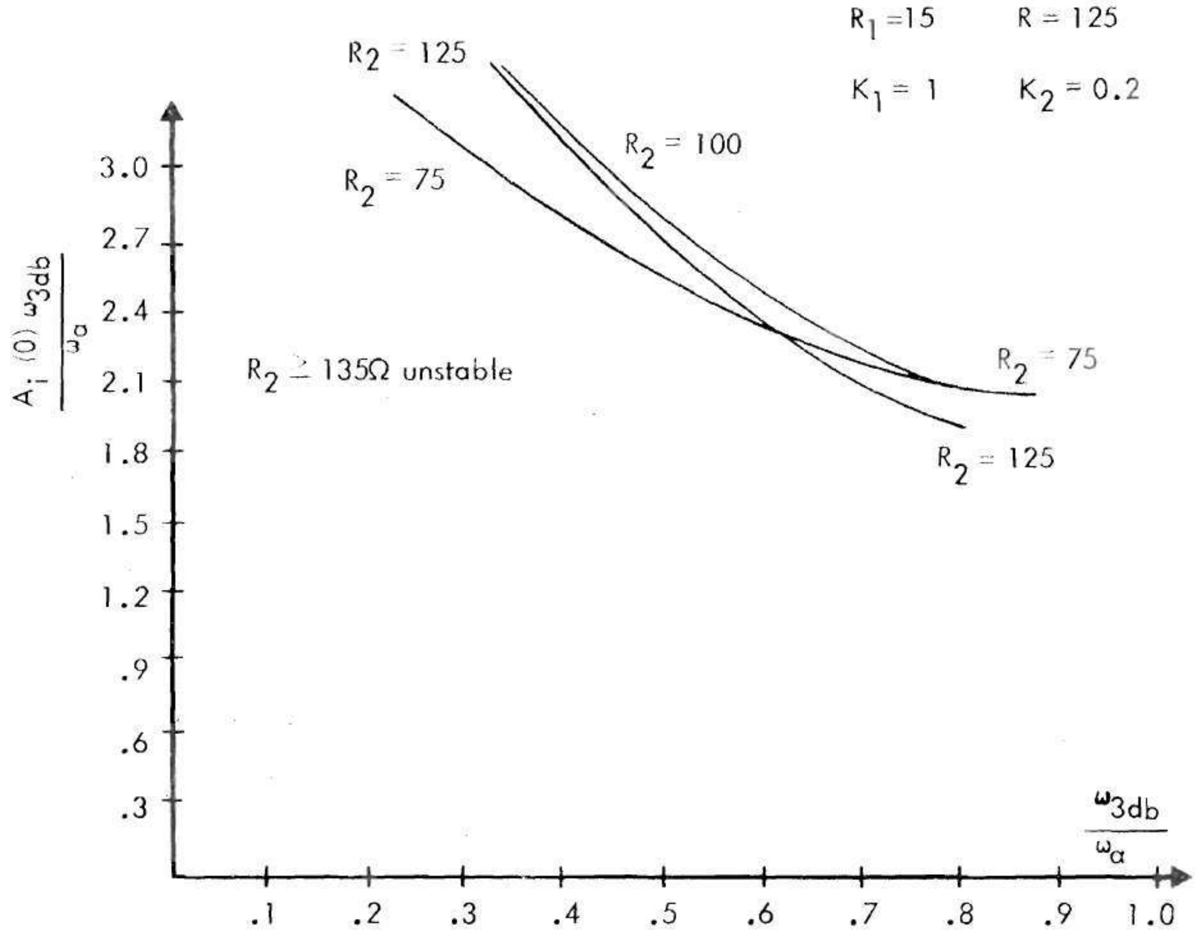

Figure 68. Normalized Gain-bandwidth versus Normalized ω_{3db} for Parallel Combination of Figure 33.

For $K_1 = 1$, $K_2 = 0.2$, $R_{avg.} = 125\Omega$, and $R_{1_{avg.}} = 15\Omega$ the computer data is plotted in the form of Figure 65. R and R_1 have small variance from their average values, and K_1 and K_2 are picked to be their respective values for maximum gain-bandwidth. Therefore this graph may be used to find if the design objectives can be met. The average value of f_α for the 2N2189 is 150 MHz and 75 MHz is 0.5 f_α. Since there is some variance of f_α, it is required that normalized ω_{3db} be at least 0.6 so that the minimum bandwidth criterion of 75 MHz is met. Then for a minimum gain of three, normalized gain-bandwidth must be at least 3 x .06 or 1.8. Thus if the design objectives are to be met, normalized gain-bandwidth at normalized ω_{3db} equal to 0.6 must be at least 1.8 for the range of values for R_2. Consideration of Figure 68 reveals that the objectives can be met. It was decided to choose element values so that the design center value of $A_i(0)$ would be 3.5. The variance of the elements somewhat from their design center values should still yield an $A_i(0)$ of at least three.

The design is now complete. The tunnel diode time constant is adjusted to equal one times ω_α average. No external capacitance is placed across R_3 and due to stray capacitance K_2 is considered to be 0.2. The transistor Q point is -1.5 ma, -9 volts. Finally R_3 is chosen to yield an $A_i(0)$ equal to 3.5 for the average values of R_1 and R. These average values are 15 ohms and 125 ohms respectively. Using the gain equation

$$A_i(0) = \frac{-R'}{R_1 + R_3 - R'} \tag{6.1}$$

R_3 is found to be 75 ohms.

The general amplifier apparatus was used to build four such amplifiers using four different 2N2189's. The results are given in Table 3. It is seen that the design objectives were met for each amplifier. Since average f_T for the 2N2189 is about 100 MHz, the average gain-bandwidth of about 270 MHz obtained in this example was 2.7 times the present limit obtainable with ordinary broadbanding techniques. The data in Table 3 can also be considered as further confirmation of the methods for theoretical investigation of combination behavior.

Table 3. Performance of Experimental Amplifiers in Design Example.

Amplifier Number	$A_i(0)$	f_{3db} MHz	GBW MHz
1	3.06	80	248
2	3.32	85	283
3	3.56	80	285
4	3.06	85	260

CHAPTER VII

CONCLUSIONS AND RECOMMENDATIONS

As a means of achieving gain-bandwidths greater than ω_T, it was initially proposed to use the tunnel diode as an interstage element between common-base transistor stages. To this end, a class of tunnel diode-common-base transistor combinations was evolved. Methods for theoretically investigating and predicting combination behavior were developed. The validity of these methods was established by comparing the predicted and experimental performance of a set of amplifiers.

For various combinations with either six or seven normalized network variables, it was found that gain-bandwidths as large as ten times ω_T, the current limit are easily obtainable. In studying combination behavior only values of the network variables were allowed that corresponded to actual devices and also satisfied stability and biasing requirements. Two of the combinations studied have been given in the dissertation to illustrate the development of the methods for investigating combination behavior. Four more are discussed in Appendix III. Quite obviously only a finite set of the infinite number of possible combinations could be investigated. From the investigation of other members of the class of combinations it may be found that further increases in gain-bandwidth are obtainable.

For situations requiring gain-bandwidths greater than the current limit, the class of combinations affords a means of achieving gain-bandwidths at least an order of magnitude larger. There are, however, small signal stability and biasing complexity problems associated with the class of combinations. In a practical situation, one must weigh the advantages of a given combination against its disadvantages. Small signal stability does not seem to be a serious problem. Careful consideration must be given to the circuit size, layout, and method of construction for the frequency range of interest. If the circuit size is such that the lumped element methods of analysis developed are valid, then stability predictions should be accurate. It was discussed that small signal stability predictions could be in error as the normalized tunnel diode time constant approaches one. For the experimental work performed by the author, stability predictions for normalized tunnel diode time constants as small as one were found to be accurate.

Biasing requirements were found to be the main disadvantage of such combinations. The bias source must have very low internal resistance and must be capable of very fine voltage adjustments. The effect of temperature on biasing stability must also be considered. For a given small signal gain, the slope of the volt-ampere characteristic in the negative resistance region of the series combination of tunnel diode, emitter-base junction, and external resistance decreases as the tunnel diode peak current decreases. Since the stringency of the requirements on the bias source are directly proportional to the steepness of this slope, it is recommended that the tunnel diode peak current be as small as possible consistent with meeting gain-bandwidth objectives.

For a given small signal gain the steepness of this slope is normally less for a parallel combination than for a series combination of same degree of complexity. Therefore, if maximum gain-bandwidths are about the same for both combinations, the parallel combination should be chosen over the series combination in order to relax the restrictions on the bias source.

In conclusion, it should be noted that many approaches using the tunnel diode as an amplifying device have been primarily theoretical, in that biasing and sometimes small signal stability considerations have not received sufficient attention. The inclusion of these considerations would force radical changes in many of the proposed amplifier configurations and would render others unusable. The emphasis in this investigation has been on developing a class of combinations which could be stably biased and for which small signal stability could be predicted. Toward this end, only values of the network variables have been allowed which correspond to actual devices, allow stability predictions to be made, and are practical from biasing considerations.

APPENDIX I

METHOD FOR OBTAINING ELEMENT VALUE RANGES OF UNILATERAL H MODEL

The method of obtaining the parameter value ranges of the unilateral common-base hybrid model of Figure 32 for a particular type of transistor is illustrated for the 2N2189. For convenience, the model of Figure 32 is repeated in Figure 69. In Table 4 pertinent data from the

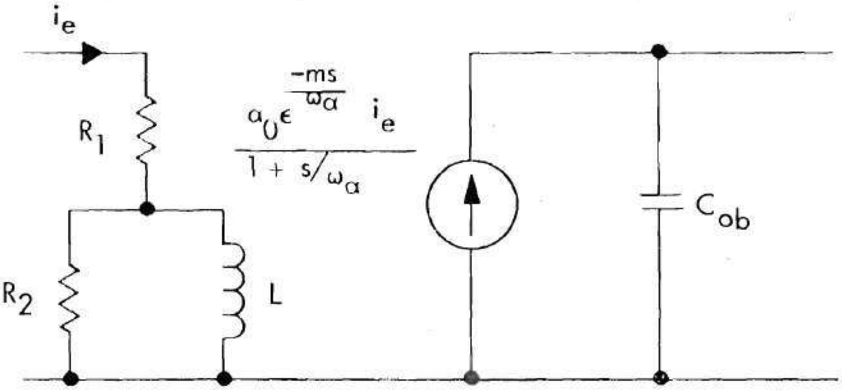

$$R_1 = r_e' + (1-\alpha_0)\, r_b' \qquad R_2 = \alpha_0\,(1+m)\, r_b' + \alpha_0 R r_b' C_c \omega - r_e'$$

$$L = \frac{\alpha_0\,(1+m)\, r_b' - r_e'}{\omega_\alpha} + \alpha_0 R r_b' C_c$$

$$R = Z_L|_{\omega \to 0}$$

Figure 69. Unilateral Common-base Hybrid Model.

the 2N2189 data sheet are given. First, the most stringent condition for model use should be checked. This condition is that $1/r_b'C_c$ should be much greater than ω_α. In Table 4 it is seen that maximum $r_b'C_c$ equals 125 picoseconds. Therefore minimum $1/r_b'C_c$ is 8×10^9 which is much greater than 9.4×10^8, the average ω_α.

Table 4. Data from the Texas Instruments Inc. 2N2189 Data Sheet

Parameter	Test Conditions	Minimum	Average	Maximum	Units
h_{fe}	$f = 1KHz$ $I_C = -1.5ma$ $V_{CE} = -9v$	60	135	180	
f_T	$I_C = -1.5ma$ $V_{CE} = -9v$	102	110	-	MHz
$f_{h_{fb}}$	$I_E = 1.5ma$ $V_{CB} = -9v$	-	150	-	MHz
C_{ob}	$V_{CB} = -9v$ $I_E = 0$ $f = 1MHz$	-	1.6	2.5	pF
$r_b'C_c$	$V_{CB} = -9v$ $I_E = 1.5ma$ $f = 31.9MHz$	-	90	125	psec

At $I_E = 0$, the average value of C_{ob} is 1.6pF and the maximum value is 2.5pF. C_{ob} is the capacitance measured between collector and base when the emitter is a small signal open circuit. At $I_E = 0$, C_{ob} equals $C_c + C_{cb} + \frac{C_{ce}C_{eb}}{C_{ce}+C_{eb}}$ where C_{cb}, C_{ce}, and C_{cb} are header capacitances including overlap diode capacitances. The 2N2189 is encapsulated in a TO-58 case and has a $(C_{cb} + \frac{C_{ce}C_{eb}}{C_{ce}+C_{eb}})$ value of approximately 1.05pF. Therefore maximum C_c equals about 1.45pF and average C_c equals about 0.55pF. Since minimum C_{ob} is not given, minimum C_c will have to be estimated. Such estimates must be based upon experience, the physical structure of the transistor, and consultation with the manufacturer. From such considerations, minimum C_c is assumed to be 0.25pF. Therefore minimum C_{ob} is about 1.3pF and the range of C_{ob} has been specified for $I_E = 0$. For $I_E > 0$ and $\omega \ll \omega_\alpha$, C_{ob} equals $(C_c + C_{cb} + (1 - \alpha_o)C_{ce})$ or C_{ob} essentially equals $(C_c + C_{cb})$. Therefore for $I_E = 1.5$ma, the range of C_{ob} is from about 1.25pF to about 2.45pF.

It should be noted that C_{ob} was measured at the desired quiescent point V_{CB}. If V_{CB} for the C_{ob} measurement is different from the desired V_{CB}, then one must first calculate the range of C_c at the C_{ob} measurement V_{CB} as above. Then the range of C_c at the desired V_{CB} is calculated from the power law variation of this capacitance with V_{CB}. Finally the range of C_{ob} at the desired V_{CB} is found by adding C_{cb} to the adjusted range of C_c values.

It is seen that r_b' and $r_b'C_c$ appear in the expression for several of the parameters of the model. Maximum $r_b'C_c$ is given as 125 picoseconds, and average $r_b'C_c$ is given as 90 picoseconds. The minimum value of $r_b'C_c$ must also be estimated. A reasonable value for this type of transistor is about 15 picoseconds. The range of $r_b'C_c$ is now specified. This range in conjunction with the range of C_c is used to estimate the range of r_b'. Assuming low correlation between r_b' and C_c, the maximum value of $r_b'C_c$ occurs for maximum r_b' and maximum C_c. Therefore

$$r_b'{}_{max} \approx \frac{(r_b'C_c)_{max.}}{C_{c\ max.}} \tag{A1.1}$$

Using the maximum values of $r_b'C_c$ and C_c, maximum r_b' is found to be about 90 ohms for the 2N2189. Likewise, it is seen that

$$r_b'{}_{min} \approx \frac{(r_b'C_c)_{min.}}{C_{c\ min.}} \tag{A1.2}$$

Using the minimum values of $r_b'C_c$ and C_c, the minimum value of r_b' is found to be about 60 ohms.

Since $f_{h_{fb}} \approx (1+m)f_T$ for a transistor with $\frac{1}{r_b'C_c} > \omega_\alpha$, m can be found by calculating $(\frac{f_{h_{fb}}}{f_T} - 1)$. In Table 4 it is seen that only f_T average is given. Therefore m average is found to be 0.365 and the minimum and maximum values must be estimated. A reasonable range for m seems to be from about 0.34 to 0.39.

Next the range of α_o and $(1 - \alpha_o)$ should be found. Since minimum and maximum h_{fe} are given, this is easily accomplished because $\alpha_o = \frac{h_{fe}}{1+h_{fe}}$. For maximum h_{fe} of 180, one calculates a maximum α_o of 0.99443 and a minimum $(1 - \alpha_o)$ of 5.57×10^{-3}. For minimum h_{fe} of 60, one calculates a minimum α_o of 0.9833 and a maximum $(1 - \alpha_o)$ of 1.67×10^{-2}.

The parameter r_e' equals kT/qI_E and at room temperature $KT/q \approx .025$. Assuming I_E equals 1.5 ma, r_e' is approximately 16.65 ohms. Since normal room temperature will vary somewhat, assume that r_e' is between 15 and 17.5 ohms.

For $1/r_b'C_c \gg \omega_\alpha$, the frequency $f_{h_{fb}}$, at which common-base h_{21} is down 3db from its low frequency value, equals f_α. The average value of $f_{h_{fb}}$ and hence f_α is given as 150 MHz. The minimum and maximum values of $f_{h_{fb}}$ are not given. If one assumes that the ratio of average to minimum $f_{h_{fb}}$ to be approximately the same as the ratio of average to minimum f_T, the minimum f_α is found to equal approximately 135 MHz. The maximum value of f_T is not given, so maximum f_α is estimated to be about 165 MHz.

Using the above derived and estimated ranges, the parameter ranges of R_1, R_2, and L can be found. Assuming fairly low correlation between r_e', α_o, and r_b'; then

$$R_{1\,min} \approx r_e{}'_{min} + (1 - \alpha_o)_{min} \cdot r_b{}'_{min} \tag{A1.3}$$

For the 2N2189 values minimum R_1 is found to be about 15 ohms. Likewise

$$R_{1\,max} \approx r_e{}'_{max} + (1 - \alpha_o)_{max} \cdot r_b{}'_{max} \tag{A1.4}$$

The maximum value of R_1 is found to be about 19 ohms.

Examination of the R_2 expression reveals that

$$R_{2\,max} \approx \alpha_{o\,max}\,(1 + m_{max})r_b{}'_{max} + \alpha_{o\,max}\,50(r_b{}'C_c)_{max}\,\omega_{\alpha\,max} - r_e{}'_{min} \tag{A1.5}$$

This value is found to be approximately 120 ohms for the 2N2189. Likewise it is seen that

$$R_{2\,min} \approx \alpha_{o\,min}\,(1 + m_{min})r_b{}'_{min} + \alpha_{o\,min}\,50(r_b{}'C_c)_{min}\,\omega_{\alpha\,min} - r_e{}'_{max} \tag{A1.6}$$

The minimum value of R_2 is found to be 65 ohms.

In similar fashion an examination of the L expression yields

$$L_{max} \approx \frac{\alpha_{o\,max}\,(1 + m_{max})r_b{}'_{max} - r_e{}'_{min}}{\omega_{\alpha\,min}} + \alpha_{o\,max}\,50(r_b{}'C_c)_{max} \tag{A1.7}$$

The value of maximum L is calculated to be about 1.4×10^{-7} henries. Similarly

$$L_{min} \approx \frac{\alpha_{o\ min}(1 + m_{min})r_{b\ min}' - r_{e\ max}'}{\omega_{\alpha\ max}} + \alpha_{o\ min}\ 50(r_b'C_c)_{min} \qquad (A1.8)$$

This value is found to be about 6.3×10^{-8} henries for the 2N2189.

Now the parameter value ranges have been established. The unilateral model with the ranges derived for the 2N2189 is given in Figure 70. In the previous discussion it has been seen that usually only the maximum or the minimum value of most parameters, but not both, is given on the data sheet. One can obtain the missing value either through measurements or from the manufacturer. This value can also be estimated from experience with the type of transistor structure and some knowledge of semiconductor physics. If the parameters in the unilateral common-base hybrid model have been derived using estimates, then one can allow for possible error by increasing the parameter value ranges by a certain amount. Using the slightly increased ranges, one then does a worst case design.

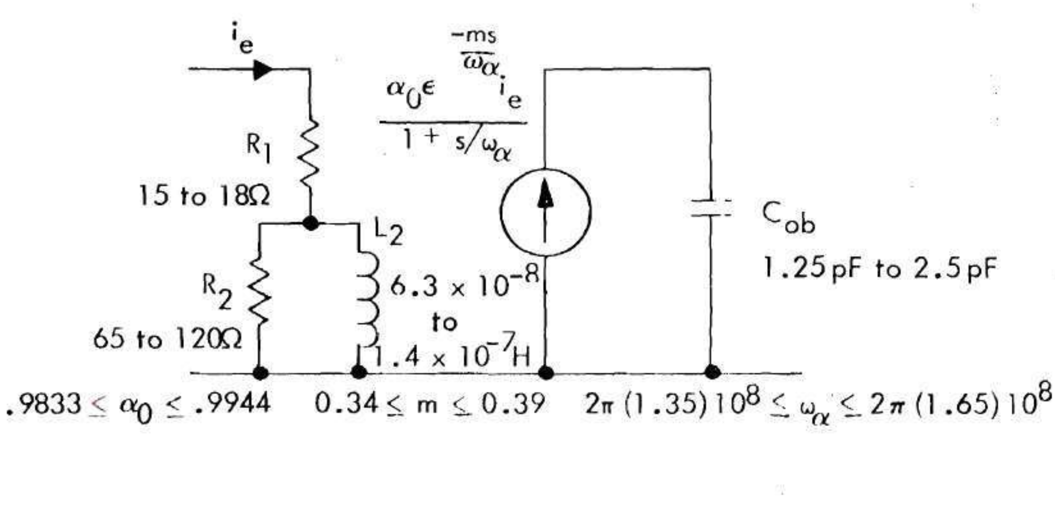

Figure 70. Unilateral Common Base Hybrid Model for the 2N2189.

APPENDIX II

COMPUTER PROGRAMS

The computer programs for the two combinations given in Chapter II for illustration purposes are presented in the following pages. It is to be noted that a variable R_4 appears in both programs that is not present in the combination gain equations. This variable does not appear in the program equations but is merely entered as a variable and printed out. This is done to facilitate the investigation of the two combinations which are the same as the ones in Chapter III except that a resistance is placed in parallel with the tunnel diode. These combinations are discussed in Appendix III. One simply considers R in the programs to be the equivalent negative resistance of the combination. Since the program is run at a given time for one value of peak current tunnel diode, the printout of R_4 tells one what resistance was combined with the tunnel diode in order to produce the value of R given in the program. Due to computer language rules, the network variable R_1' is called R_1 in the program for the series combination. Likewise R' is designated R and C' is designated C in the program for the parallel combination. Both programs are written in extended Algol 60 computer language.

```
          BEGIN
FILE OUT        FO 6(2,15) ;
REAL            K3,P,A,B,C,D,E,F,G,H,M,K2,Y,X,K1,RA;
INTEGER         R,R1,R2,I,J     ;
          ARRAY    POLY,IRT,RRT,YRT,GBW[0:3]  ;
 PROCEDURE FUNCTION(REALE,IMAG,REVAL,IEVAL,ORDER,COEF);COMMENT THE USER
MUST INSERT THE CODING FOR THIS PROCEDURE."REALE"AND "IMAG"ARE THE REAL
AND IMAGINARY PARTS OF THE DEPENDENT VARIABLE.THE REAL AND IMAGINARY PAR
TS OF THE FUNCTION EVALUATED AT THIS POINT MUST BE "REVAL"AND "IEVAL",RE
SPECTIVELY.ORDER IS THE ORDER OF THE POLYNOMIAL BEING EVALUATED WHILE CO
EF IS A COLUMN ARRAY DECLARED FROM ZERO AND CONTAINING THE I TH COEFFICI
ENT AT COEF[I];VALUE REALE,IMAG,ORDER ;INTEGER ORDER ;REAL REALE,IMAG,RE
VAL,IEVAL ;ARRAY COEF[0];BEGIN INTEGER I,I1 ;ARRAY REIM[0:ORDER,0:2];REI
M[1,1]←REALE ;REIM[1,2]←IMAG ;FOR I ←2 STEP 1 UNTIL ORDER DO BEGIN I1 ←I
-1 ;REIM[I,1]←REIM[I1,1]×REALE -REIM[I1,2]×IMAG ;REIM[I,2]←REIM[I1,1]×I
MAG +REIM[I1,2]×REALE ;END ;REVAL ←COEF[0];IEVAL ←0 ;FOR I ←1 STEP 1 UNT
IL ORDER DO BEGIN REVAL ←REVAL +COEF[I]×REIM[I,1];IEVAL ←IEVAL +COEF[I]×
REIM[I,2];END ;END ;
 PROCEDURE MULLER(P1,P2,P3,MXM,NRTS,EP1,EP2,SW1,SW2,SW3,SWR,RRT,IRT,COEF
,OT) ;COMMENT PROCEDURE MULLER FINDS REAL AND COMPLEX ROOTS OF AN ARBIT
RARY FUNCTION.P1,P2,AND P3 ARE STARTING VALUES.THE ROOTS NEAREST TO THES
E POINTS WILL BE FOUND FIRST.MXM IS THE MAXIMUM NUMBER OF ITERATIONS TO
BE MADE IN FINDING ANY ONE ROOT.EP1 AND EP2 ARE CONVERGENCE CRITERION FA
CTORS.IF ABS((X(I+1)-X(I))/X(I+1))IS LESS THAN EP1 OR IF THE FUNCTION VA
LUE AND MODIFIED FUNCTION VALUE ARE BOTH LESS THAN EP2,A ROOT HAS BEEN FO
UND.SW1,SW2,SW3,AND SWR ARE BOOLEAN VARIABLES.IF SW1 IS TRUE,THEN EACH
ITERANT OF EACH ROOT WILL BE PRINTED.IF SW2 IS TRUE THE VALUE OF EACH RO
OT FOUND WILL BE PRINTED.IF SW3 IS TRUE,THEN,WHEN APPLICABLE,THE COMPLEX
 CONJUGATE OF EACH ROOT FOUND WILL BE ADMITTED AS A ROOT.IF SWR IS TRUE
ONLY REAL ROOTS ARE FOUND.SWR SHOULD BE SET TRUE IF IT IS KNOWN THAT THE
 FUNCTION HAS ALL REAL ROOTS.ARRAYS RRT AND IRT CONTAIN THE REAL AND IMA
GINARY PARTS,RESPECTIVELY,OF THE ROOTS FOUND.PROCEDURE FUNCTION IS THE F
UNCTION GENERATOR AND PROCEDURE COMPLEX PERFORMS THE NECESSARY COMPLEX A
RITHMETIC.COEF IS A COLUMN ARRAY WHICH IS PASSED TO THE PROCEDURE FUNCTI
ON .R.D.RODMAN,MRS,22 5018 (PROFESSIONAL SERVICES DIVISIONAL GROUP),CARD
 SEQUENCE BEGINS WITH MULL0001,FIRST RELEASE 5/1/63 ;VALUE P1,P2,P3,MXM,
NRTS,EP1,EP2,SW1,SW2,SW3,SWR ;INTEGER MXM,NRTS ;BOOLEAN SW1,SW2,SW3,SWR
```

```
;REAL P1,P2,P3,EP1,EP2 ;ARRAY RRT,IRT[0],COEF[0];FILE OT1 ;BEGIN BOOLEAN00002000
 BOOL;INTEGER C1,RTC,I,ITC ;REAL RX1,RX2,RX3,IX1,IX2,IX3,RROOT,IROOT,RDN00002100
R,IDNR,T1,IT1,FRROOT,FIROOT,RFX1,RFX2,RFX3,IFX1,IFX2,IFX3,RH,IH,RLAM,ILA00002200
M,RDEL,IDEL,T2,IT2,T3,IT3,T4,IT4,RG,IG,RDEN,IDEN,RFUNC,IFUNC ;LABEL M0,M00002300
1,M2,M3,M4,M9,M8,M6,M7,FIN1,FIN2,FIN3,M10,M12,M11,EXIT ;SWITCH J ←M2,M3,00002400
M4,M7,M11 ;FORMAT OUT F2(X46,"REAL",X12,"IMAGINARY"/X37,E18.11,X4,E18.1100002500
 /X39,"THE FUNCTION EVALUATED AT THIS POINT IS"/X46,"REAL",X12,"IMAGINAR00002600
Y"/X37,E18.11,X4,E18.11 /X35,"THE MOD""IFIED FUNCTION EVALUATED AT THIS 00002700
POINT IS"/X46,"REAL",X12,"IMAGINARY"/X37,E18.11,X4,E18.11 ),F4(///X29,I300002800
," ITERATIONS HAVE BEEN MADE.  THE VALUE OF ""THE ITERANT IS NOW"),F6(//00002900
X37,"SUCCESSIVE ITERANTS MEET CONVERGENCE CRITERION"/X39,"AFTER",I3," IT00003000
ERATIONS.  THE ROOT FOUND IS"),F8(//X33,"THE FUNCTION VALUES OF THE LAST00003100
 ITERANT ARE"" SUFFICIENTLY"/X33,"NEAR ZERO. ",I4," ITERATIONS WERE MA""00003200
DE.  THE ROOT FOUND IS"),F10(//X35,I3," ITERATIONS COMPLETED AND SUCCESS00003300
FUL CONVE""RGENCE"/X41,"HAS NOT OCCURRED.  THE LAST ITERANT IS"),F12(//X00003400
40,"THE PREVIOUS ROOT FOUND WAS COMPLEX.  THE"/X40,"CONJUGATE OF THIS VA00003500
LUE IS ALSO A ROOT.");PROCEDURE COMPLEX(A,IA,B,IB,K,C,IC);VALUE A,IA,B,I00003600
B,K ;INTEGER K ;REAL A,IA,B,IB,C,IC ;BEGIN REAL TEMP ;LABEL MPY,DVD,SQT,00003700
EXIT ;SWITCH JUNCTION ←MPY,DVD,SQT ;GO TO JUNCTION[K];MPY:C ←A×B −IA×IB 00003800
;IC ←A×IB +IA×B ;GO TO EXIT ;DVD:IF B =0 AND IB =0 THEN BEGIN C←1 ;IC←0 00003900
;GO TO EXIT END ;TEMP ←B×B +IB×IB ;C ←(A×B +IA×IB)/TEMP ;IC ←(IA×B −A×IB00004000
)/TEMP ;GO TO EXIT ;SQT:IF (IA=0)AND (A<0)THEN BEGIN C ←0 ;IC ←SQRT(−A)E00004100
ND ELSE IF IA=0 THEN BEGIN C ←SQRT(A);IC←0 END ELSE BEGIN TEMP ←SQRT(A×A00004200
 +IA×IA);C ←SQRT((TEMP+A)/2);IC ←IF (TEMP −A)<0 THEN 0 ELSE SQRT((TEMP−A00004300
)/2)END ;IF((B+C)×(B+C)+(IB+IC)×(IB+IC))<((B−C)×(B−C)+(IB−IC)×(IB−IC))TH00004400
EN BEGIN C ←B−C ;IC ←IB−IC END ELSE BEGIN C ←B+C ;IC ←IB+IC END ;EXIT:EN00004500
D ;FOR I ←1 STEP 1 UNTIL NRTS DO RRT[I]←IRT[I]←0 ;RTC←0 ;M0:IX1←IX2←IX3←00004600
C1←IROOT←ITC←0 ;RROOT←P1 ;BOOL ←FALSE ;M1:C1←C1+1 ;RDNR ←1 ;IDNR ←0 ;FOR00004700
 I ←1 STEP 1 UNTIL RTC DO BEGIN COMPLEX(RDNR,IDNR,RROOT−RRT[I],IROOT−IRT00004800
[I],1,T1,IT1);RDNR ←T1 ;IDNR ←IT1 END ;FUNCTION(RROOT,IROOT,T1,IT1,NRTS,00004900
COEF );COMPLEX(T1,IT1,RDNR,IDNR,2,FRROOT,FIROOT);GO TO J[C1];M2:RFX1←FRR00005000
OOT ;IFX1←FIROOT ;RROOT←P2 ;GO TO M1 ;M3:RFX2←FRROOT ;IFX2←FIROOT ;RROOT00005100
←P3 ;GO TO M1 ;M4:RFX3←FRROOT ;IFX3←FIROOT ;RX1←P1 ;RX2←P2 ;RX3←P3 ;RH ←00005200
RX3−RX2 ;IH ←IX3−IX2 ;COMPLEX(RH,IH,RX2−RX1,IX2−IX1,2,RLAM,ILAM);RDEL ←R00005300
LAM +1 ;IDEL ←ILAM ;M9:IF(RFX1=RFX2)AND(RFX2=RFX3)AND(IFX1=IFX2)AND(IFX200005400
=IFX3)THEN BEGIN RLAM ←1 ;ILAM ←0 ;GO TO M8 END ;COMPLEX(RFX1,IFX1,RLAM,00005500
ILAM,1,T1,IT1);COMPLEX(RFX2,IFX2,RDEL,IDEL,1,T2,IT2);T1 ←T1−T2+RFX3 ;IT100005600
```

```
←IT1-IT2+IFX3 ;COMPLEX(RDEL,IDEL,RLAM,ILAM,1,T2,IT2);COMPLEX(T1,IT1,T2,00005700
IT2,1,T3,IT3);COMPLEX(RFX3,IFX3,T3,IT3,1,T1,IT1);T1 ←-4×T1 ;IT1 ←-4×IT1 00005800
;COMPLEX(RFX3,IFX3,RLAM+RDEL,ILAM+IDEL,1,T2,IT2);COMPLEX(RDEL×RDEL-IDEL×00005900
IDEL,2×RDEL×IDEL,RFX2,IFX2,1,T3,IT3);COMPLEX(RLAM×RLAM-ILAM×ILAM,2×RLAM×00006000
ILAM,RFX1,IFX1,1,T4,IT4);RG←T4-T3+T2 ;IG←IT4-IT3+IT2 ;IF SWR AND ((RG×RG00006100
+T1)<0)THEN BEGIN RDEN ←RG ;IDEN ←IG ←0 END ELSE COMPLEX(RG×RG-IG×IG+T1,00006200
2×RG×IG+IT1,RG,IG,1,RDEN,IDEN);COMPLEX(-2×RFX3,-2×IFX3,RDEL,IDEL,1,T1,IT00006300
1);COMPLEX(T1,IT1,RDEN,IDEN,2,RLAM,ILAM);M8:ITC ←ITC +1 ;RX1←RX2 ;RX2←RX00006400
3 ;RFX1←RFX2 ;RFX2←RFX3 ;IX1←IX2 ;IX2←IX3 ;IFX1←IFX2 ;IFX2←IFX3 ;COMPLEX00006500
(RLAM,ILAM,RH,IH,1,T1,IT1);RH←T1 ;IH←IT1 ;M6:RDEL←RLAM+1 ;IDEL←ILAM ;RX300006600
←RX2+RH ;IX3←IX2+IH ;C1←3 ;RROOT←RX3 ;IROOT←IX3 ;GO TO M1 ;M7:RFX3←FRRO00006700
T ;IFX3←FIROOT ;FUNCTION(RX3,IX3,RFUNC,IFUNC,NRTS,COEF);COMPLEX(RFX3,IFX00006800
3,RFX2,IFX2,2,T1,IT1);IF (T1×T1 +IT1×IT1)>100 THEN BEGIN RLAM←RLAM/2 ;RH00006900
←RH/2 ;ILAM←ILAM/2 ;IH←IH/2 ;GO TO M6 END ;IF SW1 THEN BEGIN WRITE(OT1,F00007000
4,ITC);WRITE(OT1,F2,RX3,IX3,RFUNC,IFUNC,RFX3,IFX3)END ;T1 ←RX3-RX2 ;IT1 00007100
←IX3-IX2 ;COMPLEX(T1,IT1,RX2,IX2,2,T2,IT2);IF SQRT(T2×T2+IT2×IT2)≤EP1 TH00007200
EN GO TO FIN1 ;IF(SQRT(RFUNC×RFUNC+IFUNC×IFUNC)≤EP2)AND (SQRT(RFX3×RFX3+00007300
IFX3×IFX3)≤EP2)THEN GO TO FIN2 ;IF ITC>MXM THEN GO TO FIN3 ELSE GO TO M900007400
 ;FIN1:IF (NOT SW2)THEN GO TO M12 ELSE WRITE(OT1,F6,ITC);GO TO M10 ;FIN200007500
:IF (NOT SW2)THEN GO TO M12 ELSE WRITE(OT1,F8,ITC);GO TO M10 ;FIN3:BOOL 00007600
←TRUE ;IF (NOT SW2)THEN GO TO M12 ELSE WRITE(OT1,F10,ITC);M10:WRITE(OT1,00007700
F2,RX3,IX3,RFUNC,IFUNC,RFX3,IFX3);M12:RTC ←RTC+1 ;RRT[RTC]←RX3 ;IRT[RTC]00007800
←IX3 ;IF RTC ≥NRTS THEN GO TO EXIT ;IF(ABS(IX3)>EP1)AND (SW3)AND (NOT BO00007900
OL)THEN BEGIN IX3←-IX3 ;FUNCTION(RX3,IX3,RFUNC,IFUNC,NRTS,COEF);RROOT ←R00008000
X3 ;IROOT ←IX3 ;C1 ←4 ;GO TO M1 ;M11:IF SW2 THEN BEGIN WRITE(OT1,F12);WR00008100
ITE(OT1,F2,RX3,IX3,RFUNC,IFUNC,FRROOT,FIROOT)END ;RTC ←RTC+1 ;RRT[RTC]←R00008200
X3 ;IRT[RTC]←IX3 END ELSE GO TO M0 ;IF RTC <NRTS THEN GO TO M0 ;EXIT:END00008300
 ;                                                                       00008400
FORMAT OUT      FMT1(/, "FIXING THE FOLLOWING PARAMETERS AT",//,
                     "R1 = ", F8.3, X8, "R = ", F8.3, X8, "R2 = ", F8.3,
                     X7, "K1 = ", F8.3, X8, "P = ", F8.3, X8, "R4 = ",
                     F8.3,//, "ONE OBTAINS", //, X12, "R3", X12, "Y",
                     X11, "IM(X)", X9, "RE(X)", X9 , "GAW", /),
                FMT2(X8, F8.3, X3, R11.4, X3, R11.4, X3, R11.4, X3,
                     F9.4, //),
                FMT3(X19, R11.4, X3, R11.4, X3, R11.4, X3, F9.4, //),
                FMT4(/X10,"R3=",F8.3,X10,"A=",R10.3,X10,"C=",R10.3,X10,
```

```
                "D=",R10.3,X10,"BC-AD=",R10,3) ;
        WRITE(FO[NO]) ;
        R1 ←  10  ;
        R ← 120   ;
        FOR R2 ← 50                      DO
        FOR K1 ← 1,2          DO
        FOR P  ← .005                         DO
       FOR R4 ←   101.8                       DO
BEGIN
        WRITE (FO [PAGE] ) ;
       WRITE (FO,FMT1,R1,R,R2,K1,P ,R4) ;
        FOR R3 ← 107,108,109,109.5                      DO
BEGIN
       K2 ← R3 × P  ;
       A  ← R1 + R3 - R  ;
       B  ← K2×(R1-R) - K1×(R1+R3) + R1 + R2 + R3 - R  ;
       C  ← K2×(R1+R2-R) -K1×(R1+R2+R3) - R1×K1×K2  ;
       D  ← -K1×K2×(R1+R2)  ;
       J ← B×C - A×D ;
       IF (A>0 AND C>0 AND D>0 AND J>0) OR
          (A<0 AND C<0 AND D<0 AND J>0) THEN
BEGIN
       E  ← -K1  ;
       F  ← D*2 ;
       G  ← C*2 - 2×B×D  ;
       H  ← B*2 - 2×A×C - 2×A*2×E*2  ;
       M  ← - A*2  ;
       POLY[0] ← M ; POLY[1] ← H ; POLY[2] ← G ; POLY[3] ← F ;
       MULLER(-1,-2,-3,30,3,@-10,@-10,FALSE,FALSE,TRUE,FALSE,
               RRT,IRT,POLY,FO ) ;
       FOR I←1 STEP 1 UNTIL 3 DO
BEGIN
       YRT[I] ← SQRT( ABS(RRT[I]) );
       GBW[I] ← YRT[I] × ( -R3/(R3+R1-R) ) ;
END ;
       WRITE (FO,FMT2,R3,YRT[1],IRT[1],RRT[1],GBW[1]) ;
       FOR I←2 STEP 1 UNTIL 3 DO WRITE (FO,FMT3,YRT[I],
```

```
              IRT[I],RRT[I],GBW[I]) ;
END    ELSE WRITE(FO,FMT4,R3,A,C,D,J) ;
 END;
 END;
 END.
```

```
         BEGIN
FILE OUT           FU 6(2,15) ;
REAL              R3,P,A,B,C,D,E,F,G,H,M,K2,Y,X,K1,R4;
INTEGER           R,R1,R2,I,J    ;
          ARRAY     POLY,IRT,RRT,YRT,GBW[0:3]   ;
 PROCEDURE FUNCTION(REALE,IMAG,REVAL,IEVAL,ORDER,COEF);COMMENT THE USER
MUST INSERT THE CODING FOR THIS PROCEDURE."REALE"AND "IMAG"ARE THE REAL
AND IMAGINARY PARTS OF THE DEPENDENT VARIABLE.THE REAL AND IMAGINARY PAR
TS OF THE FUNCTION EVALUATED AT THIS POINT MUST BE "REVAL"AND "IEVAL",RE
SPECTIVELY.ORDER IS THE ORDER OF THE POLYNOMIAL BEING EVALUATED WHILE CO
EF IS A COLUMN ARRAY DECLARED FROM ZERO AND CONTAINING THE I TH COEFFICI
ENT AT COEF[I];VALUE REALE,IMAG,ORDER ;INTEGER ORDER ;REAL REALE,IMAG,RE
VAL,IEVAL ;ARRAY COEF[0];BEGIN INTEGER I,I1 ;ARRAY REIM[0:ORDER,0:2];RE
M[1,1]←REALE ;REIM[1,2]←IMAG ;FOR I ←2 STEP 1 UNTIL ORDER DO BEGIN I1 ←I
 -1 ;REIM[I,1]←REIM[I1,1]×REALE -REIM[I1,2]×IMAG ;REIM[I,2]←REIM[I1,1]×I
MAG +REIM[I1,2]×REALE ;END ;REVAL ←COEF[0];IEVAL ←0 ;FOR I ←1 STEP 1 UNT
IL ORDER DO BEGIN REVAL ←REVAL +COEF[I]×REIM[I,1];IEVAL ←IEVAL +COEF[I]×
REIM[I,2];END ;END ;
 PROCEDURE MULLER(P1,P2,P3,MXM,NRTS,EP1,EP2,SW1,SW2,SW3,SWR,RRT,IRT,COEF
,DT1 );COMMENT PROCEDURE MULLER FINDS REAL AND COMPLEX ROOTS OF AN ARBIT
RARY FUNCTION.P1,P2,AND P3 ARE STARTING VALUES.THE ROOTS NEAREST TO THES
E POINTS WILL BE FOUND FIRST.MXM IS THE MAXIMUM NUMBER OF ITERATIONS TO
BE MADE IN FINDING ANY ONE ROOT.EP1 AND EP2 ARE CONVERGENCE CRITERION FA
CTORS.IF ABS((X(I+1)-X(I))/X(I+1))IS LESS THAN EP1 OR IF THE FUNCTION VA
LUE AND MODIFIED FUNCTION VALUE ARE BOTH LESS THAN EP2,A ROOT HAS BEEN F
OUND.SW1,SW2,SW3,AND SWR ARE BOOLEAN VARIABLES.IF SW1 IS TRUE,THEN EACH
ITERANT OF EACH ROOT WILL BE PRINTED.IF SW2 IS TRUE THE VALUE OF EACH RO
OT FOUND WILL BE PRINTED.IF SW3 IS TRUE,THEN,WHEN APPLICABLE,THE COMPLEX
 CONJUGATE OF EACH ROOT FOUND WILL BE ADMITTED AS A ROOT.IF SWR IS TRUE
ONLY REAL ROOTS ARE FOUND.SWR SHOULD BE SET TRUE IF IT IS KNOWN THAT THE
 FUNCTION HAS ALL REAL ROOTS.ARRAYS RRT AND IRT CONTAIN THE REAL AND IMA
GINARY PARTS,RESPECTIVELY,OF THE ROOTS FOUND.PROCEDURE FUNCTION IS THE F
UNCTION GENERATOR AND PROCEDURE COMPLEX PERFORMS THE NECESSARY COMPLEX A
RITHMETIC.COEF IS A COLUMN ARRAY WHICH IS PASSED TO THE PROCEDURE FUNCTI
ON .R.D.RODMAN,MRS:22 5018 (PROFESSIONAL SERVICES DIVISIONAL GROUP),CARD
 SEQUENCE BEGINS WITH MULL0001,FIRST RELEASE 5/1/63 ;VALUE P1,P2,P3,MXM,
NRTS,EP1,EP2,SW1,SW2,SW3,SWR ;INTEGER MXM,NRTS ;BOOLEAN SW1,SW2,SW3,SWR
```

PARALLEL PROGRAM

```
;REAL P1,P2,P3,EP1,EP2 ;ARRAY RRT,IRT[0],COEF[0];FILE OT1 ;BEGIN BOOLEAN00002000
 BOOL;INTEGER C1,RTC,I,ITC ;REAL RX1,RX2,RX3,IX1,IX2,IX3,RROOT,IROOT,RDN00002100
R,IDNR,T1,IT1,FRROOT,FIROOT,RFX1,RFX2,RFX3,IFX1,IFX2,IFX3,RH,IH,RLAM,ILA00002200
M,RDEL,IDEL,T2,IT2,T3,IT3,T4,IT4,RG,IG,RDEN,IDEN,RFUNC,IFUNC ;LABEL M0,M00002300
1,M2,M3,M4,M9,M8,M6,M7,FIN1,FIN2,FIN3,M10,M12,M11,EXIT ;SWITCH J ←M2,M3,00002400
M4,M7,M11 ;FORMAT OUT F2(X46,"REAL",X12,"IMAGINARY"/X37,E18.11,X4,E18.1100002500
 /X39,"THE FUNCTION EVALUATED AT THIS POINT IS"/X46,"REAL",X12,"IMAGINAR00002600
Y"/X37,E18.11,X4,E18.11 /X35,"THE MOD""IFIED FUNCTION EVALUATED AT THIS 00002700
POINT IS"/X46,"REAL",X12,"IMAGINARY"/X37,E18.11,X4,E18.11 ),F4(///X29,I300002800
," ITERATIONS HAVE BEEN MADE.  THE VALUE OF ""THE ITERANT IS NOW"),F6(//00002900
X37,"SUCCESSIVE ITERANTS MEET CONVERGENCE CRITERION"/X39,"AFTER",I3," IT00003000
ERATIONS.  THE ROOT FOUND IS"),F8(//X33,"THE FUNCTION VALUES OF THE LAST00003100
 ITERANT ARE"" SUFFICIENTLY"/X33,"NEAR ZERO. ",I4," ITERATIONS WERE MA""00003200
DE.  THE ROOT FOUND IS"),F10(//X35,I3," ITERATIONS COMPLETED AND SUCCESS00003300
FUL CONVE""RGENCE"/X41,"HAS NOT OCCURRED.  THE LAST ITERANT IS"),F12(//X00003400
40,"THE PREVIOUS ROOT FOUND WAS COMPLEX.  THE"/X40,"CONJUGATE OF THIS VA00003500
LUE IS ALSO A ROOT.");PROCEDURE COMPLEX(A,IA,B,IB,K,C,IC);VALUE A,IA,B,I00003600
B,K ;INTEGER K ;REAL A,IA,B,IB,C,IC ;BEGIN REAL TEMP ;LABEL MPY,DVD,SQT,00003700
EXIT ;SWITCH JUNCTION ←MPY,DVD,SQT ;GO TO JUNCTION[K];MPY:C ←A×B -IA×IB 00003800
;IC ←A×IB +IA×B ;GO TO EXIT ;DVD:IF B =0 AND IB =0 THEN BEGIN C←1 ;IC←0 00003900
;GO TO EXIT END ;TEMP ←B×B +IB×IB ;C ←(A×B +IA×IB)/TEMP ;IC ←(IA×B -A×IB00004000
)/TEMP ;GO TO EXIT ;SQT:IF (IA=0)AND (A<0)THEN BEGIN C ←0 ;IC ←SQRT(-A)E00004100
ND ELSE IF IA=0 THEN BEGIN C ←SQRT(A);IC←0 END ELSE BEGIN TEMP ←SQRT(A×A00004200
 +IA×IA);C ←SQRT((TEMP+A)/2);IC ←IF (TEMP -A)<0 THEN 0 ELSE SQRT((TEMP-A00004300
)/2)END ;IF((B+C)×(B+C)+(IB+IC)×(IB+IC))<((B-C)×(B-C)+(IB-IC)×(IB-IC))TH00004400
EN BEGIN C ←B-C ;IC ←IB-IC END ELSE BEGIN C ←B+C ;IC ←IB+IC END ;EXIT:EN00004500
D ;FOR I ←1 STEP 1 UNTIL NRTS DO RRT[I]←IRT[I]←0 ;RTC←0 ;M0:IX1←IX2←IX3←00004600
C1←IROOT←ITC←0 ;RROOT←P1 ;BOOL ←FALSE ;M1:C1←C1+1 ;RDNR ←1 ;IDNR ←0 ;FOR00004700
 I ←1 STEP 1 UNTIL RTC DO BEGIN COMPLEX(RDNR,IDNR,RROOT-RRT[I],IROOT-IRT00004800
[I],1,T1,IT1);RDNR ←T1 ;IDNR ←IT1 END ;FUNCTION(RROOT,IROOT,T1,IT1,NRTS,00004900
COEF );COMPLEX(T1,IT1,RDNR,IDNR,2,FRROOT,FIROOT);GO TO J[C1];M2:RFX1←FRR00005000
OOT ;IFX1←FIROOT ;RROOT←P2 ;GO TO M1 ;M3:RFX2←FRROOT ;IFX2←FIROOT ;RROOT00005100
←P3 ;GO TO M1 ;M4:RFX3←FRROOT ;IFX3←FIROOT ;RX1←P1 ;RX2←P2 ;RX3←P3 ;RH ←00005200
RX3-RX2 ;IH ←IX3-IX2 ;COMPLEX(RH,IH,RX2-RX1,IX2-IX1,2,RLAM,ILAM);RDEL ←R00005300
LAM +1 ;IDEL ←ILAM ;M9:IF(RFX1=RFX2)AND(RFX2=RFX3)AND(IFX1=IFX2)AND(IFX200005400
=IFX3)THEN BEGIN RLAM ←1 ;ILAM ←0 ;GO TO M8 END ;COMPLEX(RFX1,IFX1,RLAM,00005500
ILAM,1,T1,IT1);COMPLEX(RFX2,IFX2,RDEL,IDEL,1,T2,IT2);T1 ←T1-T2+RFX3 ;IT100005600
```

```
←IT1−IT2+IFX3 ;COMPLEX(RDEL,IDEL,RLAM,ILAM,1,T2,IT2);COMPLEX(T1,IT1,T2,
IT2,1,T3,IT3);COMPLEX(RFX3,IFX3,T3,IT3,1,T1,IT1):T1 ←−4×T1 ;IT1 ←−4×IT1 
;COMPLEX(RFX3,IFX3,RLAM+RDEL,ILAM+IDEL,1,T2,IT2);COMPLEX(RDEL×RDEL−IDEL×
IDEL,2×RDEL×IDEL,RFX2,IFX2,1,T3,IT3);COMPLEX(RLAM×RLAM−ILAM×ILAM,2×RLAM×
ILAM,RFX1,IFX1,1,T4,IT4);RG←T4−T3+T2 ;IG←IT4−IT3+IT2 ;IF SWR AND ((RG×RG
+T1)<0)THEN BEGIN RDEN ←RG ;IDEN ←IG ←0 END ELSE COMPLEX(RG×RG−IG×IG+T1,
2×RG×IG+IT1,RG,IG,3,RDEN,IDEN);COMPLEX(−2×RFX3,−2×IFX3,RDEL,IDEL,1,T1,IT
1);COMPLEX(T1,IT1,RDEN,IDEN,2,RLAM,ILAM);M8:ITC ←ITC +1 ;RX1←RX2 ;RX2←RX
3 ;RFX1←RFX2 ;RFX2←RFX3 ;IX1←IX2 ;IX2←IX3 ;IFX1←IFX2 ;IFX2←IFX3 ;COMPLEX
(RLAM,ILAM,RH,IH,1,T1,IT1);RH←T1 ;IH←IT1 ;M6:RDEL←RLAM+1 ;IDEL←ILAM ;RX3
←RX2+RH ;IX3←IX2+IH ;C1←3 ;RROOT←RX3 ;IROOT←IX3 ;GO TO M1 ;M7:RFX3←FRROO
T ;IFX3←FIROOT ;FUNCTION(RX3,IX3,RFUNC,IFUNC,NRTS,COEF);COMPLEX(RFX3,IFX
3,RFX2,IFX2,2,T1,IT1);IF (T1×T1 +IT1×IT1)>100 THEN BEGIN RLAM←RLAM/2 ;RH
←RH/2 ;ILAM←ILAM/2 ;IH←IH/2 ;GO TO M6 END ;IF SW1 THEN BEGIN WRITE(OT1,F
4,ITC);WRITE(OT1,F2,RX3,IX3,RFUNC,IFUNC,RFX3,IFX3)END ;T1 ←RX3−RX2 ;IT1 
←IX3−IX2 ;COMPLEX(T1,IT1,RX2,IX2,2,T2,IT2);IF SQRT(T2×T2+IT2×IT2)≤EP1 TH
EN GO TO FIN1 ;IF(SQRT(RFUNC×RFUNC+IFUNC×IFUNC)≤EP2)AND (SQRT(RFX3×RFX3+
IFX3×IFX3)≤EP2)THEN GO TO FIN2 ;IF ITC>MXM THEN GO TO FIN3 ELSE GO TO M9
 ;FIN1:IF (NOT SW2)THEN GO TO M12 ELSE WRITE(OT1,F6,ITC);GO TO M10 ;FIN2
:IF (NOT SW2)THEN GO TO M12 ELSE WRITE(OT1,F8,ITC);GO TO M10 ;FIN3:BOOL 
←TRUE ;IF (NOT SW2)THEN GO TO M12 ELSE WRITE(OT1,F10,ITC);M10:WRITE(OT1,
F2,RX3,IX3,RFUNC,IFUNC,RFX3,IFX3);M12:RTC ←RTC+1 ;RRT[RTC]←RX3 ;IRT[RTC]
←IX3 ;IF RTC ≥NRTS THEN GO TO EXIT ;IF(ABS(IX3)>EP1)AND (SW3)AND (NOT BO
OL)THEN BEGIN IX3←−IX3 ;FUNCTION(RX3,IX3,RFUNC,IFUNC,NRTS,COEF);RROOT ←R
X3 ;IROOT ←IX3 ;C1 ←4 ;GO TO M1 ;M11:IF SW2 THEN BEGIN WRITE(OT1,F12);WR
ITE(OT1,F2,RX3,IX3,RFUNC,IFUNC,FRROOT,FIROOT)END ;RTC ←RTC+1 ;RRT[RTC]←R
X3 ;IRT[RTC]←IX3 END ELSE GO TO M0 ;IF RTC <NRTS THEN GO TO M0 ;EXIT:END
 ;
FORMAT OUT      FMT1(/, "FIXING THE FOLLOWING PARAMETERS AT",//,
                      "R1 = ", F8.3, X8, "R = ", F8.3, X8, "R2 = ", F8.3,
                      X7, "K1 = ", F8.3, X8, "K2 = ", F8.3, X8, "R4 = ",
                      F8.3,//, "ONE OBTAINS", //, X12, "R3", X12, "Y",
                      X11, "IM(X)", X9, "RE(X)", X9 , "GRW", /),
                FMT2(X8, F8.3, X3, R11.4, X3, R11.4, X3, R11.4, X3,
                      F9.4, //),
                FMT3(X19, R11.4, X3, R11.4, X3, R11.4, X3, F9.4, //),
                FMT4(/X10,"R3=",F8.3,X10,"A=",R10.3,X10,"C=",R10.3,X10,
```

```
               "D=",R10.3,X10,"BC-AD=",R10.3) ;
     WRITE(FO[NO]) ;
     R2 ← 15 ;
     R ←150 ;
     FOR R1 ← 50,100,150,200                 DO
     FOR K1 ← 1,2,4            DO
     FOR K2 ← 2,1,.5,.2            DO
    FOR R4 ← 000                     DO
BEGIN
     WRITE (FO [PAGE] ) ;
    WRITE (FO,FMT1,R1,R,R2,K1,K2,R4) ;
     FOR R3 ← 127.5,120,110,100,90,75,60                 DO
BEGIN
     A  ← R1 + R3 - R  ;
     B  ← K2×(R1-R) - K1×(R1+R3) - R1 + R2 + R3 - R  ;
     C  ← K2×(R1+R2-R) -K1×(R1+R2+R3) - R1×K1×K2  ;
     D  ← -K1×K2×(R1+R2)  ;
     J ← B×C - A×D ;
     IF (A>0 AND C>0 AND D>0 AND J>0) OR
        (A<0 AND C<0 AND D<0 AND J>0) THEN
BEGIN
     E  ←  K2  ;
     F  ← D*2 ;
     G  ← C*2 - 2×B×D  ;
     H  ← B*2 - 2×A×C - 2×A*2×E*2  ;
     M  ← - A*2  ;
     POLY[0] ← M ; POLY[1] ← H ; POLY[2] ← G ; POLY[3] ← F ;
     MULLER(-1,-2,-3,30,3,@-10,@-10,FALSE,FALSE,TRUE,FALSE,
             RRT,IRT,POLY,FO ) ;
     FOR I←1 STEP 1 UNTIL 3 DO
BEGIN
     YRT[I] ← SQRT( ABS(RRT[I]) );
     GBW[I] ← YRT[I] × ( -R/(-R+R3+R1) ) ;
END ;
     WRITE (FO,FMT2,R3,YRT[1],IRT[1],RRT[1],GBW[1]) ;
     FOR I←2 STEP 1 UNTIL 3 DO WRITE (FO,FMT3,YRT[I],
        IRT[I],RRT[I],GBW[I]) ;
```

```
END
     ELSE
     WRITE(FO,FMT4,K3,A,C,D,J) ;
END;
END;
END.
```

APPENDIX III

SEVERAL OTHER MEMBERS OF THE CLASS OF COMBINATIONS

Four other combinations were investigated using the computer method. Two of these are a very simple extension of the two combinations given in the dissertation for illustration purposes. These two combinations are the same as those discussed except that a resistance is placed in parallel with the tunnel diode as shown in Figure 71. Using model (d)

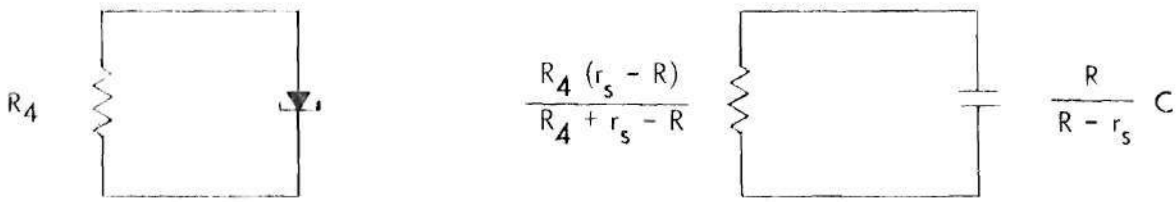

Figure 71. Parallel Combination of Tunnel Diode and Resistance.

for the tunnel diode, the small signal model for the parallel combination is that given in the right half of the figure. These combinations are investigated by using the same equations developed for the previous two combinations. One merely uses a different equivalent negative resistance for the tunnel diode.

The addition of a positive resistance R_4, greater than the R of the tunnel diode, produces a larger equivalent negative resistance. In going from one value of tunnel diode peak current to the next higher manufactured value, the average negative resistance decreases by a factor of two to three. The parallel combination affords a method of realizing the values between the two average values of negative resistance. For a given type of transistor, some of its model element values may be such that maximum gain-bandwidth can only be achieved using this method. The main disadvantage of the method is that the sensitivity of equivalent negative resistance to R is increased. The absolute value of the derivation of the equivalent negative resistive resistance with R_4 equal to infinity is obviously unity. For finite R_4

$$\frac{\partial}{\partial R}\ \frac{R_4(r_s - R)}{R_4 + r_s - R} = \frac{R_4^2}{(R_4 + r_s - R)^2} \qquad \text{(A3.1)}$$

Since R_4 must be greater than $(r_s - R)$ for the equivalent negative resistance to be greater than $(r_s - R)$, this derivative must be greater

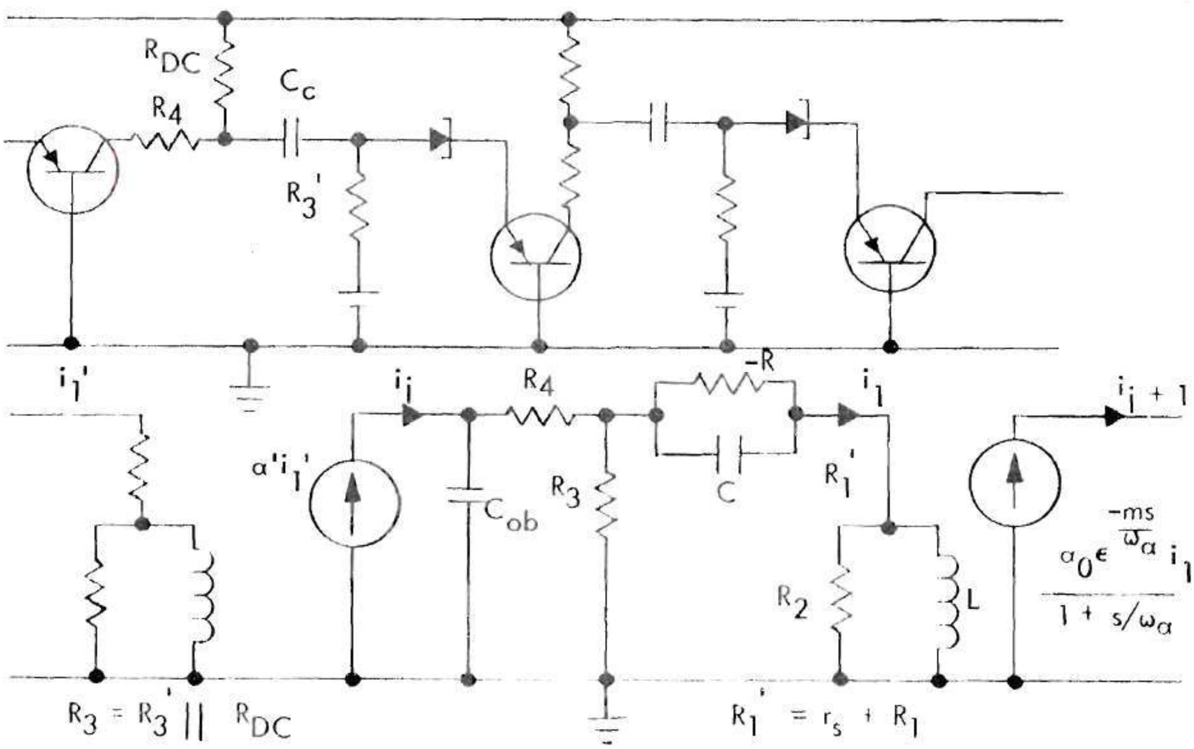

Figure 72. A Series Combination.

than unity.

The third combination considered is given in Figure 72. Again the gain equations are written in terms of the transfer current gain from one dependent current source to the next. The current gain is in the form

$$\frac{i_{j+1}}{i_j} = \frac{K(1 + es)}{a + bs + cs^2 + ds^3} \tag{A3.2}$$

where

$$a = R_2(R_1 + R_3 - R) \tag{A3.3}$$

$$b = (R_1 + R_2 + R_3 - R)L - R_2RC(R_1 + R_3) + R_2C_{ob}[R_3R_4 + (R_1 - R)(R_3 + R_4)] \tag{A3.4}$$

$$c = -(R_1 + R_2 + R_3)RLC - R_2RCC_{ob}[R_3R_4 + R_1R_3 + R_1R_4] + (R_1 + R_2 - R)(R_3 + R_4)LC_{ob} + R_3R_4C_{ob}L \tag{A3.5}$$

$$d = -[(R_1 + R_2)(R_3 + R_4) + R_3R_4]\, RLCC_{ob} \tag{A3.6}$$

$$e = - RC \tag{A3.7}$$

$$K = R_3R_2 \tag{A3.8}$$

Normalization of equation (A3.2) is accomplished by letting

$$\frac{R_2}{L} = \omega_a \tag{A3.9}$$

$$RC = \frac{K_1}{\omega_a} \tag{A3.10}$$

$$C_{ob} = \frac{P}{\omega_\alpha} \tag{A3.11}$$

Each coefficient of the denominator and K is also divided by R_2. The resulting equation for i_{j+1}/i_j normalized with respect to ω_α has the coefficients

$$a = (R_1 + R_3 - R) \tag{A3.12}$$

$$b = (R_1 + R_2 + R_3 - R) - K(R_1 + R_3) \tag{A3.13}$$

$$c = -(R_1 + R_2 + R_3)K_1 - K_1P[R_3R_4 + R_1R_3 + R_1R_4] + (R_1 + R_2 - R)(R_3 + R_4)P + R_3R_4P \tag{A3.14}$$

$$d = -K_1P[(R_1 + R_2)(R_3 + R_4) + R_3R_4] \tag{A3.15}$$

$$e = -K_1 \tag{A3.16}$$

$$K = R_3 \tag{A3.17}$$

The previously discussed restrictions on the network variable ranges, definition of gain-bandwidth, and computer method are adequate to investigate the gain-bandwidth properties of this normalized gain equation.

The fourth combination is given in Figure 73. The total gain can be written in terms of the transfer current gains i_{j+1}/i_j. This transfer current gain from one dependent source to the next is in the form

$$i_{j+1}/i_j = \frac{K(1 + es)}{a + bs + cs^2 + ds^3} \tag{A3.18}$$

where

$$a = (R_3 - R) + R_1' \tag{A3.19}$$

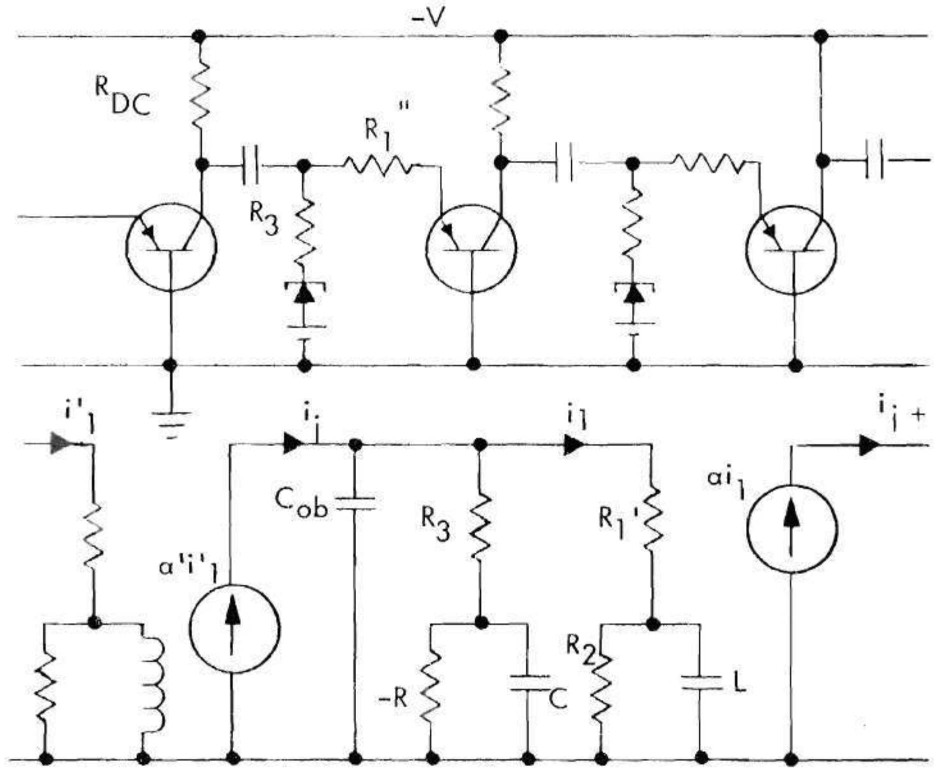

$R_1' = R_1 + R_1''$ $\qquad$ R_{DC} large $\qquad$ $\alpha = \dfrac{\alpha_0 \epsilon^{\frac{-ms}{\omega_\alpha}}}{1 + s/\omega_\alpha}$

Figure 73. A Parallel Combination.

$$b = -(R_1' + R_3)RC + R_1' C_{ob}(R_3 - R) + (R_1' + R_2 + R_3 - R)\frac{L}{R_2} \tag{A3.20}$$

$$c = -(R_1' + R_2 + R_3)R\frac{L}{R_2}C - R_1' R_3 RCC_{ob} + (R_1' + R_2)\frac{L}{R_2}C_{ob}(R_3 - R) \tag{A3.21}$$

$$d = -(R_1' + R_2)R_3 R\frac{L}{R_2}C\,C_{ob} \tag{A3.22}$$

$$e = \frac{-R_3 RC}{R_3 - R} \tag{A3.23}$$

$$K = R_3 - R \tag{A3.24}$$

To normalize gain equation (A3.18) one makes the following definitions.

$$\frac{R_2}{L} = \omega_a \tag{A3.25}$$

$$RC = \frac{K_1}{\omega_a} \tag{A3.26}$$

$$C'_{ob} = \frac{P}{\omega_a} \tag{A3.27}$$

The resulting equation for i_{j+1}/i_j normalized with respect to ω_a has the coefficients

$$a = (R_3 - R) + R_1' \tag{A3.28}$$

$$b = -(R_1' + R_3)K_1 + R_1'(R_3 - R)P + (R_1' + R_2 + R_3 - R) \tag{A3.29}$$

$$c = -(R_1' + R_2 + R_3)K_1 + (R_1 + R_2)(R_3 - R)P + R_1 R_3 K_1 P \tag{A3.30}$$

$$d = -(R_1 + R_2)R_3 K_1 P \tag{A3.31}$$

$$e = \frac{R_3 K_1}{R - R_3} \tag{A3.32}$$

The network variable range restrictions and computer method given in Chapter III are adequate to investigate the gain-bandwidth properties of the normalized gain equation.

As previously discussed, the investigation of these four combinations revealed that gain-bandwidth improvements over the current limit of an order of magnitude are possible. For all six combinations investigated by the author, a factor of ten improvement over the current limit was found to be possible for realistic values of the network variables.

BIBLIOGRAPHY

1. Bode, H. W., Network Analysis and Feedback Amplifier Design, P. Van Nostrand Co., Inc., 1945.

2. Hanson, W. W., "On Maximum Gain-Bandwidth Product in Amplifiers," Journal of Applied Physics, September, 1945, pp. 528-534.

3. Ghausi, M. W., Principles and Design of Linear Active Networks, McGraw Hill, New York, 1965.

4. Carlin, H. J., "Synthesis Techniques for Gain-Bandwidth Optimization in Passive Transducers," Proceedings of the IRE, vol. 48, no. 10, pp. 1705-1714, October, 1960.

5. Chang, K. K. N., Parametric and Tunnel Diodes, Prentice Hall, Englewood Cliffs, N. J., 1964.

6. Chow, W. F., Principles of Tunnel Diode Circuits, John Wiley and Sons, New York, 1964.

7. Engineering Staff of Texas Instruments Incorporated, Transistor Circuit Design, McGraw Hill, New York, 1963.

8. Linvill, J. G., Models of Transistors and Diodes, McGraw Hill, New York, 1963.

9. Su, K. L., Active Network Synthesis, McGraw Hill, New York, 1965.

10. Gray, et al., Physical Electronics and Circuit Models of Transistors (SEEC Vol. 2), John Wiley and Sons, New York, 1964.

11. Thornton, et al., Characteristics and Limitations of Transistors (SEEC Vol. 4), John Wiley and Sons, New York, 1964.

12. Lewin, M. H., Negative Resistance Elements as Digital Computer Components, Ph.D. Thesis, Princeton University, 1960.

VITA

James Stephen Gray was born in Rochester, New York, on December 27, 1940. He is the son of Ralph E. and Ambrozine Robinson Gray. He was married to Susan Hatch Horton of Sheffield, Alabama, in September of 1962. They have one child, James Stephen Gray, Jr., born June 18, 1964.

Mr. Gray attended public school in Memphis, Tennessee and was graduated from Central High School in 1958. He attended Southwestern at Memphis on an academic scholarship and received a B.S. in Mathematics and Psychology in 1962.

In September 1962 he entered Electrical Engineering graduate school at the Georgia Institute of Technology. He received the M.S.E.E. in 1965. During his graduate career Mr. Gray was both a graduate teaching assistant and a graduate research assistant. From September 1965 to September 1966 he held an NSF Trainee Fellowship. During part of this time he served as Vice-President of the Graduate Student Senate.